Handbook of Fiber Chemistry

Third Edition

Edited by

Menachem Lewin

CRC Press
Taylor & Francis Group

Handbook of Fiber Chemistry

Third Edition

INTERNATIONAL FIBER SCIENCE AND TECHNOLOGY SERIES

Series Editor

MENACHEM LEWIN
Hebrew University of Jerusalem
Jerusalem, Israel
Herman F. Mark Polymer Research Institute
Polytechnic University
Brooklyn, New York

The Editor and Publisher gratefully acknowledge
the past contributions of our distinguished

INTERNATIONAL FIBER SCIENCE AND TECHNOLOGY SERIES

Series Editor: **MENACHEM LEWIN**

1. Handbook of Fiber Science and Technology (I): Chemical Processing of Fibers and Fabrics-Fundamentals and Preparation (in two parts), *edited by Menachem Lewin and Stephen B. Sello*
2. Handbook of Fiber Science and Technology (II): Chemical Processing of Fibers and Fabrics-Functional Finishes (in two parts), *edited by Menachem Lewin and Stephen B. Sello*
3. Carbon Fibers, *Jean-Baptiste Donnet and Roop Chand Bansal*
4. Fiber Technology: From Film to Fiber, *Hans A. Krässig, Jürgen Lenz, and Herman F. Mark*
5. Handbook of Fiber Science and Technology (III): High Technology Fibers (Part A), *edited by Menachem Lewin and Jack Preston*
6. Polyvinyl Alcohol Fibers, *Ichiro Sakurada*
7. Handbook of Fiber Science and Technology (IV): Fiber Chemistry, *edited by Menachem Lewin and Eli M. Pearce*
8. Paper Structure and Properties, *edited by J. Anthony Bristow and Petter Kolseth*
9. Handbook of Fiber Science and Technology (III): High Technology Fibers (Part B), *edited by Menachem Lewin and Jack Preston*
10. Carbon Fibers: Second Edition, Revised and Expanded, *Jean-Baptiste Donnet and Roop Chand Bansal*
11. Wood Structure and Composition, *edited by Menachem Lewin and Irving S. Goldstein*
12. Handbook of Fiber Science and Technology (III): High Technology Fibers (Part C), *edited by Menachem Lewin and Jack Preston*
13. Modern Textile Characterization Methods, *edited by Mastura Raheel*
14. Handbook of Fiber Science and Technology (III): High Technology Fibers (Part D), *edited by Menachem Lewin and Jack Preston*
15. Handbook of Fiber Chemistry: Second Edition, Revised and Expanded, *edited by Menachem Lewin and Eli M. Pearce*
16. Handbook of Fiber Chemistry: Third Edition, *edited by Menachem Lewin*

Handbook of Fiber Chemistry

Third Edition

Edited by

Menachem Lewin

Taylor & Francis
Taylor & Francis Group
Boca Raton London New York

CRC is an imprint of the Taylor & Francis Group,
an informa business

CRC Press
Taylor & Francis Group
6000 Broken Sound Parkway NW, Suite 300
Boca Raton, FL 33487-2742

Printed in the United States of America on acid-free paper
10 9 8 7 6 5 4 3 2 1

International Standard Book Number-10: 0-8247-2565-4 (Hardcover)
International Standard Book Number-13: 978-0-8247-2565-5 (Hardcover)

Library of Congress Cataloging-in-Publication Data

Handbook of fiber chemistry / edited by Menachem Lewin. -- 3rd ed.
p. cm. -- (International fiber science and technology series ; 16)
Includes bibliographical references and index.
ISBN 0-8247-2565-4
1. Textile fibers. 2. Textile chemistry. I. Lewin, Menachem, 1918- II. Series.

TS1540.H26 2006
677'.02832--dc22 2006044600

Visit the Taylor & Francis Web site at
http://www.taylorandfrancis.com

and the CRC Press Web site at
http://www.crcpress.com

Preface

The third edition of the *Handbook of Fiber Chemistry*, expanded from the second edition, contains 13 chapters dealing with the most important natural, human-made, and synthetic fibers, including the additional chapter on the highly important and broadly used Kevlar fiber. Almost a decade has passed since the the second edition, and relatively little change has taken place during this time in the use of the basic fibers. Some important technological advances that have happened during this period are fully discussed in the present volume. Thus, the fibers described in this book maintain their unchallenged economic positions. The technologies used in their production and applications have been greatly improved, as indicated by the considerable number of patents published; thus the current production systems have not been discarded or replaced by inherently new systems. Similarly, the markets for these fibers were not only maintained, but have expanded and diversified.

Fiber science in its present state of development cannot be considered as a mature science. New fibers, including nanofibers and biologically and electronically active fibers, are under development for specific applications at present for relatively limited markets. Several of these fibers are discussed in the four volumes on high-technology fibers included in this series. Their development is, however, derived from the scientific and technological principles of the conventional fibers described in this book. The definitions, morphology, and fine structure, properties, testing, processing methods, and equipment, and the conversions into marketable products are basically similar.

The chapters in this revised and expanded volume, except for the chapters on acrylic and wool fibers, are either new or extensively updated; hence this edition should be considered as entirely a new book. A wide array of new data have become available in the past decade based, to a large extent, on new scientific techniques, instruments, and disciplines. These data have enabled us to gain a better insight into the structure of fibers and structure–property relationships, and have brought about a better understanding of fiber-related phenomena. We have made a serious effort to include the most important developments in fiber science during the last decade in the present volume.

The chapters in this edition are authored by leading experts in the field of fiber science. Many of the chapters (rayon, acetate, silk, polypropylene, polyamide, polyester) are new and written by authors who have not contributed to the previous edition. Other chapters (vinyl fibers, cotton, jute and kenaf, long vegetable fibers) have been fully updated. Of particular importance is the updated comprehensive chapter on cotton fibers. This was prepared by 16 recognized authorities and compiled by P. Wakelyn and R. Bertoniere. It contains a vast amount of up-to-date information presented in a lucid and concise format, and covers all aspects of the science and technology of cotton and cellulose. The recently revived interest in other vegetable fibers is clearly illustrated in the chapters on long vegetable fibers, and on jute and kenaf.

This volume is aimed at a wide audience of scientists, technologists, and engineers in chemistry, physics, biology, medicine, agriculture, materials, textiles, and polymers. We hope that this book will help experts working in these various disciplines to understand the vigorous and complex field of fibers, and as a result, to interact with scientists working on

fibers so as to provide new, better routes for developing novel and innovative products and technologies.

I wish to thank all the authors who have contributed to this book, and the editorial staff of the Taylor & Francis Group who helped me in its publication.

Contributors

Subhash K. Batra
North Carolina State University
Raleigh, North Carolina

Noelie R. Bertoniere
Southern Regional Research Center
Agricultural Research Service
U.S. Department of Agriculture
New Orleans, Louisana

Peggy Cebe
Departments of Biomedical Engineering,
Chemical & Biological Engineering & Physics
Tufts University
Medford, Massachusetts

Anthony J. East
Medical Device Concept Lab
New Jersey Institute of Technology
Newark, New Jersey

J. Vincent Edwards
Southern Regional Research Center
Agricultural Research Service
U.S. Department of Agriculture
New Orleans, Louisiana

Alfred D. French
Southern Regional Research Center
Agricultural Research Service
U.S. Department of Agriculture
New Orleans, Louisiana

Bruce G. Frushour
High Performance Materials
Monsanto Company
St. Louis, Missouri

Vlodek Gabara
Spruance Plant
E.I. DuPont
Richmond, Virginia

Gary R. Gamble
Cotton Quality Research Station
Agricultural Research Service
U.S. Department of Agriculture
Clemson, South Carolina

Wilton R. Goynes, Jr.
Southern Regional Research Center
Agricultural Research Service
U.S. Department of Agriculture
New Orleans, Louisiana

Jon D. Hartzler
Spruance Plant
E.I. DuPont
Richmond, Virginia

Lawrance Hunter
Council for Scientific and Industrial Research
Port Elizabeth, South Africa

Michael Jaffe
Department of Biomedical Engineering
New Jersey Institute of Technology
Newark, New Jersey

Leslie N. Jones
Division of Wool Technology
CSIRO
Belmont, Victoria, Australia

David L. Kaplan
Departments of Biomedical Engineering,
Chemical & Biological Engineering & Physics
Tufts University
Medford, Massachusetts

Hyeon Joo Kim
Departments of Biomedical Engineering,
Chemical & Biological Engineering & Physics
Tufts University
Medford, Massachusetts

Raymond S. Knorr
Fibers Division
Solutia, Inc.
Pensacola, Florida

Richard Kotek
College of Textiles
North Carolina University
Raleigh, North Carolina

Herman L. LaNieve
Warren, New Jersey

Kiu-Seung Lee
DuPont Experimental Station
Wilmington, Delaware

Akira Matsumoto
Departments of Biomedical Engineering, Chemical & Biological Engineering & Physics
Tufts University
Medford, Massachusetts

David D. McAlister
Cotton Quality Research Station
Agricultural Research Service
U.S. Department of Agriculture
Clemson, South Carolina

Takuji Okaya
The University of Shiga Prefecture
Shiga, Japan

Donald E. Rivett
Division of Biomolecular Engineering
CSIRO
Melbourne, Victoria, Australia

David J. Rodini
Spruance Plant
E.I. DuPont
Richmond, Virginia

Marie-Alice Rousselle
Southern Regional Research Center
Agricultural Research Service
U.S. Department of Agriculture
New Orleans, Louisiana

Roger M. Rowell
Modified Lignocellulosic Materials
Forest Products Laboratory
University of Wisconsin
Madison, Wisconsin

Ichiro Sakurada*
Institute for Chemical Research
Kyoto University
Kyoto, Japan

Harry P. Stout*
British Jute Trade Research Association
Dundee, Scotland

Devron P. Thibodeaux
Southern Regional Research Center
Agricultural Research Service
U.S. Department of Agriculture
New Orleans, Louisiana

Barbara A. Triplett
Southern Regional Research Center
Agricultural Research Service
U.S. Department of Agriculture
New Orleans, Louisiana

Daryl J. Tucker
School of Biological and Chemical Sciences
Deakin University
Geelong, Victoria, Australia

Irene Y. Tsai
Departments of Biomedical Engineering, Chemical & Biological Engineering & Physics
Tufts University
Medford, Massachusetts

Phillip J. Wakelyn
National Cotton Council of America
Washington, D.C.

Xianyan Wang
Departments of Biomedical Engineering, Chemical & Biological Engineering & Physics
Tufts University
Medford, Massachusetts

H.H. Yang
Richmond, Virginia

Mei-Fang Zhu
Shanghai, China

*Deceased

Table of Contents

Chapter 1 Polyester Fibers 1

Michael Jaffe and Anthony J. East

Chapter 2 Polyamide Fibers 31

H.H. Yang

Chapter 3 Polypropylene Fibers 139

Mei-Fang Zhu and H.H. Yang

Chapter 4 Vinyl Fibers 261

Ichiro Sakurada and Takuji Okaya

Chapter 5 Wool and Related Mammalian Fibers 331

Leslie N. Jones, Donald E. Rivett, and Daryl J. Tucker

Chapter 6 Silk 383

Akira Matsumoto, Hyeon Joo Kim, Irene Y. Tsai, Xianyan Wang, Peggy Cebe, and David L. Kaplan

Chapter 7 Jute and Kenaf 405

Roger M. Rowell and Harry P. Stout

Chapter 8 Other Long Vegetable Fibers: Abaca, Banana, Sisal, Henequen, Flax, Ramie, Hemp, Sunn, and Coir 453

Subhash K. Batra

Chapter 9 Cotton Fibers 521

Philip J. Wakelyn, Noelie R. Bertoniere, Alfred D. French, Devron P. Thibodeaux, Barbara A. Triplett, Marie-Alice Rousselle, Wilton R. Goynes, Jr., J.Vincent Edwards, Lawrance Hunter, David D. McAlister, and Gary R. Gamble

Chapter 10 Regenerated Cellulose Fibers 667

Richard Kotek

Chapter 11 Cellulose Acetate and Triacetate Fibers 773

Herman L. LaNieve

Chapter 12 Acrylic Fibers 811
Bruce G. Frushour and Raymond S. Knorr

Chapter 13 Aramid Fibers 975
Vlodek Gabara, Jon D. Hartzler, Kiu-Seung Lee, David J. Rodini, and H.H. Yang

Index 1031

1 Polyester Fibers

Michael Jaffe and Anthony J. East

CONTENTS

1.1 Introduction 2
1.2 PET History 3
1.3 PET Polymerization 3
1.3.1 Monomer Production 3
1.3.2 Polymerization 4
1.3.3 Characterization of Poly(ethylene Terephthalate) Chip 5
1.3.4 PET Processing—Melt Spinning 5
1.3.5 PET Processing—Drawing 10
1.3.6 PET Yarn after Processing—Heat-Setting and Bulking 12
1.3.7 Polyester Yarns for Specific Applications 12
1.3.8 Physical Properties of PET 13
1.4 Other Polyesters 14
1.4.1 Polyester Fibers Based on Terephthalic Acid 14
1.4.2 High-Performance Polyester Fibers—PEN and LCPs 15
1.4.3 Fibers from Main-Chain Thermotropic Polyesters—LCPs 15
1.4.3.1 Chemical Structure of LCPs 15
1.4.3.2 Processing of Thermotropic Polyesters 16
1.4.3.3 Structure–Property Relationships 17
1.5 Biodegradable Fibers 18
1.6 Modification of Polyester Fibers—Specific Solutions for Specific Applications 19
1.6.1 Spin Finishes 19
1.6.2 Tire Cord 19
1.6.3 Low-Pill Staple Polyester 19
1.6.4 Noncircular Cross-Section Fibers 20
1.6.5 Antistatic and Antisoiling Fibers 20
1.7 Dyeing Polyesters 21
1.7.1 Introduction 21
1.7.2 Disperse Dyes 21
1.7.3 Anionic and Cationic Dyes for Polyester 22
1.7.4 Mass Dyeing 22
1.8 Bicomponent Fibers and Microfibers 23
1.8.1 Side–Side Bicomponent Fibers 23
1.8.2 Core–Sheath Bicomponent Fibers 24
1.8.3 Multiple Core Bicomponent Fibers 24
1.8.4 Hollow Fibers 24

1.9 Novel Fiber Forms 25
1.9.1 Microfibers 25
1.9.2 Melt-Spinning Microfibers 25
1.10 World Markets and Future Prospects for Polyester Fibers 26
References 26

1.1 INTRODUCTION

Polyester fiber, specifically poly(ethylene terephthalate) (PET), is the largest volume synthetic fiber produced worldwide. The total volume produced in 2002 was 21 million metric tons or 58% of synthetic fiber production worldwide. The distribution of synthetic fiber production by chemistry is shown in Figure 1.1 [1].

If one assumes the total production is a single 5 denier per filament (dpf) (~20 μm in diameter) filament, the total length would be about 0.01 light years (~10^{14} m) or the equivalent of about one million trips to the moon. While other polyesters are commercially produced in fiber form—poly(ethylene naphthalate) (PEN); poly(butylene terephthalate) (PBT); poly(propylene terephthalate) (PPT); and poly(lactic acid) (PLA); thermotropic polyester (liquid crystalline polymer (LCP)—these are of insignificant volume compared to PET. Hence this chapter focuses primarily on PET.

The reasons for the dominating success of PET fiber are:

- Low cost
- Convenient processability
- Excellent and tailorable performance

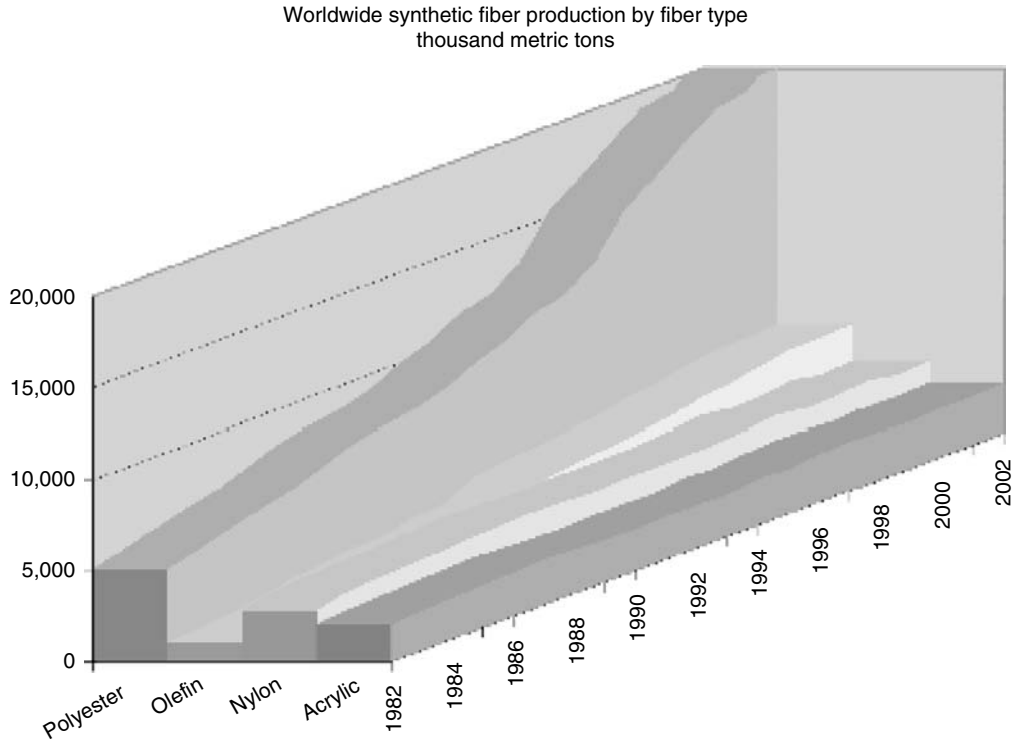

FIGURE 1.1 Worldwide fiber production.

The basis of the low cost lies in the high efficiency of the conversion of mixed xylenes to terephthalic acid, the melting temperature (280°C) being well within the range of commercial heating fluids, and the glass transition temperature (75°C), allowing the convenient stabilization of spinline- or drawline-introduced morphology and molecular orientation. The excellent performance results from the ability to accurately control fiber morphology (distribution and connectivity of crystalline and noncrystalline load-bearing units), allowing the balance of thermal and dimensional stabilities, transport, and mechanical properties to be controlled. Over the decades, since its introduction in the 1960s, polyester technology has evolved into a large number of products that range from cotton-blendable staple to high-performance tire cord. It is likely that PET will continue to dominate as the synthetic fiber of choice in future, although profitability has constantly eroded with time and production has shifted from the United States and Europe to Asia.

Polyester fibers have been reviewed in many publications [2–4], most recently by East [5], and the reader is directed to these publications for additional details. This work provides the reader with an overview of polyester fiber technology, sufficient to allow the vast and detailed open and patent literature related to polyester fibers generally, and PET fiber specifically, to become more meaningful.

1.2 PET HISTORY

The development of PET fiber began with the pioneering work on condensation polymers led by W.H. Carothers of DuPont in the 1930s [6].

Carothers focused on aliphatic polyesters and the resulting properties were poor compared to the aliphatic nylons that were simultaneously explored by his group. Much improved fiber performance was achieved in the early 1940s by the team comprising Whinfield and Dickson [7], Calico Printers Association Laboratory in Great Britain. Their work focused on aromatic–aliphatic polyesters from terephthalic acid (TA) and ethylene glycol. The same studies examined other aliphatic–aromatic polyester compositions, including PBT, PPT, and PEN. Commercialization of PET was rapid after World War II with the introduction of Terylene in Great Britain by ICI and the introduction of Dacron in the United States. Other products soon followed and PET successfully entered the textile market as both filament yarn and staple, and the industrial market as a rubber reinforcement filament yarn, primarily for use in the sidewalls of passenger car tires. Key properties were wash-and-wear characteristics in textiles and high modulus, coupled with excellent modulus retention, in industrial applications. The detailed review of Brown and Reinhart [8] described this history.

1.3 PET POLYMERIZATION

PET is the condensation product of terephthalic acid and ethylene glycol. The key to successful PET polymerization is monomer purity and the absence of moisture in the reaction vessel. PET polymerization has recently been reviewed in detail by East [9].

1.3.1 Monomer Production

The enabling technological breakthrough that allowed for the cost-effective polymerization of PET was the development of low-cost, pure TA from mixed xylenes by the Amoco company in the mid-20th century [10,11]. An alternative to TA, and the monomer of choice before the availability of low-cost TA, is dimethyl terephthalate (DMT). While direct esterification of TA is the preferred method of PET synthesis, ester interchange between DMT and ethylene glycol is still utilized in some PET manufacture, partially because of local choice and partially

because DMT is a product of polyester recycling by methanolysis or glycolysis [12]. The second monomer, ethylene glycol, is a major material of commerce, produced by the oxidation of ethylene followed by ring opening with water [13]. The large-scale production of all PET monomers assures low-cost polymers and makes competition from new compositions of fiber-forming polymers very difficult.

1.3.2 Polymerization

The first stage of PET polymerization is, in essence, the production of bishydroxyethylterephthalate (BHET). In the direct esterification of TA, this reaction

$$\begin{aligned} &HOOC-C_6H_4-COOH + 2HOCH_2CH_2OH \\ &\quad \rightarrow HOCH_2CH_2OCO-C_6H_4-COOCH_2CH_2OH + 2H_2O \end{aligned} \tag{1.1}$$

actually results in a mixture of low amounts of free BHET with a variety of PET oligomers. Water removal is critical to the ultimate achievement of high molecular weights. Similarly, in the first stage of the ester interchange process, BHET is formed along with a mixture of PET oligomers, i.e.,

$$\begin{aligned} &CH_3OCO-C_6H_4-COOCH_3 + 2HOCH_2CH_2OH \\ &\quad \rightarrow HOCH_2CH_2OCO-C_6H_4-COOCH_2CH_2OH + 2CH_3OH \uparrow \end{aligned} \tag{1.2}$$

The reaction catalysts for the ester interchange reaction have been the subject of intense research for many years and many catalyst compositions are found in the patent literature [14–16]. The introduction of ester interchange catalysts requires the killing of these catalysts later in the polymerization sequence as they are equally effective as depolymerization catalysts.

The next step in the polymerization is the melt polymerization stage. In this reaction step, an ester interchange reaction occurs between two molecules of BHET to split off a molecule of glycol and build polymer molecular weight. The reaction must be catalyzed, and antimony trioxide (Sb_2O_3) is almost universally the moiety of choice. High vacuum is applied to push the reaction to high molecular weights. Typical melt polymerization temperatures are 285°C or higher, and viscosities are on the order of 3000 poise, making uniform stirring and the imparting of a constant shear history across the polymerization mixture difficult, although the power requirement to the stirrer thus becomes a useful QC tool. Recent variations of this method have been patented by DuPont (elimination of vacuum) [19–21] and Akzo (new, nonantimony-based catalyst) [17,18]. As neither DuPont nor Akzo has produced PET fiber in 2005, it is unclear whether these apparent process improvements are actually utilized.

After achieving molecular weight targets, the polymer may be extruded into strands and cut into chips for subsequent melt spinning (batch process) or fed directly into a spinning machine and converted to fiber (continuous process—CP spin-draw). In the case of chipped polymer, the molecular weight can be further increased through solid-state polymerization. In this process, thoroughly dried PET chip is first crystallized at about 160°C to prevent the amorphous as-polymerized chip from sticking together (sintering), and then heated just below the melting point under high vacuum and extreme dryness to advance the molecular weight upward to values of inherent viscosity (IV) of 0.95 (textile grade chip has an IV of about 0.65). [22,23]. The effects of the process thermal history of PET chip and fiber have been extensively studied and are conveniently monitored by thermal analysis techniques. Jaffe et al. [24] have reviewed the thermal behavior of PET and described the expected response of PET to process history in detail.

A variety of side reactions and end-group-induced reactions can lower the thermal stability and cause degradation of PET during spinning. The formation of diethylene glycol through the coupling of two hydroxyl ends from the glycol ends (or BHET ends) by dehydration, forming a diethyleneglycol (DEG) unit in the chain, is especially troublesome. DEG is a foreign unit in the backbone, although it does not directly affect the polymer chain length. This unit reduces crystallinity and lowers the glass transition, thermal stability, and hydrolytic stability of the polymer. It is impossible to completely eliminate DEG formation and about 1.0–1.5 mol% of DEG is always present. Depression of the polymer melting point is easily measured by differential scanning calorimetry (DSC), and this parameter provides an accurate measure of DEG content [24]. Finally, any melt-processed PET always has some cyclic trimer content, which, while not a direct problem for polymer performance, does tend to exude during processing and may cause process upsets.

In reality, commercially produced PET is always made by a continuous process involving a number of linked vessels between which the polymer is continuously pumped until the final product specifications are achieved. While some process descriptions have been published [25], most processing details are highly protected as proprietary information. The process usually involves at least four steps, i.e., an initial esterifier followed by a series of three polymerizers, each designed to further advance the polymer molecular weight. Extreme care is taken to promote within and between batch uniformity, eliminate dead zones where polymer may degrade, and remove all low molar mass reaction products such as glycol or water. A typical PET polymerization process is shown in Figure 1.2.

1.3.3 Characterization of Poly(ethylene Terephthalate) Chip

PET chip or representative samples of CP spin-draw polymer are conveniently characterized as by their molecular weight, cleanliness, and thermal behavior. Molecular weight is characterized by the polymer intrinsic viscosity [η], usually in halogenated solvents; the best halogenated solvents are hexafluoroisopropanol/pentafluorophenol mixtures. Intrinsic viscosity is related to molecular weight by the Mark-Houwink equation, i.e.,

$$[\eta] = KM_{\mathrm{v}}^{\alpha}$$

where K and α are solvent-dependent, but K is about $1.5\times10^{-2} - 1\times10^{-1}$ and α is about 0.60–0.85 [26]. High molecular weight or high crystallinity can make polymer dissolution difficult and be responsible for erratic results. Polymer cleanliness is measured microscopically (optical techniques, polarized light microscopy) and is often expressed in units such as the number of black specks or the number of gels per gram of polymer. Acceptable values are determined empirically and are meaningful only in a known process context. Thermal parameters are conveniently monitored by DSC, allowing a quick assessment of DEG content, crystallinity, etc.

1.3.4 PET Processing—Melt Spinning

The melt spinning of PET has been extensively treated in the patent literature, but less in the open literature [27], although the recent chapters by Bessey and Jaffe [28] and Reese [2] are good introductions to the process. We will concentrate here on how changes in the key process variables of spinline stress and temperature profile affect assembly at the molecular level (morphology), and, in turn, how the morphology affects the resulting performance of the yarn. The relationships described here are equally valid for all semicrystalline polymers; LCPs will be treated separately. The average value of key properties and the standard deviation

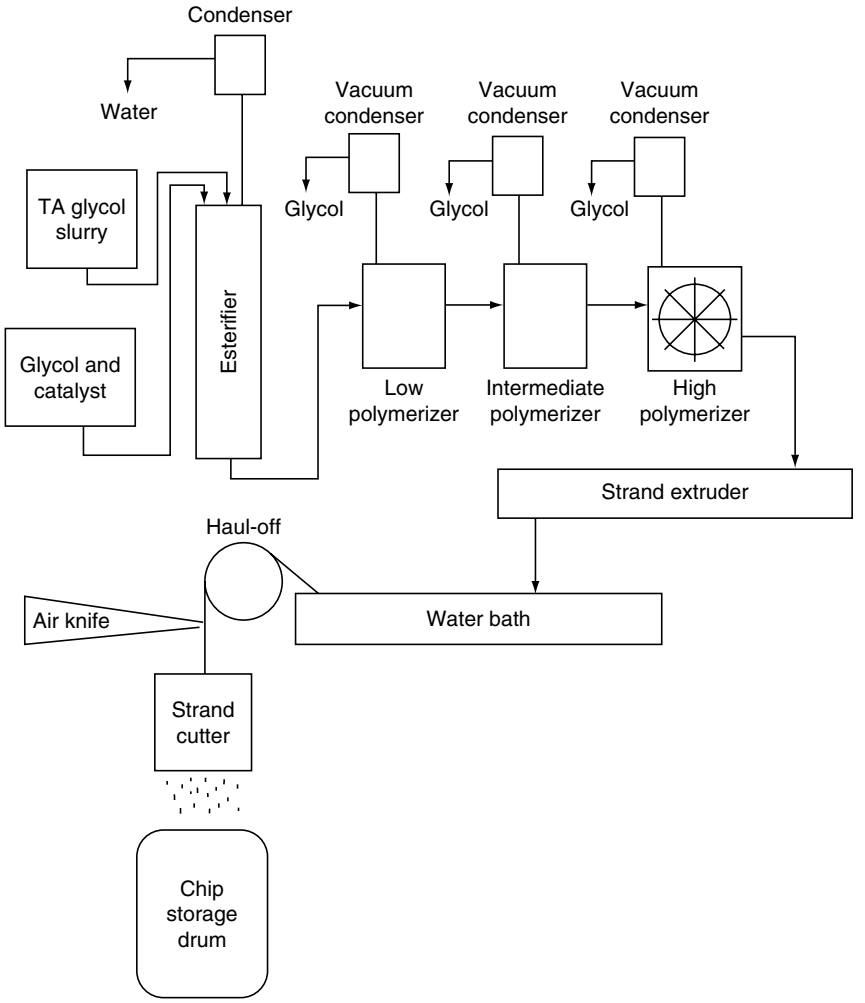

FIGURE 1.2 Typical PET production process.

associated with the mean value must be controlled for fiber products to have commercial value. In general, variation in properties, hence variation in morphology, must be controlled to about 10% for the yarn to be commercially acceptable. Variation means differences between filaments in a yarn or along a given filament. The frequency of variation is also critical; high frequency changes that may be averaged over a critical use length are, in general, more acceptable than a smaller variation along or between filaments that occurs at a lower frequency.

Polymer is introduced into the manifold of the spinning machine either as a dried chip or as produced by the CPU. The manifold may feed as few as one or as many as 200 separate spinnerets and is designed to keep the directed polymer streams as uniform as possible in shear and thermal history. The PET spinning temperature is typically between 280 and 300°C; local shear heating may increase this temperature by as much as 10–15°C. The molten polymer stream is then fed through metering pumps to the spinning pack (assembly that starts with a series of filters and ends at the spinneret—see Figure 1.3). The spinneret consists of five (hosiery yarn) to several thousand holes, typically ranging from 180 to 400 μm in

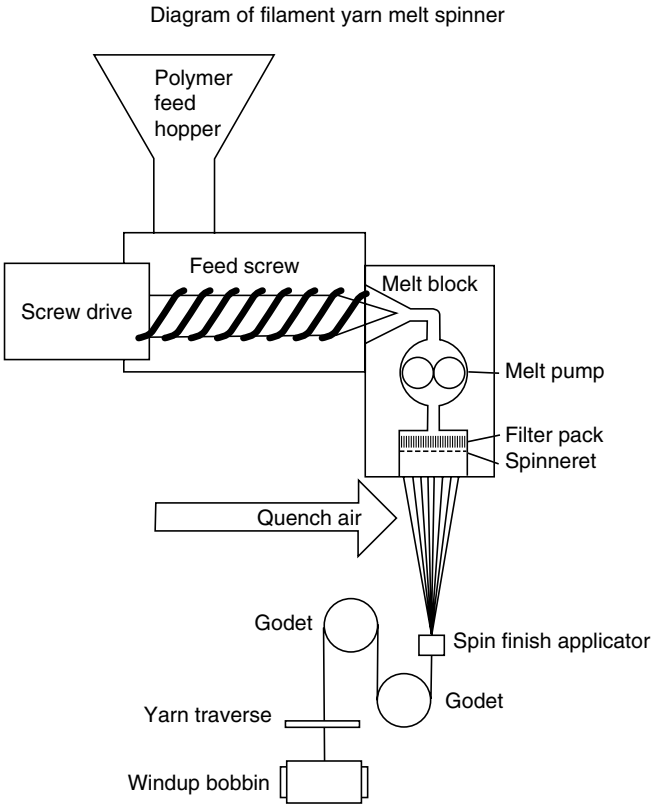

FIGURE 1.3 Key elements of polyester filament yarn melt-spinning machine.

diameter. Pack and spinneret designs are the subject of specialized expertise and the reader is referred to the open and patent literature for the depth of engineering detail available on these subjects [29]. The purpose of pack and spinneret is to insure that filtered (clean) polymer is fed to each hole of the spinneret as uniformly as possible. Passage through the spinneret subjects the polymer to a complex rheological environment (see, for example, the work of Denn [30]), resulting in local increases of molecular orientation and a distribution of orientation between the spinneret wall and center line. On exiting the spinneret, the combined effects of surface tension and relaxation of molecular orientation result in die swell (increase of the filament diameter to greater than the spinneret hole diameter).

From a molecular point of view, the starting polymer melt is best visualized as an entangled network, characterized by the polymer molecular weight, molecular weight distribution, the entanglement density, and the average chain length between entanglements. This is shown diagrammatically in Figure 1.4.

The processes that occur in the spinline, between the exit of the polymer from the spinneret and the point of stress isolation on the first godet or roller at the base of the spin line, involve the changing of this fluid network to the solid-state molecular chain topology of the filament. Within a distance of 3–5 m, and under the influence of an applied force (take-up tension) and quench media, at speeds in excess of 100 miles per hour—less than 0.01 sec residence time—the fiber is transformed from a fluid network to a highly interconnected semicrystalline morphology, characterized by the amount, size, shape, and net orientation

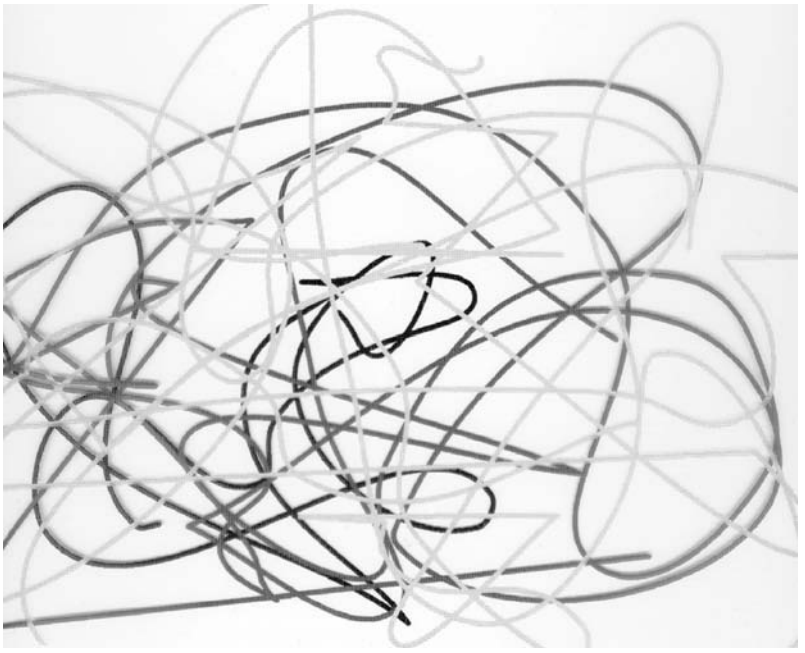

FIGURE 1.4 Diagramatic representation of an entangled polymer melt.

(with respect to the fiber or long axis) of crystalline units, and the orientation of spatial distribution of noncrystalline areas. All of these units are interconnected by molecules that traverse more than one local region (tie molecules) of the load-bearing elements of the fiber structure.

It has been noted [31] that the crystallization rate of polymers increases by up to six orders of magnitude when the crystallization event occurs when the polymer is under an applied stress rather than in a quiescent state. This large increase in crystallization rate is accompanied by a change in crystal habit, the shape of the crystalline phase produced transformed, over a narrow stress regime, from a spherulitic (spherically symmetrical) to a columnar habit (see Figure 1.5).

This transition is surprisingly sharp—occurs at a stress of about 0.1 g/d. Increasing the spinline stress increases the number of rows and decreases the diameter of the fibrillar structure. As the fibrils are stable only in the presence of the spinning stress, they may or may not be visible in the final fiber morphology. A useful way of conceptualizing the process is to divide the spinline into three regions, namely:

- Region 1. Increase local and global molecular orientation
- Region 2. Fibril formation at points of maximum orientation (transient mesogen, mechanical steady state)
- Region 3. Fibril decoration (folded chain crystal growth)

A cartoon of this model of morphology and molecular chain topology development in melt spinning of PET is shown in Figure 1.6.

In Region 1, the spinline stress leads to filament drawdown, causing a net increase of molecular orientation of the molten and amorphous polymers. A consequence of this stress is

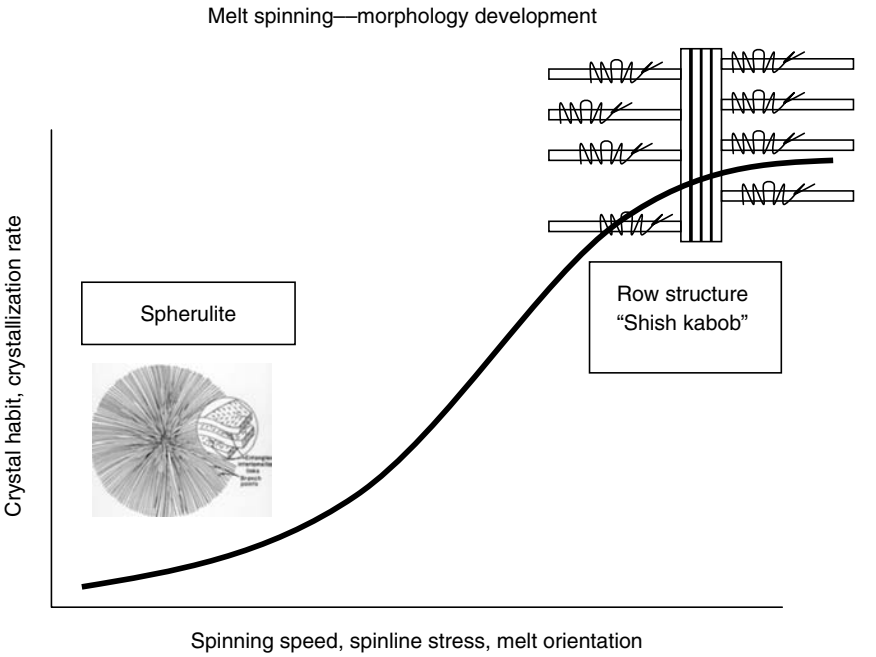

FIGURE 1.5 Morphology development in melt spinning as a function of key spinning parameters.

the disentangling of some of the starting network chains and the increase in the local molecular chain orientation in the proximity of remaining entanglements. As these bundles of locally oriented chains grow in aspect ratio, they satisfy the conditions for nematic phase formation [32–34], leading to a biphasic array comprised of fibrillar mesogenic structures

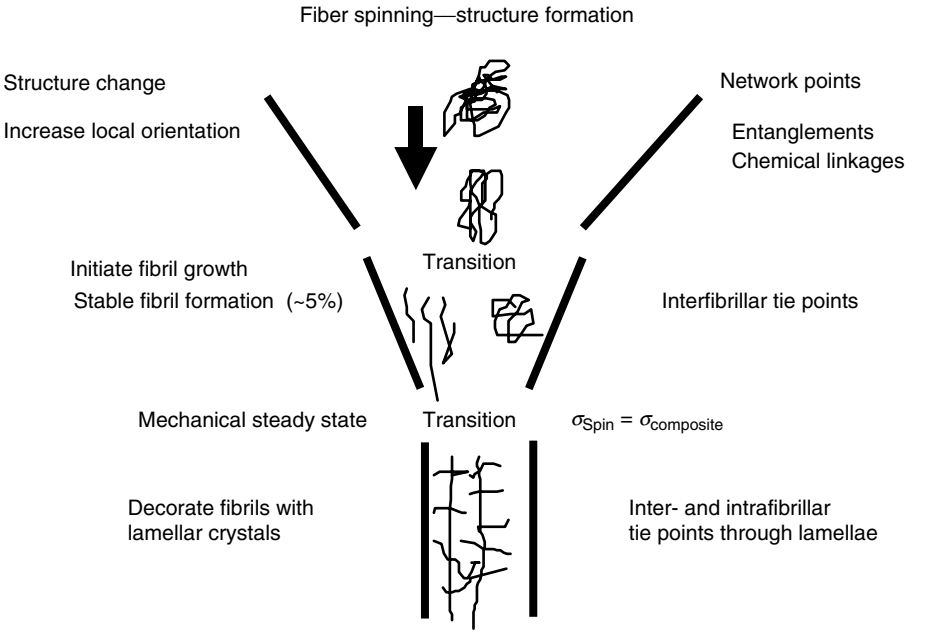

FIGURE 1.6 A cartoon of morphology development in PET melt spinning.

sitting in a lesser oriented amorphous matrix. When the spinline stress is completely supported by these fibrillar structures, the matrix chains are able to relax and the conditions for fibril formation are no longer extant. As one enters the lower temperature ranges, the fibril acts as an effective high nucleation density for lamellar crystal overgrowth of the fibrils, leading to increases of up to six orders of magnitude in the effective crystallization rate. Fibrils may or may not be evident in the final structure, but the high orientation of the wholly semicrystalline structure is always evident. The transient fibrillar structures act as the template for all further structure formation. It is also evident that molecular chains can participate in more than one element of the structure; these tie molecules provide the stress transfer elements as subsequent fiber deformation [35]. Conceptually, three types of tie molecules are possible in the model: interfibrillar, interlamellar (between lamellae on a given fibril or between lamellae on different fibrils), and between fibril and lamella. It is the tie molecule distribution, combined with the remaining entanglement distribution, that defines the residual draw ratio of the fiber structure [36].

The detailed proof of this conceptual model is difficult experimentally, although it is generally supported by the existing experimental data and melt spinning process model. The overall veracity of the model is less important than the utility of the model in predicting process–structure–property relationships. Important implications of the model are as follows:

- The order of molecular chain orientation and crystallization steps in fiber spinning is critical.
  - The formation of a transient fibrillar mesophase is the template for all further morphology development and defines the nucleation density for subsequent crystallization.
- As chain orientation prior to crystallization is increased, the load-bearing aspects of the crystalline network produced also increases, while the noncrystalline load-bearing elements of the structure decrease.
  - Leads to the decoupling of molecular orientation responsible for increased modulus and strength, from oriented chains responsible for entropic shrinkage, allowing for high modulus low shrinkage fiber products.
- The network defined in spinning remains the template for structure formation in all subsequent processing steps.

The melt spinning of all semicrystalline polymers can be fit into the general framework described above. Details of specific PET melt spinning processes are well documented in the chapter by Reese, Bessey, and Jaffe, or in the papers of Ward. The structural state of the spun yarn, while complex, is often described by a single parameter: the spun yarn birefringence, an average measure of orientation. Jaffe has shown that the spun yarn shrinkage is an excellent predictor of the remaining yarn draw ratio as shown in Figure 1.7 [33], where DRmax is defined as the highest stable draw ratio available to a given spun yarn.

1.3.5 PET Processing—Drawing

Despite the orientation introduced during spinning, additional increases in molecular order are often brought about by a separate drawing process. Fiber-forming polymers show a phenomenon called "cold drawing on stretching," provided the molecular weight is sufficiently high to prevent premature breakage. Undrawn fiber produces a distinct "neck," which localizes the point of drawing at which deformation and crystallization occur, at once evident from the change in opacity in the drawn filament due to its optical anisotropy. As-spun PET fibers can be amorphous or crystalline, depending on the spinning conditions (see Figure 1.5).

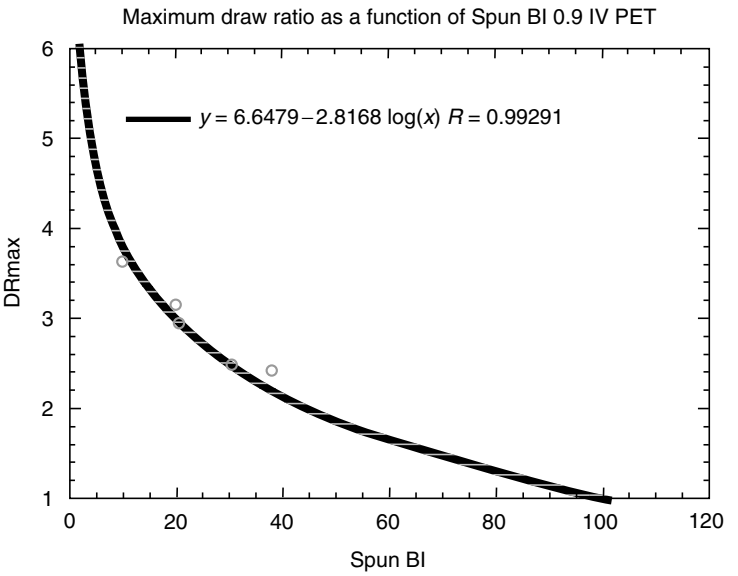

FIGURE 1.7 Variation of maximum draw ratio of high IV PET yarn as a function of molecular orientation imparted during spinning.

All fibers become more crystalline and better oriented when drawn. Faster crystallizing polymers like PBT, PPT, or nylon-6,6 always form crystalline spun fibers, although they often need a drawing stage to induce and complete crystallite orientation. The combination of molecular entanglements and the presence of polymer chain crystallites lock this orientation into place. This, in turn, affects such parameters as tenacity, modulus, elongation at break, and heat-shrinkage. The fiber must be drawn close to its maximum draw ratio for the drawing to be effective. Draw ratio is the ratio of yarn feed velocity to draw-roll haul-off speed: this ranges from about 1.5 to 6.0. The draw point is the actual place where fiber necking takes place and it must be stabilized. In early processes, this was done by a heated metal snubber pin around which the yarn was passed. The pin temperature was set to about 10°C above T_g, i.e., about 85–90°C for PET process. However, this alone was not sufficient and the drawn yarn had an unacceptable degree of heat shrinkage. The latter defect was prevented by heat-setting the fiber by passing it over a long hot plate at about 130–140°C, well above the effective T_g (~125°C) of the drawn, crystallized yarn. This simple system was adequate when draw speeds were low (500 m/min), but, as draw speeds rose considerably, it was necessary to use separately heated feed rolls and draw rolls to achieve the same effect at much higher speeds. The heated rolls allowed for longer yarn contact times for thermal transfer, with the yarn wrapped several times around the roll and over an attendant idler roll. The draw ratio has a major effect on yarn elongation and tenacity. High draw ratios give high-tenacity yarns with higher yarn moduli and lower extensions to break as expected; low draw ratios give lower tenacities with higher extensions. Jaffe [34], Ward [35], and others showed that a consequence of high-speed spinning is to shift the load supporting of the network chains of the fiber structure from noncrystalline to crystalline regions of the fiber morphology. This limits the draw ratio available to fully orient these fibers, resulting in fibers with nearly equivalent tensile properties, but significantly lower shrinkage at an elevated temperature.

1.3.6 PET Yarn after Processing—Heat-Setting and Bulking

Drawn filament yarn can be treated in a number of ways. It may simply be wound onto a yarn package, twisted on a ring frame, or sent for a yarn bulking process such as false-twist bulking. One of the major breakthroughs in the 1970s was the introduction of high-speed yarn winders, which gave large cylindrical yarn packages (up to 15 lb of yarn) and ran at 3000 m/min (113 mph). The yarn traverse was a major technological enabler, as without a reliable high-speed traverse to keep pace with the windup speeds, the process was not runnable (i.e., conversion efficiency of polymer to salable yarn was <~90%). The problem was that the traverse guide had to reverse instantaneously and reliably at the end of each traverse stroke. Any "dwell" would cause a buildup yarn at the bobbin edges and the yarn would simply slough off. Engineering solutions were eventually found and nowadays windup speeds can be 6000 m/min or even higher.

Many apparel yarns need to be textured or "bulked" to give desirable esthetic properties, particularly for cotton blends and women's wear markets. This may be done during drawing (draw-bulking) or in a separate process. The number of bulking processes is numerous and for those wanting more detailed descriptions, a reference to a specialist publication is provided [37]. The principle of the so-called "false-twist" bulking is to create minor side-to-side variations in molecular orientation across a given yarn, causing the yarn to bend during controlled thermal shrinkage to create a 3D structure with a bulky feel. The process entails running a continuous yarn through a device that twists it in the middle. Since no net twist is applied, it is called a "false" twist; the yarn ahead of the machine is wound up and the false twist escapes, but the yarn behind the twister passes through a long tube heated above fiber T_g, so that, as it exits, the false twist is "set" into the yarn. When this twist tries to spring back and unwind, it causes the treated yarn to bulk up into a spiral crimp. The degree of twist is quite high, several hundred twists per meter, so that, if the yarn is running at productive speeds, the rotation of the twister device has to be extremely high, of the order of 1 million rpm. This produces formidable mechanical problems. One ingenious solution is the friction-bulking process, in which the yarn itself is twisted either by running against the internal surface of a rotating friction bush or by contact with the edges of a series of friction disks. Since the yarn diameter is very small compared to that of the bush or the disk, a very high "gear-up" ratio is achieved and the friction device can rotate at far more reasonable speeds. A typical texturing process is shown in Figure 1.8.

Bulked continuous filament (BCF) carpet yarns are heavy decitex bundles of fiber that are bulked by passage through a turbulent blast of steam or hot air well above T_g. The turbulence blows the yarn about and entangles the filaments, and then heat sets them into place, giving them a permanent crimp. Polymers like PET do not have very good resilience as carpet fibers, but PTT ($T_g = 45°C$) lends itself very well to the BCF process and has excellent resilience [38].

1.3.7 Polyester Yarns for Specific Applications

For industrial use, high-tenacity yarns, such as the tire cord, have to be drawn under conditions where low heat shrinkage, low extension, and high modulus products are produced. In fact, a tire cord is a highly specialized product, and complete integrated continuous polymerization spinning and drawing plants (cp-spin-draw) have been developed. The process is little discussed in the open literature and the reader is directed to the patents of DuPont, Fiber Industries, and Allied Chemical Corporation (none of these companies currently exist as fiber producers).

The demands of staple fiber are different from those of filament yarns. Staple fiber is a continuous filament cut into short lengths in centimeters. Staple fibers are discontinuous and are crimped and chopped to the desired staple fiber length to blend at the carding stage with cotton (short staple), wool (long staple), or other natural fibers. The raw polyester fibers are

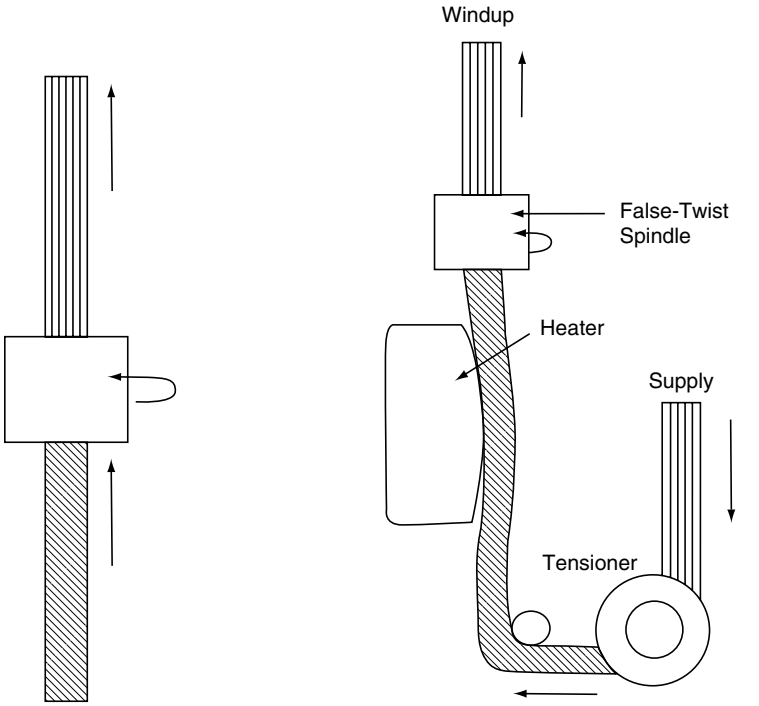

Diagrammatic representation of the insertion of false-twist in a moving yarn. The sketch shows that the twist is restricted to the yarn entering the false-twist spindle, and that it leaves the twist spindle twist-free.

Sketch illustrating the principle of false-twist texturing. Note the heater to set the twist inserted below the false-twist spindle, and the untwisted yarn leaving the false-twist spindle for windup.

FIGURE 1.8 Typical polyester yarn bulking process, false-twist texturing.

melt-spun through many hundreds of holes in a staple spinneret, and hauled off via a godet, but not wound up in the conventional way. Instead, they are deposited via an air ejector loosely into a large drum or "yarn can." When the yarn can is full, fiber bundles from many cans are combined into a thick bundle of fibers called a "tow." These tows may have a yarn count of several million decitex. The thick bundle of fibers is then drawn on a massively constructed drawframe (because the mechanical forces involved are heavy) using multiple sets of draw rolls and feed rolls. The yarn is heat-set in a steam-heated hot box, because this method gives the best thermal transfer to the individual fibers in the tow. The drawn tow then passes to a crimper, often of the stuffer-box type. The tow is overfed into a heated wedge-shaped box with a sprung lid, where it is compressed to form a concertina-type crimp. The bulked tow is finally cut to the desired staple length using a continuous staple cutter. The loose cut fiber is then transferred by an air handler to a bin and compressed into bales. A schematic diagram of a staple line is shown in Figure 1.9.

1.3.8 Physical Properties of PET

PET is a semicrystalline polymer and its physical parameters have been repeatedly determined over many years. The summary of the most recent widely accepted values [39] is shown in Table 1.1.

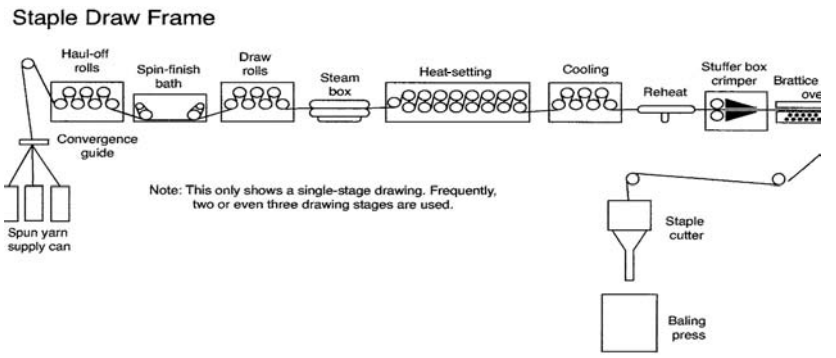

FIGURE 1.9 Schematic diagram of staple spinning line.

1.4 OTHER POLYESTERS

1.4.1 Polyester Fibers Based on Terephthalic Acid

PBT was examined in detail in the early 1950s both in Europe and the United States as a textile fiber. It had many attractive properties compared to PET; it could be melt-spun at lower temperatures and, owing to its polymer chemistry, it was inherently whiter than PET. As a fiber, it was much more elastic and had excellent resilience and recovery from small deformations. It dyed easily with disperse dyes at the boil, not needing to be dyed under pressure like PET. PBT fiber resisted the common photo-oxidative yellowing and it seemed to have a bright commercial future. However, the reason why PBT never achieved the success of PET in textiles was because 1,4-butanediol is significantly more expensive than ethylene glycol. Also, PBT did not have the pleat-retaining properties of PET in blends. However, it succeeded as a polyester carpet fiber, where its resilience and ease of dyeing were assets, although it had to compete against nylon.

Another of the pioneer polyesters was polytrimethylene terephthalate (PTT). This was recognized very early on as a fiber with outstanding resilience. PTT has been known in many ways as an ideal textile fiber for over 60 years. It remained on the shelf until, in the last decade, it became a commercial product owing to two new routes to the crucial intermediate 1,3-propanediol. One route is petrochemically derived (hydroformylation of ethylene oxide), while the other is a fermentation route using corn sugar to make 1,3-propanediol directly using genetically modified bacteria [40].

TABLE 1.1

Crystal habit	Triclinic: one polymer chain per unit cell
Cell parameters	$a = 0.444$ nm; $b = 0.591$ nm; $c = 1.067$ nm, $\alpha = 100°$; $\beta = 117°$; $\gamma = 112°$
Cell density	$1.52\,g/cm^3$
T_m (DSC)	260–265°C
ΔH_f	140 J/g; 33.5 cal/g
T_g (solid chip)	78°C (DSC)
T_g (drawn fiber)	120°C (dynamic loss)
Specific gravity	1.33 (amorphous, undrawn), 1.39 (crystalline drawn fiber)

Eastman Kodak introduced a new polyester as a staple fiber called "Kodel" in 1958. A new diol was introduced to derive a patent-free composition of matter; a mixture of *cis*- and *trans*-1,4- cyclohexanedimethanol made by the exhaustive hydrogenation of dimethyl terephthalate. This polyester had a higher T_g than PET and also a higher melting point, but it was successful enough to find a market. In recent years, the polyester has found use in polyester carpets [41,42].

1.4.2 High-Performance Polyester Fibers—PEN and LCPs

The polyester derived from ethylene glycol and naphthalene-2,6-dicarboxylic acid was first discovered by ICI in the late 1940s [43]. It has a much higher T_g than PET and gives strong, high-modulus fibers, but the inaccessibility of the diacid was an insurmountable problem until recently. Now, firms like Amoco (now Solvay) are able to supply the dimethyl ester of 2,6-NDA, and the polymer (PEN) is increasingly used in high-performance polyester films and for high-softening-point blow-molded bottles and containers. Recently, Honeywell have started producing a high-performance PEN fiber under the name PENTEX. This absorbs UV light owing to the naphthalene ring. In Japan, stretch-blow-molded PEN bottles are used to package vitamins and baby food, which would otherwise be adversely affected by UV light.

1.4.3 Fibers from Main-Chain Thermotropic Polyesters—LCPs

It was recognized early in the development of polymer science that the tensile modulus of polymers should correlate with both the chemical and physical structures, and that maximum property levels would be achieved when all the molecular chain backbone bonds were lined up in the direction of measurement [44,45]. The all-aromatic main chain thermotropic polyesters are semirodlike molecules that naturally organize into nematic liquid crystal domains and many variants are commercially available in resin and fiber form (see literature and websites of Ticona and DuPont). The nematic state can be viewed as similar to "logs floating in a river," leading to ease of flow parallel to the molecular axis (low elongational viscosity) and an extended chain structure in the solid state. Hence, the nematic state in polymers brings both processing ease and high axial tensile properties. Figure 1.10 illustrates the processing of LCPs and the morphology produced, in contrast to conventional polymers such as PET or nylon.

All of the LCPs are composed of stiff, highly aromatic molecules and are characterized by a very high local molecular orientation in the solid state (orientation function >0.95). If processed into fibers, the local orientation is transformed to global. These globally oriented LCP fibers are further characterized by very high specific tensile properties and intrinsically low density when compared with metals, ceramics, and carbon. The highly anisotropic nature of these oriented LCP fibers, causing inherent weakness in shear and compression, limiting their use almost exclusively to applications in tension, is not shown in Figure 1.10. It should also be noted that, in the absence of global orientation, the tensile properties of the thermotropic polymers are similar to filled plastics, and compressive behavior is less of a critical issue.

1.4.3.1 Chemical Structure of LCPs

Thermotropic polyester backbone chemistry is characterized by a high degree of aromaticity, planarity, and linearity in the chain backbone. Most common moieties are *p*-phenylene, 1,4-biphenyl, and 2,6-naphthalyl moieties linked by ester or amide linkages. Polymers that form liquid crystal phases in the melt are thermotropic, whereas those that form liquid crystalline phases in solution are lyotropic. The all-aromatic polyester homopolymers tend to be intractable, decomposing at temperatures well below their melting points and insoluble in most

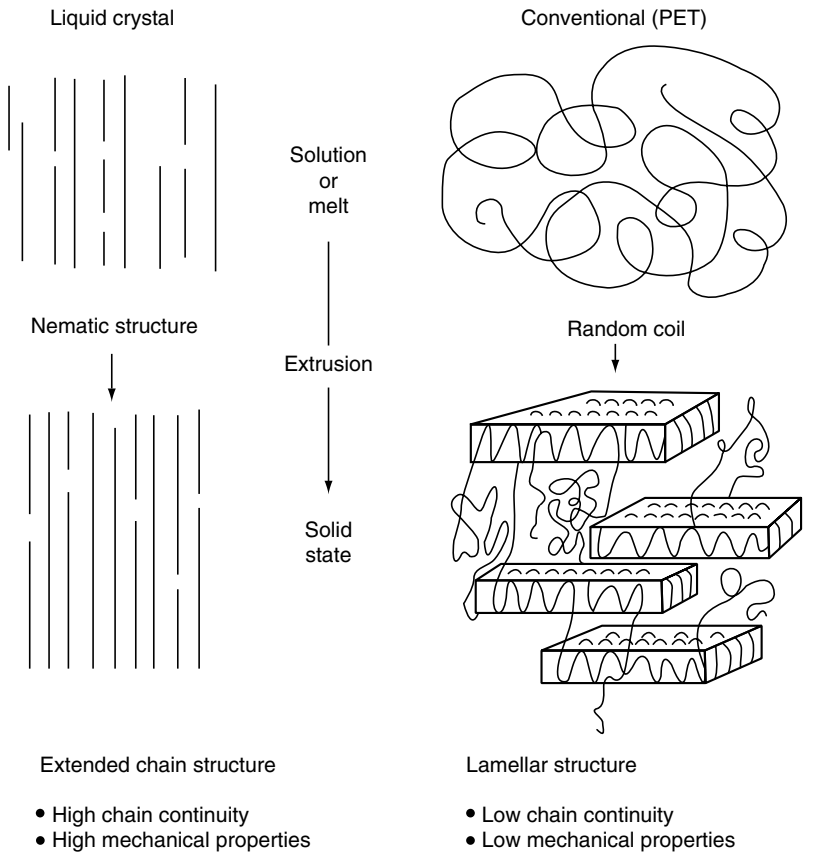

FIGURE 1.10 Structure development during spinning LCP versus PET.

solvents. Successful melting point reduction strategies include incorporation of comonomers to lessen crystal packing, decrease chain linearity, and increase chain-to-chain distance. All these approaches lower the polymer melting point and, when the melting temperature is reduced to below the polymer decomposition temperature, stable melt processing is possible. These approaches have led to large numbers of melt processable thermotropic polyesters. Typical LCP monomer and polymer chemistries of industrial importance are shown in Figure 1.11. Much of the cost of LCP fibers is the result of high monomer cost and limited monomer availability.

1.4.3.2 Processing of Thermotropic Polyesters

Thermotropic polyesters are melt-spun from the nematic phase and orient easily in an elongational flow field (moderate drawdowns/forces are sufficient). In the fiber case, highly oriented fibers form easily with an initial modulus close to theory—typical values range from about 70 to 150 GPa. Ward [46] has shown that the tensile modulus may be described by an "aggregate model," i.e., the modulus is a function of the inherent chain modulus, the molecular chain orientation, and the shear modulus (which described the stress transfer between chains). The tensile strength of LCP fibers follows the prediction of the "lag-shear model" [47]. Both the aggregate model and the lag shear model treat the LCP as though it

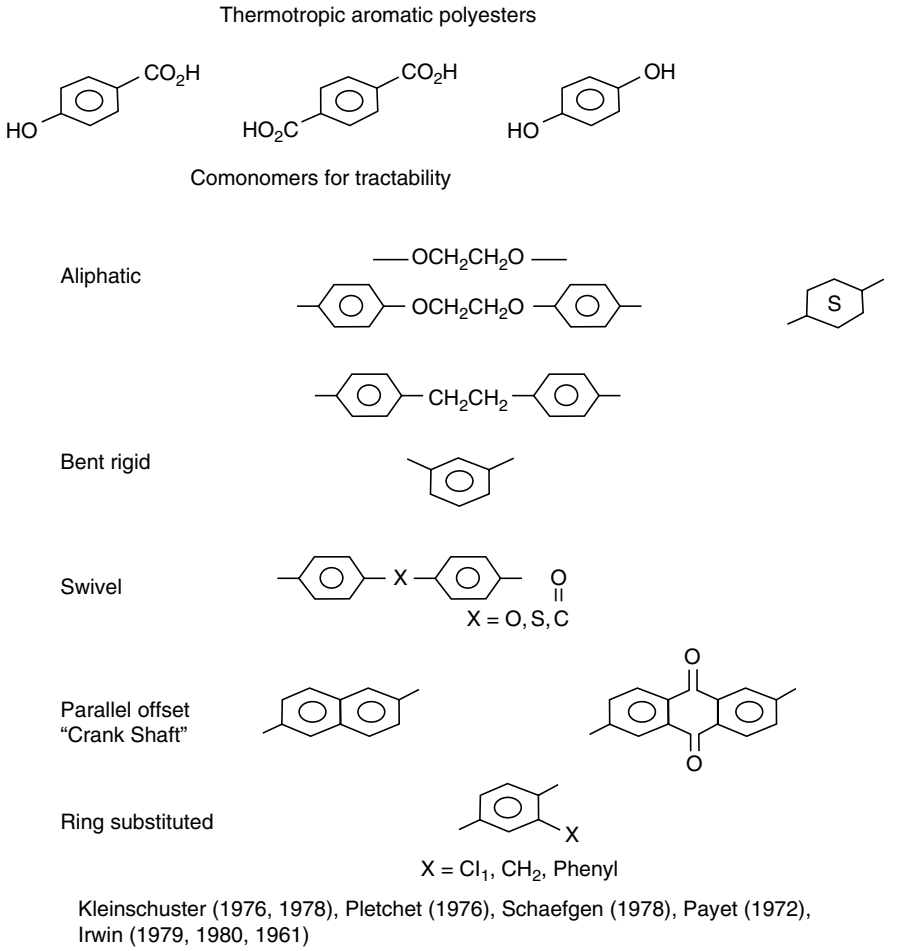

FIGURE 1.11 Typical LCP monomers.

were a self-reinforced short-fiber-reinforced composite. As-spun tensile strength of the thermotropic copolyesters tends to be on the order of about 1 GPa, and can be advanced to about 3 GPa by annealing free to shrink close to the melting temperature. Kinetics of strength improvement follow those of solid-state polymerization, leading many researchers to associate strength increases with molecular weight increase [48]. The failure of strength and elongation to increase in tandem suggests a mechanism of flaw reduction. Structural perfection and improved intermolecular bonding also play a role in the observed property improvement. Modulus increase during annealing is usually minimal with the thermotropic polyesters, unless structural perfection leads to an increase in overall molecular chain orientation.

1.4.3.3 Structure–Property Relationships

The unifying feature of all fibers spun from LCPs is the very high axial molecular orientation, which leads to extreme anisotropy of microstructure and mechanical properties. In the transverse direction, the strength is only about 20% of the axial strength and the modulus is typically less than 10% of the axial value. The microstructure of LCP fibers reflects the very

TABLE 1.2
Typical Fiber Mechanical Properties

Fiber	Tensile modulus (GPa)	Shear modulus (GPa)	Tensile strength (GPa)	Composite compression strength (GPa)
p-Aramid	70–130	1.8	3.2	240–290
Thermotropic copolyester	70–130	1.3	3.2	100–200
PBO	240		3.5	
M5	285	**5.2**	3.5	**500**
Carbon-HM370	370	17.5	2.2	700–900

high orientational molecular anisotropy, and may be described as a hierarchy composed of fibrillar structures ranging in diameter from microns to about 10 nm [49,50].

The properties of the most important LCP fibers are listed in Table 1.2. The key application areas for LCP fibers include hard armor (vehicles, helmets), soft ballistic protection (vests), cut protection (gloves), and a variety of composite uses that include honeycomb structure, pressure vessels, and rubber reinforcement. Ropes and cables find utility in the mooring of huge offshore structures such as oil-drilling platforms and the reinforcement and support of optical cables. LCP fibers also find specialty niche markets such as sails for racing yachts, specialized fishing nets, etc.

1.5 BIODEGRADABLE FIBERS

Biodegradable polyesters comprise a diverse field, but the most well-developed fiber (monofil) market is resorbable surgical sutures, which slowly disappear *in vivo* and do not need subsequent surgical removal. The first commercial samples were introduced in the early 1970s by Ethicon Corporation [51]. These sutures were monofil fibers spun from a copolymer of glycolic acid and D-lactic acid. Such aliphatic hydroxy acids are completely biocompatible and harmless: in U.S. Food and Drug Administration (FDA) terms, these materials are ''generally recognized as safe (GRAS).'' The properties of polyglycolide and stereochemically pure D- or L-polylactide polymers are quite good, and they form strong, highly crystalline fibers by melt spinning. Other biodegradable polyester fibers have been explored. Synthetic lactones such as ε-caprolactone and 2-dioxanone have been copolymerized with glycolide and lactide [52,53]. ICI began working on poly (3-hydroxybutyric acid) in the 1970s and later developed a copolymer with 3-hydroxyvaleric acid. Both polyhydroxyacids are stereochemically pure and give crystalline polymers, which can be processed into fibers and films. The interesting feature of these polymers is that they are made in very high molecular weight form by bacteria. Certain microorganisms, when cultivated and starved of nitrogen sources, synthesize aliphatic polyesters instead of proteins. The number average molecular weight of the as-harvested polymer can be several million daltons and it must be reduced to allow the polymer to be processed and fabricated. ICI (now Astra-Zeneca) first developed ''Biopol'' as one product and although others have been introduced by different companies, little has been targeted towards fiber end-use [54]. All the polyhydroxyacids are unstable and degrade on exposure or composting, but the degradation rate is very much governed by the ratio of hydrophobic/hydrophilic properties. While hydrolysis is important, catalyzed degradation by various lipases is also a factor.

1.6 MODIFICATION OF POLYESTER FIBERS—SPECIFIC SOLUTIONS FOR SPECIFIC APPLICATIONS

This wide topic covers both chemical and physical modifications to both the polymer and the fiber. We shall deal with only a few of the more important variations possible on this theme, but all are based on an understanding of polyester chemistry and processing described earlier in this chapter.

1.6.1 Spin Finishes

Fibers need to be treated with surface finishes or lubricants to allow high-speed processing. The various processing steps such as drawing, bulking, and textile processing would be impossible without these spin finishes because so many of them rely on specific frictional properties of the fiber (for example, friction twisting). Spin finishes are often water emulsions of various surface-active agents and lubricant oils; their formulation is a complex process and sometimes more of an art as well as a science. Finish application is made early in the process, before the cooling threadline from the spinner hits the first godet. Earlier, finish was applied from a lick roll rotating slowly in a bath. As spinning speeds increased, the finish was applied directly via a special hollow ceramic yarn guide as a neat oil formulation and metered at precise levels via a metering pump. Staple fiber is sprayed with emulsified finish or the whole tow may be immersed in large baths of finish. Some staple processes use a draw stage in a hot bath of finish.

1.6.2 Tire Cord

During the manufacture of tires (typically radial ply construction for passenger cars), the polyester tire core is subjected to drastic hydrolytic conditions. The rubber is molded into the basic tire shape and rubber vulcanization uses various accelerators, some of which cause severe aminolysis of the polyester chain. The process is run at 175°C in the presence of steam. While PET is fairly resistant to strong aqueous ionic base at moderate temperatures, nonpolar bases like ammonia, hydrazine, and simple aliphatic amines can easily diffuse into the PET structure and cause aminolytic breakdown [55].

To maintain the high strength engineered into the tire cord, it is essential that the IV (molecular weight) drop be minimized. The rate of degradation of the tire cord is directly related to the level of free COOH groups on the chain ends. This reaction is autocatalytic under vulcanization conditions, and reduction from their usual level (about 40 micro equivalents per gram of fiber) improves in-rubber stability. For some years, tire cord manufacturers employed a process in which the yarn was treated with epoxy compounds such as phenyl–glycidyl ether to esterify excess COOH end-groups [56]. This process was convenient because tire cords were treated with various "activating finishes" to improve their rubber adhesion. However, the glycidyl ethers were carcinogens and the process was abandoned in favor of the drastic alternative of melt-injecting ethylene oxide gas under high pressure into the molten polymer during the last stages of polymerization [57]. This reduced the free COOH end-group concentration to about 4–10 $\mu e/g$ by forming harmless BHET ends, and IV drop at tire molding was significantly reduced.

1.6.3 Low-Pill Staple Polyester

PET staple blends with wool and cotton were highly successful from the very first introduction of PET in the 1950s. However, consumers soon noticed an annoying problem. It was the formation of small fuzzy balls (called "pills") on the surface of fabrics. This phenomenon is

known as "pilling" and it is common to all staple fibers, particularly if the level of yarn twist is low, so that the fiber has many loose ends. The pills rub off harmlessly with wool because wool is a weak fiber. However, PET is a strong fiber (tenacity ca. 5 g/decitex) and therefore pills do not rub off; instead, they cling and have a negative impact on fabric esthetics. To reduce pilling, the IV of the polyester is reduced to make weaker fibers. These do not pill so obviously because the pills break away. A polymer of IV = 0.42 was selected as the best compromise for a low-pill PET staple fiber, but it caused many problems. The melt viscosity was so low and the molten polymer so fluid that the process became unstable. A method had to be found to raise the effective melt viscosity of the polymer while maintaining the low-pill properties to give an acceptable melt-spinning process. The method adopted was to introduce branching points into the polymer chain by adding a multifunctional component (either a polyacid or a polyhydric alcohol) so as to produce a star-branched polymer. Such polymers are known to have higher melt viscosities for the same (nominal) polymer IV. The branching agent added (ca. 1 mol%) was usually pentaerythritol. Too much additive would lead to gel formation by forming cross-linked networks, but this is not a problem at low levels [2].

1.6.4 Noncircular Cross-Section Fibers

Synthetic fibers like PET and nylon are normally round in cross section, however no natural fiber has a circular cross section. Wool is irregular, cotton is "dogbone" shaped, and silk is triangular. In the early 1970s, people began to study the effect of noncircular cross-section (NCCS) fibers on yarn and fabric esthetics, which is a subjective topic involving such arcane terms as "feel," "drape," and "handle." Fortunately, a melt-spun fiber lends itself NCCS well to the production of (NCCS) fibers by varying the shape of spinneret orifice, provided the melt viscosity is high enough so that surface tension does not cause the filament to resume a circular shape. Since the holes had to be very small (about 0.015 in. overall), machining a multiplicity of holes at a uniform size and shape was a major engineering problem, particularly in the hard metal alloys used for spinneret plates. Laser etching is one technique used. A hole shaped like a T gave trilobal filaments. In the pioneering days, much of this work was entirely heuristic, but gradually emerged some rules of thumb. Multilobed yarn cross sections (trilobal and octalobal) can give quite different appearances. Trilobal is glittery as the incident light reflects off the fiber surface, while octalobal gives an opaque matte effect, as the light is effectively absorbed by multiple reflections from the many acute angles. Sharp-edged filaments have the prized rustle and high frictional characteristics of pure silk, where it is called "scroop." Flat rectangular filaments give fabrics an unpleasant "slimy" handle. Gradually, these principles were applied to commercial yarns, and many filament yarns for the apparel and BCF carpet markets now use NCCS fibers.

1.6.5 Antistatic and Antisoiling Fibers

These topics are related because the origins of the problems are interrelated. Synthetic fibers in general, and PET in particular, are hydrophobic materials—PET has a moisture regain of 0.4% at 60% RH. PET fibers are difficult to wet and rapidly build up static electrical charges by friction because as water effectively leaks away, voltage is produced. It is possible to build up potentials as high as 50 kV by rubbing a polyester fabric, e.g., by walking on a polyester carpet when the relative humidity is low (5%). Such a potential, discharged by grasping a grounded door handle, would give a very unpleasant electric shock. Static charges also lead to attraction of dust and dirt.

To avoid these problems, the moisture uptake of the polyester should be increased by combining it with hydrophilic materials that are wash-fast. One additive that has been used

repeatedly is polyethylene oxide (PEG), a stable, functional, highly hydrophilic, water-soluble, and humectant polymer (see below):

$$HO-CH_2CH_2O[CH_2CH_2O-]_n-H$$

The MW can be from a few hundred to many millions. Copolymers of PET with PEG having a molecular weight of approximately 500–2000 Da were made, and it was possible to incorporate permanently enough PEG without drastic reduction of the PET properties to greatly improve the fiber moisture uptake, but at the expense of severe reduction in the light stability of dyed fibers [58]. Other processes used a PET/PEG block copolymer in aqueous dispersion that was padded and baked onto the fiber as a textile finish. This relied on cocrystallization of the PET segments with the polymer to make the treatment wash-fast [59]. The most satisfactory technique is probably to make a bicomponent fiber with a thin coating of a PET/PEG copolymer on a PET core in a core–sheath configuration. This does not affect fiber properties and minimizes the light fastness issue [60].

1.7 DYEING POLYESTERS

1.7.1 Introduction

Dyeing synthetic fibers is a huge subject in its own right and the reader is advised to consult one of the many publications that deal with it comprehensively [61]. When PET fibers first appeared, they presented many problems for traditional dyers. PET has no functional groups to give affinity for usual dyestuffs. Natural fibers like wool, cotton, silk, and then later man-made ones like rayon and nylon were well known and had good dye affinities because the fibers had pendant or terminal functional chemical groups such as $-NH_2$, –COOH, and –OH. These dyes were developed to interact with such groups. The only way to dye polyester was to rely on Van der Waals forces to hold the dye in the fiber. All classic cationic and anionic dyes for wool and silk or direct dyes for cotton had water-solubilizing ionic groups like $-NR_3^+$ and $-SO_3^-$. Such dyes had little or no affinity for PET.

1.7.2 Disperse Dyes

PET fiber chemistry is in some ways similar to that of cellulose acetate fibers, where the class of dye called "dispersed dyes" were in use. These dyes did not have strongly polar solubilizing groups and were actually dispersed in the aqueous dyebath with a surfactant as a suspension of fine particles in suspension. Such dyes usually had a low molecular weight and this later led to problems with PET due to dye sublimation. Polyester fabrics needed stentering (heat-setting under tension) on a pin-frame to remove creases after dyeing. This became a big problem for PET dyers. It was clear that special dyes were needed for PET. As the polyester fiber market grew, such modified dyes rapidly advanced, and were based on well-understood dye chemistry. Higher molecular weight dyes of the anthraquinone type gave reds, blues, and dark greens, while selected azos were used for yellow and orange shades. These dyes were most effective if they were somewhat water-soluble and the ethanolamino group ($-NRCH_2CH_2OH$) and sometimes its *O*-benzenesulfonate ester were incorporated, giving a weakly polar nature and bestowing solubility in polyester but without a truly ionic character. The higher molecular weight dyes reduced dye sublimation, but at the cost of slower dyeing and poor dye exhaustions. A breakthrough was achieved in the middle of the 1950s with the development of heterocyclic (nitroaminothiazole) dyes, which gave very stable light-fast azo blues [62]. These had good affinities for PET. Another dye problem that became quite important was gas-fume

fading of disperse dyes due to the generation of oxides of nitrogen (NO_x) and even traces of ozone in living rooms, arising from wider use of oil and gas heating systems. It was solved largely by selecting dyes whose chromophores were stable to oxidation by NO_x.

Carriers were introduced to speed up dyeing. These were solubilizing agents that temporarily swelled the fiber and "carried" the dye into the fibrous structure. The carrier was trapped in the amorphous regions of the fiber morphology, since the dense crystalline regions could not be penetrated by the large dye molecules. The carrier itself diffused out again, so it might be regarded as a fugitive plasticizer. Phenols like 2-hydroxybiphenyl (OPP) were widely used and greatly improved the economics of dyeing polyester. An alternative was pressure dyeing, using superheated dye liquor at 135–150°C (well above the T_g of drawn PET fiber), but this was a capital-intensive process since pressure-dyeing vessels were expensive. Eventually, pollution problems with dyehouse liquor waste led to restrictions on the use of carriers. Pressure dyeing is now the norm, although more expensive. This is one reason why non-PET polyester fibers like PBT and PTT are attractive to the dyer. Both have T_gs of about 45°C, so they can be aqueously dyed to heavy shades at the boil at atmospheric pressure. The reluctance of polyester to dye can be turned into a commercial advantage. The argument is that "a fiber that does not readily dye will also not easily stain."

1.7.3 Anionic and Cationic Dyes for Polyester

Since much polyester was originally used in blends with wool, it was natural that attempts should be made to modify PET to make it acid-dyeable with anionic dyes. The most popular theme was to incorporate basic additives by copolymerizing an aminohydroxy compound or aminoacid into the PET structure. All such attempts failed because the copolymers were discolored yellow or brown, and were of low IV. It was found, however, that certain polyamides, containing additional in-chain tertiary amine groups, when melt blended with PET and high-molecular-weight PEG (M_w 20,000) formed a three-phase mixture in which the polyamide was dispersed inside the PEG and this in turn was dispersed inside the PET. Thus, the critical components were prevented from intermixing in the melt. The mixture was melt-spun successfully into fibers at 270°C. Diamond-patterned fabrics were jacquard knitted with mixtures of the dye variant fiber and normal PET. These could be cross dyed to give patterned effects from a single dyebath containing both acid and disperse dyes. However, the process was deemed too complex and expensive for a commercial product and the light stability of the dyes was not adequate [63].

Greater success was achieved by DuPont who copolymerized, the sodium salt of 5-sulfoisophthalic acid into PET to render the polymer dyeable with cationic (basic) dyes. Basic dyeable PET was successfully launched as Dacron 64 in the form of a low-pill staple product [64]. The presence of the sulfonate groups in the polymer chain also acts as an ionic dipolar cross-link and increases the melt viscosity of the polymer quite markedly. Thus, it is possible to melt-spin polymer with IV 0.56 under normal conditions, giving a low-pill fiber variant. The fiber also has a greater affinity for disperse dyes due to the disruption of the PET structure. Continuing this theme, there are "deep dye" variant PET fibers, often used in PET carpet yarns, which are copolymers of PET with chain-disrupting copolymer units like polyethylene adipate. They have less crystallinity and a lower T_g; therefore, they may be dyed at the boil without the use of pressure equipment or carrier at the cost of some loss of fiber physical properties.

1.7.4 Mass Dyeing

Since much polyester staple fiber is dyed to dark, expensive colors (black and navy blue), the fiber is often mass dyed or mass pigmented at the polymerization stage. Clearly, thermally

stable pigments and dyes have to be used. Especially fine pigment grades of carbon black are used for black, and this is toned by adding small amounts of navy blue or very dark green melt dyes to remove any traces of brown, which dyers consider unacceptable. Mass dyeing is only economic if the demand warrants it.

A more recent development is "dope dyeing" (a term dating back to the acetate rayon industry), where a range of melt-dyed colors are produced by coloring white polymer immediately before melt spinning by adding calculated mixtures of master-batch pigmented polymer or actual neat dyestuff. This can conveniently be done by adding the dye in the form of pills or granules containing a specific amount of dye at a calculated feed rate to the molten polymer during the melt-spinning process or by adding the coloring agent as a liquid dispersion in a very high boiling point (over 300°C) inert oil, either during polymerization or at melt spinning [65]. The latter process is of particular value in melt coloration of POY feedstock yarns.

1.8 BICOMPONENT FIBERS AND MICROFIBERS

Bicomponent fibers or "heterofil" fibers are filaments made up of different polymers. There are many geometrical arrangements. The three main heterofil geometries are side-by-side, core–sheath (both concentric and eccentric), and the multiple core or "islands in a sea" configuration. The so-called "splittable pie" configurations are used in the production of microfibers (see Figure 1.12).

The two polymer components do not have to differ in "chemical" nature. They can differ only in physical parameters such as molecular weight. Usually, it is desirable that the two components have good mutual adhesion, but not always. Polyolefines do not bond well with polyesters or polyamides and this fact is exploited in the formation of microfibers (see later).

1.8.1 Side–Side Bicomponent Fibers

Side–side bicomponent fibers can be used to produce self-bulking yarns. Two PET polymers of different molecular weights, spun as a side–side heterofil, produce a self-bulking fiber

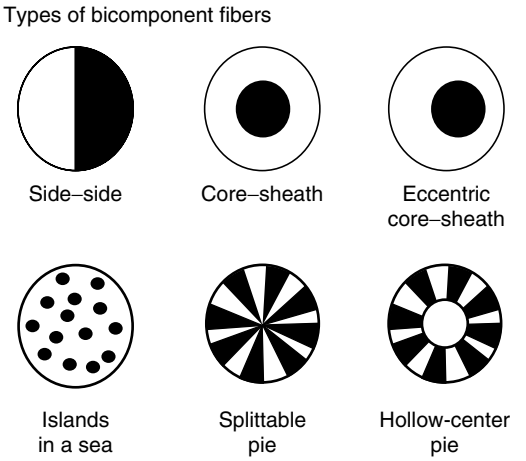

FIGURE 1.12 PET containing biocomponent fiber.

after drawing and relaxing because the spun birefringences differ. The relaxed yarn curls up like a bimetallic strip and results in a spiral crimp. A self-bulking fiber can also be made by cospinning PET with a PET copolyester containing a branching agent in a side–side configuration [66].

1.8.2 Core–Sheath Bicomponent Fibers

The core–sheath (c–s) configuration is adaptable because many different polymers may be applied as a sheath over a solid polyester core, thus giving a variety of modified surface properties while maintaining all the major fiber and textile properties of PET. An early patent by Shima and coworkers uses an eccentric core–sheath configuration to achieve spiral crimp in a yarn [67]. A recent patent by Chang and coworkers discloses the use of side–side or eccentric c–s bicomponent fibers to achieve a self-crimping yarn made from polytrimethylene terephthalate, where one component is a melt-blend of PTT with a small amount of polystyrene [68].

We have already mentioned the antisoil–antistatic fiber made by using a PET–PEG block copolymer coating on a polyester core. A widely used c–s heterofil has a normal PET core with a lower softening-point sheath polymer (typically a PET–isophthalate copolyester). When such fibers are laid randomly in a nonwoven structure and heated to a temperature above the softening point of the sheath polymer, but below the fusion point of the core polymer, the fibers adhere wherever they cross and touch. This may be done either by heated calendar rolls or simply in a forced draught hot air oven. The result is a stable nonwoven fabric [69,70]. A new development is a biodegradable, nonwoven material for disposable fabrics, made by thermally bonding a polylactide core bicomponent fiber with a low melting sheath polymer such as polyethylene [71].

1.8.3 Multiple Core Bicomponent Fibers

The multiple core or ''islands in a sea'' type of heterofil is mainly of interest in connection with microfibers and this is discussed in the following text.

1.8.4 Hollow Fibers

Hollow fibers are a type of core–sheath heterofil in which the core is composed of air. They are usually made in the form of crimped staple fiber and spun from a modified staple spinning pack [72]. With advances in melt-spinner design, more complex geometries [73] are available. One patent describes a multiple-core circular polyester staple fiber with seven cores [73]. Hollow fibers in the form of filament yarn have specialized uses in medical devices, but the largest volume market for hollow fiber is staple fiberfill for pillows, duvets, quilts, and thermal outerwear. The desired quality here is ''loft'' and it is better if the fiber is light and bulky. The most desired quality is thermal insulation. Hollow polyester fibers are well suited to this end use: the air entrapped in the hollow cores adds significantly to their insulating properties; more hollow air cores increase this effect. The fibers are frequently crimped by a stuffer-box process or made as bicomponent hollow fibers, which develop spiral crimp on drawing. Such filler fibers are frequently treated with a permanent polysiloxane finish that makes them slippery, so that they slide easily over each other and resist clumping up, which reduces their insulating effect. In this form, they compete with goose down as a thermally insulating filling material. For end-uses like fabric interlinings, it is desirable to stabilize a filled hollow fiber structure by incorporating an additional thermally bondable bicomponent fiber [75].

1.9 NOVEL FIBER FORMS

1.9.1 Microfibers

Microfiber is arbitrarily defined as a filament of less than 1.0 dpf. Normal filament yarn polyester is around 3. 0–5.0 dpf. Microfibers are many times finer than a human hair and finer than the finest silk: diameters are generally less than 10 μm. A typical polyester microfiber has a titer of about 0.5 dpf. Such fine fibers in the form of yarns have excellent textile properties. They are very flexible, giving a soft "hand" and excellent drape to fabrics. The high density of fibers in a typical microfiber fabric makes it inherently windproof and waterproof. There are only tiny gaps for air to blow through, yet the fabrics are largely unwettable, because surface tension effects prevent water from penetrating the interstices in the fabric. These fabrics are comfortable to wear as water vapor from perspiration evaporates easily. Their fabric properties make them ideal for women's wear, sportswear, active, and outdoor wear. They have (radiant) heat-insulating properties because the filaments are of the same dimensional order as the wavelengths of infrared radiation. A 0.5 dpf polyester filament (density ≈ 1.4 g/cm^3) has a diameter of about 7 μm, right in the middle of the IR wavelength range (2–20 μm). Hence, radiation is efficiently scattered by the microfibers and radiation loss of body heat is reduced.

Microfibers lend themselves very well to fabric esthetics. Dyed fabrics appear with solid, bright colors due to the fine size of individual filaments. They are semimatte in appearance, without the need for treatments such as sand washing. The vulnerability to damage from careless ironing is one disadvantage. The thermal capacity of the tiny filaments is so low that it is easy to overheat them. They also snag easily and, as with all fine fabrics, they need to be handled with a degree of care.

1.9.2 Melt-Spinning Microfibers

The first commercial microfibers were produced in Japan [76] in the 1970s and were made by spinning a bicomponent fiber with polyester fibrils dispersed in a matrix polymer in the "islands in a sea" configuration [77]. This was drawn into fibers and processed into fabric and finally the matrix polymer was dissolved, leaving tiny polyester fibrils. These were processed into a synthetic suede material marketed as Ultrasuede. The polyester fibrils were extremely fine, less than 1 μm in diameter. The process was expensive, but the product was successful. At the same time, numerous variations on this theme later followed. One ingenious idea by Sato and coworkers used was a blend of PET in a PET–sulfoisophthalate copolymer rich in SO_3Na groups, which dissolved readily in aqueous base leaving the unaffected PET.

There are many patents in the literature, mostly on static devices for melt-spinning multiple fibers with the "islands in a sea" configuration. This is usually done by a multiple series of flow-divider plates that take the initial side–side polymer flow (as in a heterofil spinner) and subdivide it and cross over the flow many times before the spinneret plate, so that each spun filament emerges with the desired structure. Some examples are further ideas of Okamoto [78] and Dugan [79]. More recently, the dissolvable matrix has been made of such materials as polylactic acid (already mentioned), thermoplastic starches, or water-soluble copolyesters. Good review articles on microfibers have been written by Robeson [80], Murata [81], and Isaacs [82].

Another method of making microfibers is the "splittable pie" technique, where a bicomponent fiber of special configurations is spun from two incompatible polymers that adhere poorly. On subjecting these fibers to mechanical stress, as during carding, they split apart to form bundles of microfibers with a wedge-shaped cross section. PET–polypropylene or

PET–nylon-6 are examples of suitable polymer combinations. Such microfibers are frequently used in nonwoven fabrics such as filter materials and specialty fabrics like cleaning cloths for microelectronic components or polishing cloths for lenses and delicate optical instruments.

1.10 WORLD MARKETS AND FUTURE PROSPECTS FOR POLYESTER FIBERS

The total world market for all synthetic fibers in 2002 was around 36,000,000 tons. Of this total, 21,500,000 tons is PET and the rate of consumption is still growing, although apparently slowing. Over the past 15 years, there have been cataclysmic changes in the polyester-producing fiber business. The gradual eclipse of the textile industry in the United States and much of western Europe and its geographical shift to Asia and other places, such as Central America and parts of Eastern Europe, has brought about these changes. Old, firms like ICI, Hoechst, Monsanto, and Eastman have disappeared completely from the fiber-producing scene. The last survivor was DuPont which announced in February 2002 that they would split off all their fiber and textile interests as a separate industry under the name Invista. In November 2003, Koch Industries announced that they would acquire Invista.

The new generation of polyester fiber producers buy polymer in the open market as a commodity item and convert it into fiber and yarn. They have revolutionized the market and superseded the old order. Koch Industries buy PPT polymer from Shell and spin Corterra fibers and market them, although Shell retains the trademark and Koch proposes to build its own polymer plant in Mexico. The emergence of China as a major consumer and producer of polyester fiber (it outstripped the United States in polyester production in 1998) will have a major effect on world markets.

The market for polyester fiber will certainly continue to grow overall, although, as a major commodity item, it is likely to be affected much more than in the past by global economics and trade cycles. Certainly, the price of raw materials like crude oil and natural gas will have an effect on process costs and markets. Nevertheless, there is still a trend to replace other fibers, both natural and synthetic, with polyester. Nylon is still losing markets to polyester. At present, nylon dominates polyester in domestic carpet yarns, but because PET is cheaper, it has a growing share of the contract carpet trade. The new microfibers and newer easy-to-dye polyesters with excellent resilience (like PTT) would be expected to make big inroads into floor coverings and the apparel markets over the next few years. It was confidently expected that PTT would have an immediate impact on the carpet business (one place where PET polyester suffers) in 1999–2000 when Corterra was first launched. So far this has not happened, but fiber price and availability are major factors as always. In the long term, there are new nonoil-based biomass-derived processes in commercial production for making not just intermediates for polyesters but even the polymers themselves. The effect of recycling polyester such as soda bottles into fiberfill and carpet yarns may also have unpredictable effects.

REFERENCES

1. Worldwide Manufactured Fiber Survey, Fiber Economic Bureau, Fiber Organon, June 2002.
2. G. Reese, Polyester fibers, in *Encyclopedia of Polymer Science & Technology*, 3rd edn, Vol. 3, John Wiley & Sons, New York, 2003, pp. 652–678.
3. Y. Murase and A. Nagai, in T. Nakjima (ed.), *Advanced Fiber Spinning*, Woodhouse Publishing, Cambridge, UK, 1994, pp. 25–64.
4. J.E. McIntyre, in J. Scheirs and T.E. Long (eds.), *Chemistry and Technology of Polyesters and Copolyesters*, John Wiley & Sons, New York, 2003, pp. 2–28.

5. A.J. East, Polyester fibres, in J.E. McIntyre (ed.), *Synthetic Fibres: Nylon, Polyester Acrylic, Polyolefine,* Woodhead Publishing Limited, Cambridge, England, 2005, Chapter 3.
6. H. Mark and G.F. Whitby (eds.), *The Collected Papers of W.H. Carothers*, Interscience Publications Inc., New York, 1940.
7. U.K. Patent 578,079 (June 14, 1946), J. Rex Whinfield and J.T. Dickson (to ICI Ltd), also U.S. Patent 2,465,319 (March 22, 1949), J.R. Whinfield and J.T. Dickson (to E I Du Pont de Nemours & Co Inc.).
8. A.E. Brown and K.A. Reinhart, Polyester fiber: from its invention to its present position, *Science*, July 16, 1971, 287–293.
9. A.J. East, *Kirk-Othmer Encyclopedia of Chemical Technology*, 5th edn, to be published.
10. W.S. Witts, *Chem. Proc. Eng*., 1970, **51**, 55.
11. U.S. Patent 3,584,039 (June 8, 1971), D.H. Meyer (to Standard Oil Co).
12. J. Milgrom, Outlook for plastics recycling in the USA, Decision Resources Inc, 1993, pp. 25–27.
13. G.O. Curme and F. Johnston, *Glycols*, ACE Monograph #114, Reinhold Publishing Corp., New York, 1952, Chapter 2.
14. R.E. Wilfong, *J. Polym. Sci*., 1961, 54, 388.
15. French Patent 1,169,659 (1959) to ICI Ltd.
16. Canadian Patent 573,301 (1959), W.K. Easley et al. (to Chemstrand Corporation).
17. U.S. Patent 5,684,116 (November 4, 1997), M. Martl et al. (to Akzo-Nobel NV).
18. U.S. Patent 5,789,528 (August 4, 1998), M. Martl et al. (to Akzo-Nobel NV).
19. U.S. Patent 5,552,513 (September 3, 1996), K.K. Bhatia (to E I DU Pont de Nemours & Co Inc.).
20. U.S. Patent 5,677,415 (October 14, 1997), K.K. Bhatia (to E I DU Pont de Nemours & Co Inc.).
21. U.S. Patent 5,865,423 (January 5, 1999), K.K. Bhatia (to E I DU Pont de Nemours & Co Inc.).
22. W. Sorenson, F. Sweeney, and T.W. Campbell, *Preparative Methods of Polymer Chemistry*, 3rd edn, John Wiley & Sons, New York, 2001, pp. 181–185.
23. D.G. Callender, *Polym. Sci. Eng*., 1985, **25**, 453–457.
24. M. Jaffe, J. Menczel, and W. Bessey, Thermal characterization of polymeric materials, in E.A. Turi (ed.) *Fibers*, 2nd edn., Vol. 1, Academic Press, San Diego, CA, 1997, Chapter 7.
25. G.W. Davis and E. Hill, *Kirk-Othmer Encyclopedia of Chemical Technology Edition III*, Vol. 18, John Wiley & Sons, 1982, p. 535.
26. S. Berkowitz, *J. Appl. Polym. Sci*., 1984, **29**, 4353–4361.
27. G.W. Davis and E.S. Hill, Polyester fibers , *Kirk-Othmer Encyclopedia of Chemical Technology*, 3rd edn, Vol. 18, John Wiley & Sons Inc., 1982, pp. 531–539.
28. M. Jaffe and W. Bessey, Solid phase processing of polymers, in I. Ward, P. Coates, and M. Dumoulin (eds.), *Solid State Processing of Polymers*, Carl Hanser Verlag, Munich, 2000.
29. A. James, Principles of spin pack design: a guide to selecting components, *Int. Fiber J*., 1997, **12**, 2.
30. M.M. Denn, Anniversary Article, Fifty years of non-Newtonian fluid dynamics, *AIChE J*., 2004, **50**(10), 2335–2345.
31. A. Zabicki and A. Wasiak, Effects of molecular deformation and orientation on the crystallization of polymers, *Chemia Stosowana*, 1981, **25**(2), 147–161.
32. I. Onsager, *N Y Acad. Sci*., 1949, **51**, 627.
33. P.J. Flory, *Proc. R. Soc. London. Ser., Part A, 1956, London.*
34. S.E. Bedford, K. Yu, and A.H. Windle, Influence of chain flexibility on polymer mesogenicity, JACS, *Faraday Trans*., 1991, **88**(13), 1765–1773.
35. U.S. Patent 4,101,525, H.L. Davis, M. Jaffe, H.L. LaNieve, and E.J. Powers, ''Polyester Yarn of High Strength Possessing an Unusually Stable Internal Structure,'' U.S. Patent 4,195,052, H.L. Davis, M. Jaffe, H.L. LaNieve, and E.J. Powers, ''Production of Improved Polyester Filaments of High Strength Possessing and Unusually Stable Microstructure.''
36. S.D. Long and I.M. Ward, Tensile drawing behavior of poly(ethylene terephthalate, *J. Appl. Polym. Sci.* 1991, **42**(7), 1911–1920.
37. J.W.S. Hearle, L. Hollick, and D.K. Wilson, *Yarn Texturing Technology*, Woodhead Publishing Co., Cambridge, U.K., 2001.
38. H. Chuah et al., *Chem. Fib. Inter*., 1996, **46**(6), 424–428.
39. Y. Kitano, Y. Kinoshita, and T. Ashida, *Polymer*, 1995, **36**, 10.

40. H.H. Chuah, Polytrimethylene terephthalate, *Encyclopedia of Polymer Science and Technology*, 3rd edn, Vol. 3, John Wiley & Sons, New York, 2003, pp. 544–557.
41. E.V. Martin and C.J. Kibler, in H.F. Mark, S.M. Atlas, and E. Cernia (eds.), *Man-Made Fiber Science and Technology*, Vol. 3, John Wiley & Sons, New York, 1968, pp. 83–134.
42. S.R. Turner, R.W. Seymour, and T.W, Smith, Cyclohexanedimethanol polyesters, *Encyclopedia of Polymer Science and Technology*, 3rd edn, Vol. 2, John Wiley & Sons, 2003, pp. 127–134.
43. U.K. Patent 604,073 (1948), J.G. Cook, H.P.W. Hugill, and A.R. Low (to ICI Ltd).
44. H. Mark, Phase transitions and elastic behavior of high polymers, *J. Indust. Eng. Chem*., 1942, **29**, 449–454.
45. Tai-Shung Chung and M. Jaffe, Liquid crystalline polymers, Mainchain, *Encyclopedia of Polymer Science and Technology*, Wiley-Interscience, 2003.
46. I.M. Ward, Mechanical anisotropy of highly oriented polymers, *J. Computer Aided Matl. Design*, 1997, **4**(1), 43–52.
47. H.N. Yoon, *Colloid Polym. Sci*., 1990, **268**, 230.
48. U.S. Patent 5,945,216, Flint, M. Jaffe, I. Haider, J. Dibiase, and J. Cornetta, "Process for making high denier filaments of thermotropic liquid crystalline polymers and compositions thereof."
49. L.C. Sawyer and M. Jaffe, *J. Mater. Sci*., 1986, **21**, 1897.
50. L.C. Sawyer et al., *J. Mater. Sci. Lett*., 1992, **11**, 69.
51. D. Goupil, Sutures, Section 7.9, in B.D. Ratner, A.S. Hoffman, F.J. Schoen, and J.E. Lemons (eds.), *Biomaterials Science*, Academic Press, 1996, pp. 356–360.
52. U.S. Patent 5,869,597 (February 9, 1999), H.D. Newman and D.D. Jamiolowski (to Ethicon Inc.).
53. U.S. Patent 4,841,968 (June 27, 1989), R.L. Dunn and coworkers (to Southern Research Institute).
54. U.S. Patent 4,427,614 (January 24, 1984), P.J. Barham and Paul Holmes (to Imperial Chemical Industries PLC).
55. G. Farrow et al., *Polymer*, 1962, **3**, 17.
56. U.S. Patent 4,016,142 (April 5, 1977), W. Alexander and coworkers (to Millhaven Fibers Ltd, Canada).
57. U.S. Patent 4,442,058 (April 10, 1984), R.L. Griffith and N.A. Favstritsky (to Fiber Industries Inc).
58. D. Coleman, Copolymerization of polyethylene terephthalate with polyoxyethylene glycols, *J. Polym. Sci*., 1954, **XIV**, 15–27.
59. U.S. Patent 3,557,039 (January 19, 1971), J.E. McIntyre and M.M. Robertson (to Imperial Chemical Industries Limited).
60. U.S. Patent 3,616,183 (October 26, 1971), J.R. Brayford, I.S. Fisher, and M.M. Robertson (to Imperial Chemical Industries Limited).
61. D.R. Waring and G. Hallas (eds.), *The Chemistry and Application of Dyes*, Plenum Press, New York, 1994.
62. J.B. Dickey, E.B. Towne, and G.F. Wright, *J. Org. Chem*., 1955, **20**, 505.
63. U.S. Patent 3,544,658 (December 1, 1970), A.J. East and W.D. Thackray (to Imperial Chemical Industries Limited).
64. U.S. Patent 3,018,272 (January 23, 1962), J.M. Griffing and W.R. Remington (to E I Du Pont de Nemours & Co Inc.).
65. U.S. Patent 6,110,405 (August 29, 200), C.M. King et al. (to Wellman, Inc.).
66. U.S. Patent 5,723,215 (March 3, 1998), I.A. Hernandez et al. (to E I Du Pont de Nemours & Co Inc.).
67. U.S. Patent 3,520,770 (July 14, 1970), T. Shima et al. (to Teijin Limited, Japan).
68. U.S. Patent 6,641,916 (November 4, 2003), J.C. Chang, J.V. Kurian and R.W. Miller (to E I Du Pont de Nemours & Co Inc.).
69. U.S. Patent 5,082,720 (January 21, 1992), D.J. Hayes (to Minnesota Mining and Manufacturing Company).
70. U.S. Patent 6,441,267 (August 27, 2002), J.S. Dugan (to Fiber Innovation Technology).
71. U.S. Patent 3,772,137 (November 13, 1973), J.W. Tolliver (to E I Du Pont de Nemours & Co Inc.).
72. U.S. Patent 5,344,297 (September 6, 1994), W.H. Hills (to BASF Corporation).
73. U.S. Patent 5,104,725 (April 14, 1992), C.R. Broaddus (to E I Du Pont de Nemours & Co Inc.).
74. U.S. Patent 4,520,066 (May 28, 1985), G. Athey (to Imperial Chemical Industries PLC).

75. M. Okamoto, Ultrafine Fiber and its Applications, Part I, *Japan. Text. News*, November 1977, pp. 94–97; Part II, *Japan. Text. News*, January 1978, pp. 77–81.
76. U.S. Patent 3,705,226 (December 5, 1972), M. Okamoto et al. (to Toray Industries, Inc.).
77. U.S. Patent 4,233,355 (November 11, 1980), Y. Sato and H. Arai (to Toray Industries, Inc.).
78. U.S. Patent 4,350,006 (September 21,1982), M. Okamoto et al. (to Toray Industries Inc.).
79. U.S. Patent 5,366,804 (November 22,1994), J.S. Dugan (to BASF Corporation).
80. Robeson, *J. Appl. Polym. Sci.,* 1994, **52**, 1837–1846.
81. Murata, *Textile World*, 1996, **144**, 42–48.
82. Isaacs, *Textile World*, August 1994, 73–74.

2 Polyamide Fibers

H.H. Yang

CONTENTS

2.1 Introduction 33
2.1.1 Historic Perspective 33
2.1.2 Aliphatic Polyamides 34
2.1.2.1 Definition of Polyamides 34
2.1.2.2 Examples of Polyamide Compositions 34
2.2 Basic Chemistry of Aliphatic Polyamides 35
2.2.1 Synthetic Routes 35
2.2.2 Amidation Reactions 36
2.2.3 Ring-Opening Reactions 38
2.2.4 Molecular Weight and Molecular Weight Distribution 40
2.2.5 Nylon-6,6 Polyamide 45
2.2.5.1 Synthetic Procedure 45
2.2.5.2 Kinetics and Thermodynamics 45
2.2.5.3 Solid-State Polymerization 46
2.2.6 Nylon-6 Polyamide 47
2.2.6.1 Synthetic Procedure 47
2.2.6.2 Kinetics and Thermodynamics 47
2.2.7 Other Polyamides 56
2.2.7.1 Nylon-3 56
2.2.7.2 Nylon-4 56
2.2.7.3 Nylon-7 56
2.2.7.4 Nylon-8 56
2.2.7.5 Nylon-11 58
2.2.7.6 Nylon-12 58
2.2.7.7 Nylon-4,2 58
2.2.7.8 Nylon-4,6 58
2.2.7.9 Nylon-6,12 58
2.2.7.10 Nylon-4,1 58
2.2.7.11 Nylon-6,1 58
2.2.7.12 Nylon-6,T 59
2.2.7.13 PACM,12 59
2.3 Polymerization Processes 59
2.3.1 Monomer Syntheses 59
2.3.1.1 Caprolactam 59
2.3.1.2 Adipic Acid 65
2.3.1.3 Hexamethylene Diamine 67

2.3.2 Industrial Processes 70
2.3.2.1 General Operations 70
2.3.2.2 Nylon-6 Polyamide 72
2.3.2.3 Nylon-6,6 Polyamide 73
2.3.2.4 Other Polyamides 73
2.3.2.5 Nanocomposites 74
2.3.2.6 Process Simulation 74
2.4 Preparation of Polyamide Fibers 78
2.4.1 Melt Spinning 78
2.4.2 Dynamics of Melt Spinning 80
2.4.3 Quenching 80
2.4.4 Spin Finish 81
2.4.5 Drawing 81
2.4.6 Process Integration 82
2.4.6.1 Draw-Twisting 83
2.4.6.2 Spinning–Drawing–Texturing 84
2.4.7 High-Speed Spinning 84
2.4.8 Textile Finishing Operations 85
2.4.8.1 Texturing 85
2.4.8.2 False-Twist Texturing 85
2.4.8.3 Crimp Texturing 86
2.4.8.4 Commingling, Interlacing, and Air-Jet Texturing 87
2.4.9 Winding and Yarn Package 87
2.5 Structures and Properties of Polyamide Fibers 87
2.5.1 Polymer Chain Structure 87
2.5.2 Characteristics of Crystalline and Amorphous Structures 88
2.5.2.1 Crystalline Forms 88
2.5.2.2 Crystalline Structures in Fibers 92
2.5.2.3 Structural Models 93
2.5.3 Thermal Transitions of Crystalline Phase 94
2.5.3.1 Melt Temperature 94
2.5.3.2 Glass Transition Temperature 96
2.5.4 Characterization of Structural Parameters 98
2.5.4.1 X-Ray Diffraction 98
2.5.4.2 Crystallite Size 99
2.5.4.3 Degree of Orientation 99
2.5.4.4 Birefringence 100
2.5.4.5 Crystallinity and Crystalline Indices 101
2.5.5 Typical Fiber Properties 105
2.5.5.1 Tensile Behavior 107
2.5.5.2 Chemical Properties 113
2.5.5.3 Degradation Behavior 113
2.5.5.4 Polymer Stabilization 118
2.5.5.5 Antistatic 118
2.5.5.6 Flammability 119
2.5.5.7 Transparency 120
2.5.5.8 Dye Diffusion 120
2.5.6 Process–Structure–Property Relationship 120
2.5.6.1 Effect of Molecular Weight 121
2.5.6.2 Effect of Water 121

2.5.6.3 Effect of Spinning and Drawing 121
2.5.6.4 Effect of Spinning Conditions 122
2.6 Commercialization and Future Outlook 122
2.6.1 Polyamide Fiber Products 122
2.6.1.1 Filament Yarn and Staple 122
2.6.1.2 Bicomponent Fibers 122
2.6.1.3 Microfibers 123
2.6.2 End-Uses 124
2.6.2.1 Textiles 124
2.6.2.2 Carpets 124
2.6.2.3 Industrial Applications 124
2.6.2.4 Specialty Fibers 124
2.6.2.5 Nonwovens 124
2.6.2.6 Nonfiber Uses 125
2.6.3 Worldwide Consumption of Polyamide Fibers 125
2.6.4 Future Outlook 126
2.6.4.1 Technology 126
2.6.4.2 Market Share 126
Acknowledgment 126
References 127

2.1 INTRODUCTION

2.1.1 Historic Perspective

The development of polyamide fibers is quite interesting in the history of synthetic fibers. Nylon, the first commercial fiber product of polyamide, was marketed for manufacturing women's hosiery by E.I. du Pont de Nemours & Company in 1938. The immediate success made nylon a household name all over the world. It also provided DuPont a string of 50 years of strong earnings. The success of nylon led to the commercialization of other synthetic fibers such as polyester, polyacrylonitrile, and polyolefin fibers, as well as inorganic fibers such as carbon and boron. These developments have been strongly supported by the progress in polymer and fiber chemistry and material science. In retrospect, therefore, one must credit the chemical industry for its pursuit of new technology and vision of new materials.

In the early 1920s, DuPont embarked on a "pure science" research program for its future business objectives. The company hired Dr. Wallace H. Carothers, a brilliant young chemist, in 1927 to study long-chain polymers, methods of polymerization, and polymer properties. Within three-and-half years, Carothers accomplished the design and syntheses of condensation polymers and the conversion of these polymers to fibers. The properties of such fibers were further enhanced by the discovery of cold drawing. He also discovered a useful synthetic rubber, polychloroprene. In the ensuing years, Carothers attempted to develop useful polyesters and polyamides. His work was hampered by inadequate polymer properties for fiber use, and by his spells of mental depression. Nevertheless, he finally learned to prepare polyamides and was particularly interested in nylon-5,10 from pentamethylene diamine and sebacic acid. This polyamide composition was unsuitable for commercialization because the monomers would always be difficult to find. Rather, he was asked to develop nylon-6,6. The monomers for nylon-6,6 were thought at least theoretically available from benzene. Thus, the first sample of nylon-6,6 was prepared in 1931. The fiber made from nylon-6,6 was coded Fiber 66. For fundamental support, Paul Flory was assigned to study the molecular weight

distribution of condensation polymers. DuPont was in the commercial production of nylon-6,6 by February 1935.

Carothers [1] filed for patent on stockings from polyamide yarns on February 15, 1937. He claimed that such stockings would fit properly and would not become baggy like other synthetic fibers. Shortly afterwards, Fiber 66 was evaluated for the full-fashioned women's stockings market. DuPont made an extensive effort to overcome problems of notably knitting, wrinkling, dyeing, and shininess. This resulted in a reasonably reproducible process for stockings by September 1938. Thus, DuPont officially announced the development of a new textile fiber called "nylon." It was described as having "filaments as strong as steel, as fine as a spider's web, yet more elastic than any of the common natural fibers." [2] Full-fashioned nylon stockings then went on sale nationwide on May 14, 1940. When World War II broke out, every ounce of nylon was required for military uses including parachutes and soft body armor. By the 1980s, women's hosiery alone consumed more than 70 million pounds of nylon a year.

Unfortunately, Carothers never saw the completion of the nylon development. He committed suicide in April 1937. Flory later published his distinguished book on polymer chemistry [3]. He went on to become one of America's most revered polymer scientists and a Nobel Laureate.

2.1.2 Aliphatic Polyamides

2.1.2.1 Definition of Polyamides

Aliphatic polyamides are macromolecules whose structural units are characteristically interlinked by the amide linkage —NHCO—. The nature of the structural unit constitutes a basis for classification. Aliphatic polyamides with structural units derived predominantly from aliphatic monomers are members of the generic class of *nylons*, whereas aromatic polyamides in which at least 85% of the amide linkages are directly adjacent to aromatic structures have been designated *aramids*. This chapter is concerned with nylons, especially those of commercial importance. Aramids are discussed in a separate chapter.

The U.S. Federal Trade Commission defines nylon fibers as "a manufactured fiber in which the fiber forming substance is a long chain synthetic polyamide in which less than 85% of the amide linkages (—CO—NH—) are attached directly to two aliphatic groups."

Polyamides that contain recurring amide groups as integral parts of the polymer backbone have been classified as condensation polymers regardless of the principal mechanisms entailed in the polymerization process. Though many reactions suitable for polyamide formation are known, commercially important nylons are obtained by processes related to either of two basic approaches: one entails the polycondensation of difunctional monomers utilizing either amino acids or stoichiometric pairs of dicarboxylic acids and diamines, and the other entails the ring-opening polymerization of lactams. The polyamides formed from diacids and diamines are generally described to be of the AABB format, whereas those derived from either amino acids or lactams are of the AB format.

2.1.2.2 Examples of Polyamide Compositions

Straight-chain aliphatic nylons are commonly identified either as nylon X,Y or nylon Z, where X, Y, and Z signify the number of carbon atoms in the respective monomeric units. The pair X,Y refers to the AABB-type nylons, where the first number X is equal to the number of carbon atoms in the diamine unit and the second number Y represents the number of carbon atoms in the corresponding diacid unit. The number Z refers to the AB-type nylons and is equal to the number of carbon atoms in the amino acid unit. A few examples are:

Nylon-6,10	-[-NH-$(CH_2)_6$-NH-CO-$(CH_2)_8$-CO-]-
Nylon-6	-[-NH-$(CH_2)_5$-CO-]-
Nylon-11	-[-NH-$(CH_2)_{10}$-CO-]-
Nylon-6,T	-[-NH-$(CH_2)_6$-OCO-(C_6H_4)-OCO-]-
mXD,6,6	-[-NH-$CH_3(C_6H_3)$ -NH-CO-$(CH_2)_4$-CO-]-
Nylon-6,6–6,10 (60:40)	-[-NH-$(CH_2)_6$-NH-{-CO- $(CH_2)_4$-CO-}$_{60}$ /{-CO-$(CH_2)_8$-CO}$_{40}$-]-

Thus, nylon-6,10 is the polyamide produced from the 6-carbon hexamethylene diamine and the 10-carbon sebacic acid, whereas nylon-6 is obtained from the 6-carbon caprolactam and nylon-11 from the 11-carbon aminoundecanoic acid. The coding of nylons derived from ring structures usually includes either a single letter or a combination of letters representing the ring-containing unit. Nylon-6,T refers to a polyamide produced from hexamethylene diamine and terephthalic acid, whereas nylon-mXD,6 is derived from *m*-xylylene diamine and adipic acid. Copolyamide compositions are represented by listing the components in the order of decreasing percentages in parenthesis. Thus, nylon-6,6–6,10 (60:40) refers to a product obtained by copolymerizing hexamethylene diamine with 60% adipic acid and 40% sebacic acid.

Among various nylon compositions, nylon-6 and nylon-6,6 are by far the most important polyamides for the commercial production of fibers and resins. This chapter will focus largely on the fiber-related aspects of these two nylons. Other nylons marketed for minor fiber applications will be discussed appropriately. A wealth of information on nylon technology exists in the literature [4–8].

2.2 BASIC CHEMISTRY OF ALIPHATIC POLYAMIDES

2.2.1 Synthetic Routes

Generally speaking, polyamides can be synthesized by direct amidation where an amine reacts with a carboxylic acid with the removal of water. The reactive amine and acid groups may be on a single amino acid molecule:

$$H_2NRCOOH \leftrightharpoons H-(HNRCO)_n-OH + H_2O$$

or in different molecules:

$$RNH_2 + R'COOH \leftrightharpoons RNH_3^+ + R'COO^- \leftrightharpoons RNHCOR' + H_2O$$

where R represents an aliphatic chain segment or aromatic unit. An ester derivative of the carboxyl group may be used in some cases to facilitate the reaction:

$$RNH_2 + R'COOR'' \leftrightharpoons RNHCOR' + R''OH$$

An alternative route involves the reaction of acid chloride and amine at low temperatures to form high-melting polyamides:

$$H_2NRNH_2 + ClCOR'COCl \leftrightharpoons H_2NRNH(COR'CONH\ RNH)_{x-1}COR'COCl + (2R-1)HCl$$

This method of synthesis avoids polymer decomposition or cross-linking at high temperatures. This reaction can be carried out by interfacial polymerization where the diacid is added in a

water-immiscible solvent to an aqueous solution of the diamine, an inorganic base, and surfactant. Polymerization will take place in the organic layer at the interface. A single-phase solution polymerization can also be used for this reaction in the presence of an acid acceptor.

For aliphatic polyamides, the method of direct amidation is used predominantly. The syntheses of the commercially important nylons may be represented by the general Equation 2.1 through Equation 2.3. Equation 2.1 refers to the formation of AABB-type nylons:

$$\begin{aligned} &H_2N-(CH_2)_x-NH_2 + HOOC-(CH_2)_{y-2}-COOH \\ &\leftrightharpoons -[-HN-(CH_2)_x-NH-OC-(CH_2)_{y-2}-CO-]- \end{aligned} \tag{2.1}$$

Equation 2.2 and Equation 2.3 pertain to the polycondensation of amino acids and to the ring-opening polymerization of lactams for the synthesis of AB-type nylons, respectively:

$$H_2N-(CH_2)_{z-1}-COOH \leftrightharpoons -[-HN-(CH_2)_{z-1}-CO-]- + H_2O \tag{2.2}$$

$$HN-(CH_2)_{z-1}-C=O \leftrightharpoons -[-HN-(CH_2)_{z-1}-CO-]- \tag{2.3}$$

Lactams may be converted to the corresponding nylons by water-initiated polymerization. The reaction may also be initiated by a base that requires anhydrous conditions and proceeds at high reaction rates [9,10]. Initiators used include carbonates, hydrides, alcoholates, and hydroxides of alkali and alkaline earth metals. The conversion of lactams to polyamides is also possible by a cationic process, entailing initiation in an anhydrous medium by either strong protonic acids or their dissociable salts [11].

2.2.2 Amidation Reactions

Nylon-6,6 and other AABB-type aliphatic polyamides are synthesized according to Equation 2.1, while that of aliphatic amino acids forms AB-type polyamides according to Equation 2.2.

These polycondensation reactions proceed by a mechanism that is characterized by carbonyl addition–elimination reactions, which may be catalyzed or uncatalyzed as indicated in the general reaction scheme (2.4)

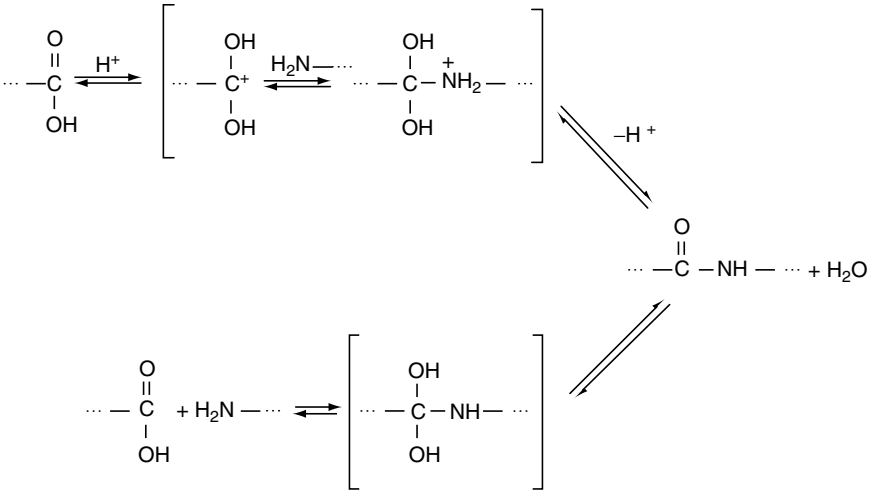

(2.4)

Assuming equivalence of all the amide groups formed and independence of the end groups from the molecular chain length, the equilibrium constant K_c, as defined by

Equation 2.5, thus governs the condensation equilibria according to Equation 2.1 and Equation 2.2.

$$K_c = [NHCO][H_2O]/[COOH][NH_2] = K_c/K_c' \tag{2.5}$$

Thus, the molecular weight of the resulting polyamides will always remain finite and will be affected considerably by any stoichiometric imbalance of the end groups. Nonequivalence of the concentration of functional groups may involve only the bifunctional reactants, or result from the presence of a monofunctional species containing a nonreactive terminal unit, or may be caused by the decomposition of the end groups. Nonequivalence of the concentration of the bifunctional reactants and the addition of monofunctional species such as acetic acid are practiced for molecular weight control. The effect of such nonequivalence on the degree of polymerization (P_n) is represented by Equation 2.6:

$$P_n = \frac{1 + r + q}{(1 + r)(1 - p) + q} \tag{2.6}$$

where p is the extent of reaction and is defined here by Equation 2.7

$$p = 1 - ([COOH] + [NH_2])/([COOH]_o + [NH_2]_o) \tag{2.7}$$

and

$$r = [NH_2]_o/[COOH]_o'; \quad q = [COOH]_o'/[COOH]_o$$

where [COOH]′ stands for the concentration of a monofunctional structure, here a monocarboxylic acid, and the subscript o refers to initial concentrations.

Applying the concept of equal reactivity of all functional groups, the rate of polycondensation according to the general Equation 2.4 may be expressed in terms of the extent of reaction by the rate equation 2.8.

$$\frac{dp}{dt} = 2k_c[COOH]_o(1 - r)\left\{\frac{r}{(1 + r)^2} - \frac{p}{2}\left[1 - \frac{p}{2}\left(1 - \frac{X_w(t)}{K_c}\right)\right]\right\} \tag{2.8}$$

where K_c is the equilibrium constant as defined by Equation 2.5; k_c is the rate constant that may assume one of the following forms:

1. $k_c = k_c^\circ$ [cat.], if the reaction is catalyzed by the addition of a catalyst.
2. $k_c = k_c^\circ + [COOH]k_c^\circ$, if the reaction is catalyzed by the carboxyl groups present in the reacting system.

In these expressions, k_c° is the rate constant for the uncatalyzed reaction and [cat.] is the concentration of any added catalyst. The momentary carboxyl group concentration [COOH] may be expressed in terms of the initial concentration and the extent of reaction of Equation 2.9:

$$[COOH] = [COOH]_o\left\{1 - \frac{p(1 + r)}{2}\right\} \tag{2.9}$$

The term $X_w(t)$ represents the fraction of the water formed by the polycondensation reaction present in the system. Thus, a solution of Equation 2.8 is only possible if an explicit expression for $X_w(t)$ can be developed. The problem obviously entails simultaneous diffusion

and reaction since X_W is related to the rate at which water is removed from the system. Approaches for corresponding analytical treatments involving specific reactor geometries [12] and modes of operations utilize differential equations such as Equation 2.10 [13,14].

$$\frac{\partial w}{\partial t} = D_w\left[\frac{\partial^2 w}{\partial Z^2} + \frac{g}{z}\frac{\partial w}{\partial z}\right] + \frac{[COOH]_o(1+r)}{2}\frac{dp}{dt} \tag{2.10}$$

where D_w is the diffusion coefficient, z is distance in the direction of diffusion, and g is a geometrical factor.

2.2.3 Ring-Opening Reactions

The polycondensation equilibrium, as represented by Equation 2.5, is also part of the more complex mechanism of the water-initiated polymerization of lactams (Equation 2.3), which entails hydrolytic ring opening (Equation 2.11), condensation (Equation 2.12), and addition (Equation 2.13), as the principal equilibrium reactions [15].

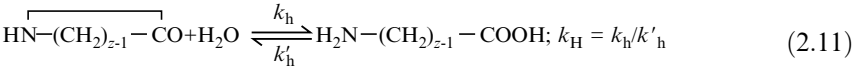

(2.11)

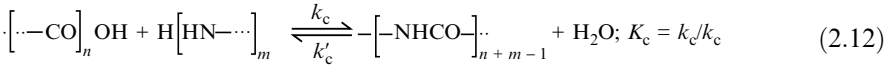

(2.12)

(2.13)

In the anionic polymerization of lactams, the reaction mechanism entails initiation (Equation 2.14) and propagation (Equation 2.15) reactions:

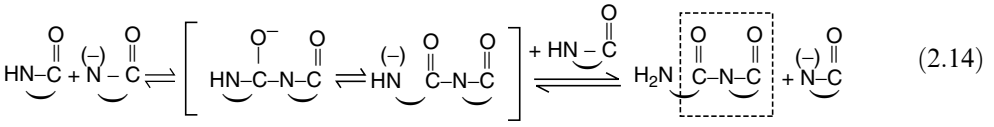

(2.14)

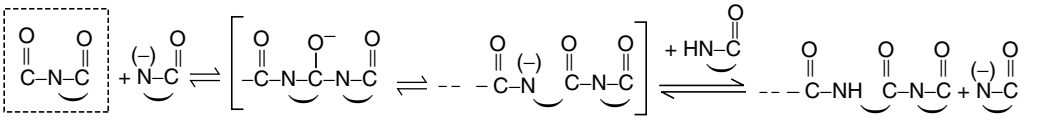

(2.15)

The initiation reaction yields an imide moiety, which constitutes a growth center for propagation reaction. Addition of certain imides such as acyl lactams as coinitiators essentially eliminates the initiation reaction and makes possible the polymerization at relatively low reaction temperatures. Mechanistic and kinetic aspects of the anionic polymerization of lactams have been treated quite extensively [16b]. The discussed subjects relate to the various equilibria governing the polymerization process. They comprise equilibria allied to monomer conversion, to the formation of cyclic oligomers, and to the effect of initiator concentrations.

Although the general reaction mechanisms of polymerization are independent of the size of the lactam ring, quantities related to the ring size mainly determine the polymerizability of a particular unsubstantiated lactam containing only carbon atoms.

As any ring-opening polymerization, the polymerization of lactams is characterized by competition between the intermolecular reaction resulting in a linear polyamide and the intramolecular reaction of cyclization. Thus, if thermodynamically feasible, as indicated by a negative value of the free-energy change of polymerization ΔG_p, the conversion of lactam to the linear polyamide can be realized if an appropriate reaction path exists for a reasonable rate in a polymer–monomer equilibrium characterized by a preponderance of linear macromolecules. The corresponding equilibrium monomer concentration $[M]_e$ is related to the standard enthalpy ΔH_p^0 and entropy ΔS_p^0 of polymerization and to temperature by Equation 2.16.

$$\Delta G_p = -RT\ln K_A = \Delta H_p^0 - TAS_p^0 = RT\ln[M]_e \tag{2.16}$$

It is readily seen that there is a reciprocal relationship between K_A and $[M]_e$. The equilibrium constant K_A is therefore a direct measure of the polymerizability of a particular lactam, and ΔH_p^0 and ΔS_p^0 are thus the corresponding principal parameters.

Polymerization in general is an exoentropic process due to the decrease of translational entropy, resulting from the ordering of individual molecules into a polymer chain. In case of the polymerization of lactams, the decrease in translational entropy is in part compensated by increases in rotational and vibrational entropies resulting from the conversion of the cyclic structures into flexible polymer chain segments. In most lactams, with the probable exception of those with more than 12 ring atoms [17], this compensation does not result in a negative entropy term in Equation 2.16. Therefore, negative values for the overall change of the free energy of polymerization of lactams containing up to 12 ring atoms result from enthalpy changes. The enthalpy change for the polymerization of these lactams is related to the difference between the strain in the particular ring structure and the strain in the corresponding linear polymer segment. Strain in lactams results from molecular deformations, which may be expressed in terms of:

1. Bond stretching (compression), related to the bond length and the motion of bonded nuclei along the internuclear line
2. Bond angle distortion (angle strain, Baeyer strain), related to the radial scissoring motion of the bond angle
3. Bond torsion (bond opposition, Pitzer strain), related to rotational motion around the bond axis and the interaction between substituents on neighboring ring atoms
4. Transannular strain (compression of van der Waals' radii), related to interaction between substituents on nonadjacent ring atoms
5. Conformational strain entailing the amide group

The extent to which each type of strain contributes to the total molecular strain depends on the ring size. Bond angle distortion is the principal source of strain in the three- and four-membered lactams, whereas torsional forces are mainly responsible for the strain in the five- to seven-membered rings. For the five- and seven-membered lactams, there is additional strain due to the inability of the amide groups to assume planar conformation resulting in a decrease of resonance stabilization [18]. Both torsional forces and nonbonded interactions originate strain predominantly in the larger rings, although decreased resonance stabilization of the amide group also contributes to the strain up to the nine-membered lactams. Regardless of any strain energy, however, the polymerization of lactams up to this size is also characterized by an

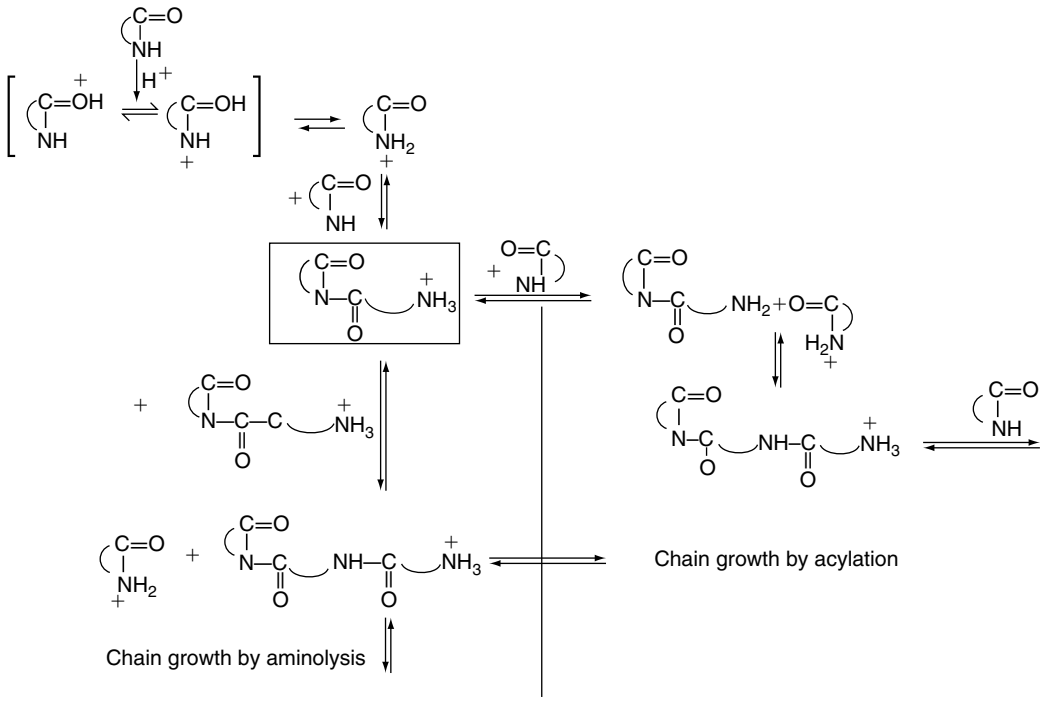

FIGURE 2.1 Mechanism of cationic polymerization of lactams.

additional energy gain of 1.4 kcal/mol due to the *cis–trans* conversion of the amide groups proceeding along with the transition of the ring structures to the linear polyamides.

In addition to the aspects discussed thus far, the polymerizability of lactams is also affected by the presence of heteroatoms in the ring moiety [19–21] and by substituents. The latter affect both enthalpy and entropy of polymerization mainly due to changes in the conformation on conversion of the cyclic structures into linear ones. The overall effects depend markedly on number, size, location, and nature of the substituents [22–26].

Kinetic presentations of the polymerization of lactams may be derived from the general mechanistic schemes presented above. The kinetics of the polymerization of caprolactam has been investigated extensively. It will be reviewed later together with the discussion on nylon-6.

This process for *cationic polymerization* of lactams has been studied extensively. Figure 2.1 shows the principal reactions of monomer conversion and chain growth [27]. Mechanistically, chain growth can commence on both the ammo-terminal end via acylation and the carboxy-terminal end via aminolysis of the polymer molecule. High extents of polymerization are rarely attained because of the occurrence of side-reactions. As shown in Figure 2.2 [27] these side-reactions result in terminal amidine groups that are incapable of adding further lactam. The cationic polymerization process has therefore not attained any practical importance.

An augmented treatment of cationic polymerization has been presented[16d]. Topics regarding initiation, type of initiators, chain growth, and the kinetic particularities of this process were addressed.

2.2.4 Molecular Weight and Molecular Weight Distribution

The polycondensation processes generally produce polyamides that are mixtures of polymer molecules of different molecular weights, the distribution of which usually follows a definite continuous function according to the "most probable distribution" model by Schulz–Flory [3]. This distribution function may, in principle, be derived from the kinetics of polymerization process, but is more readily derived from statistical considerations. In this case, the extent

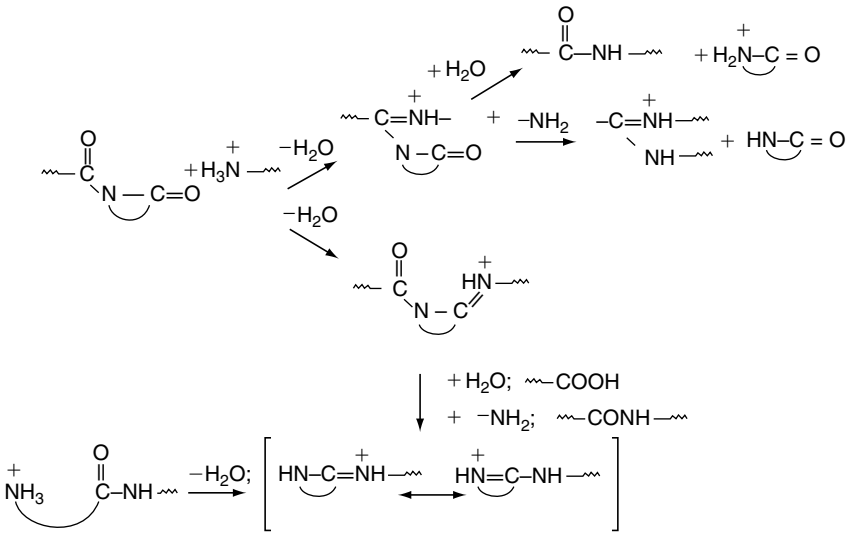

FIGURE 2.2 Formation of amidine functions during cationic polymerization of lactams. (From Reimschuessel, H.K., *J. Polym. Sci., Macromol. Rev.*, 1977, 12, 65. With permission.)

of reaction p (Equation 2.7) is defined as the probability that of all initially present reactive terminal units ($[NH_2]_o + [COOH]_o$), the fraction $2[NHCO]/([NH_2]_o + [COOH]_o)$ has reacted. The fraction of all unreacted units is thus $(1-p)$. Considering a randomly selected polymer molecule, it is now necessary to know the probability that this molecule has exactly λ linkages. The probability of the existence of one linkage is p. The same probability exists independently for any other linkages present in this molecule. Thus, the probability for the existence of λ linkages is p^{λ}. The probability for the existence of an unreacted function in this molecule is $(1-p)$. The probability for the existence of the complete molecule is equal to the product of these two probabilities:

$$p_{\lambda} = p^{\lambda}(1-p) \tag{2.17}$$

This product is equal to the fraction of all molecules that are characterized by λ linkages. The total number of these molecules is given by Equation 2.18 as

$$S_{\lambda} = Sp^{\lambda}(1-p) \tag{2.18}$$

where S is the total number of polymer molecules. Since $P_n = N/S$, where N is the total number of monomeric species converted to polymer, substitution of S by N/P_n and of P_n by Equation 2.6 yields for $r=1$ and $q=0$

$$S_{\lambda} = Np^{\lambda}(1-p)^2 \tag{2.19}$$

This is the number distribution function for a linear step-growth polycondensation at the extent of reaction p. In this instance, λ is given by the relation

$$\lambda = n_{\lambda} - 1 \tag{2.20}$$

where n_{λ} is the number of units interlinked by λ linkages. The weight of the polymer molecules consisting of n_{λ} structural units is $S_{\lambda}\, n_{\lambda}\, \bar{m}$, and $\bar{m}$ is the average mass of the

structural unit of the polymer. The total number of structural units in all polymer molecules is N, and the total weight is then $\bar{m}\,N$. The weight fraction of polymer molecules with a degree of polymerization n_λ is therefore

$$W_\lambda = S_\lambda n_\lambda / N \tag{2.21}$$

Combination of Equation 2.19 and Equation 2.20 gives

$$W_\lambda = p^\lambda (1-p)^2 = n_\lambda p_\lambda^{n-1} (1-p)^2 \tag{2.22}$$

Equation 2.22 is known as the most probable molecular weight distribution derived theoretically by Flory [3]. A presentation of either S_λ/S or W_λ vs. the degree of polymerization n_λ describes a polymer exactly with respect to its molecular weight distribution.

In many instances, however, a characterization by an average molecular weight or an average degree of polymerization is adequate. Several averages may differ considerably from each other. They are defined by the general relation Equation 2.23.

$$\overline{M}_x = \left[\frac{\sum y_i M_i^{\alpha+1}}{\sum y_i M_i} \right]^{1/\alpha} \tag{2.23}$$

where y_i is the fraction of molecules with a molecular weight of M_i.

For practical use, three molecular weight averages are of importance; they are:

$$\text{Number average } \overline{M}_\text{n} (\alpha = -1) \tag{2.23a}$$

$$\text{Weight average } \overline{M}_\text{w} (\alpha = 1) \tag{2.23b}$$

$$\text{Viscosity average } \overline{M}_\text{v} (0.5 < \alpha \geq 1) \tag{2.23c}$$

The number average may be obtained by end-group titration or osmometry, the weight average by light scattering, and the viscosity average by viscometry of dilute solutions.

Although a relative method, viscometry is the most convenient one and therefore widely used for rapid and reliable characterization of polyamides. It entails the determination of the intrinsic viscosity $[\acute{\eta}]$, which is a measure of the hydrodynamic volume of the macromolecular coil and depends, for a given solvent, on the molecular weight of the polymer. It is defined by relations such as

$$\lim_{c \to 0} \eta_\text{red} = \lim_{c \to 0} \eta_\text{sp}/c = [\eta] \tag{2.24}$$

Therefore, its determination usually entails the extrapolation of the concentration dependence of reduced viscosity quantities to zero polymer concentration. For the determination of $[\eta]$ the most frequently used are the classical Huggins [28] and Kraemer [29] equations:

$$\eta_\text{sp}/c = [\eta](1 + k_\text{H}[\eta]c) \tag{2.25}$$

$$\ln \eta_\text{rel}/\text{c} = [\eta](1 - \text{k}_\text{K}[\eta]\text{c}) \tag{2.26}$$

where η_{sp} is the specific viscosity, η_{rel} is the relative viscosity of the solution compared to the solvent, c is the concentration in g/dl, and k_H and k_K are the Huggins and Kraemer coefficients, respectively, related by the relationship $k_H + k_K = 0.5$. This relationship may not be applicable for low-molecular-weight polyamides [30,31]. For a given polymer, the intrinsic viscosity is related to the average molecular weight by the equation

$$[\eta] = KM^a \tag{2.27}$$

which has been associated with the names of a number of scientists: Staudinger, Mark, Kuhn, Houwink, and Sakurada. The parameters a and K are functions of the polymer solvent system. Theoretically, the parameter a may have values from 0.5 to 2.0. The lower value would correspond to a Gaussian molecular coil of unperturbed dimensions (impermeable, no excluded volume, θ-conditions). A value of 2 would indicate a rodlike structure. Aliphatic polyamides are flexible macromolecules for which a has values between 0.5 and 0.9. The higher values are observed in good solvents due to expansion of the molecular coil. Some of the published values for the parameters K and a (Equation 2.27) are listed in Table 2.1 [32–45]. A more complete listing and a detailed discussion on molecular weight determination and dilute solution properties of aliphatic polyamides have been presented [46].

TABLE 2.1
Parameters for Mark–Houwink Equation: $[\eta] = KM^a$

Solvent	Temperature (°C)	Calibration method	MW range ($M \times 10^{-3}$)	10^4K dl/g	a	Ref.
Nylon-4						
m-Cresol	25	LS (M_w)	10–300	4.0	0.77	32
m-Cresol	25	EG (M_n)	1.7–14	30.0	0.70	33
Nylon-6						
m-Cresol	25	LS (M_w)	5–40	5.57	0.73	34
m-Cresol	25	LS (M_w)	9–335	5.26	0.74	35
m-Cresol	25	EG (M_n)	5–30	18.0	0.65	34
Tricresol	25	OS (M_w)	8–80	2.1	0.90	36
Conc. H_2SO_4	25	EG (M_w)	4–37	6.3	0.76	37
85% HCOOH	20	V (M_v)	7–120	2.26	0.82	38
CF_3CH_2OH	25	V (M_v)	13–100	5.36	0.75	38
Nylon-6,6						
m-Cresol	25	LS (M_w)	7–80	24.0	0.61	39
90% HCOOH + 2M KCl	25	LS (M_w)	2.5–50	14.2	0.56	40
90% HCOOH	25	EG (M_n)	6–24	11.0	0.72	41
m-Cresol	20	V (M_v)	10–40	38.0	0.55	42
Nylon-6,10						
m-Cresol	25	EG (M_w)	8–24	1.35	0.96	43
Nylon-8						
m-Cresol	25	EG (M_w)	1–25	7.0	0.76	44
Nylon-12						
m-Cresol	25	LS (M_w)	3–125	8.1	0.70	45
m-Cresol	25	EG (M_n)	1–33	11.8	0.73	45

The average molecular weights as defined by Equation 2.23 correspond to average degrees of polymerization p_λ that are generally used for correlation with the extent of reaction p (Equation 2.7). The most significant averages are the number average $\bar{P}_n$ and the weight average P_w. They are defined by Equation 2.28 and Equation 2.29.

$$\bar{P}_n = (\sum_\lambda S_\lambda n_\lambda)/(\sum_\lambda S_\lambda) = \Sigma p_\lambda n_\lambda \tag{2.28}$$

$$\bar{P}_w = (\sum_\lambda S_\lambda n^2)/(\sum_\lambda S_\lambda n_\lambda) = \Sigma w_\lambda n_\lambda \tag{2.29}$$

Combining with Equation 2.17 and Equation 2.22, respectively, and evaluating the summations

$$\sum_\lambda n_\lambda p_\lambda^{n-1}(1-p)$$

and

$$\sum_\lambda n_\lambda^2 p_\lambda^{n-1}(1-p)^2$$

yields, since $p < 1$:

$$\bar{P}_n = \frac{1}{1-p} \tag{2.30}$$

$$\bar{P}_w = (1+p)/(1-p) \tag{2.31}$$

The ratio $\bar{P}_w/\bar{P}_n = 1+p$ is equal to the ratio $\bar{M}_w/\bar{M}_n$ and is referred to as the polydispersity index, since it is a measure of the polydispersity of the polymer. For linear polyamides, its value approaches 2 with increasing extents of reaction. Nonstoichiometric concentrations of bifunctional reactants or the presence of monofunctional species results in modified expressions for $\bar{P}_n$ and $\bar{P}_w$ (see Equation 2.6), but cause only negligible changes of the ratio $\bar{P}_w/\bar{P}_n$.

Both the molecular weight and the molecular weight distribution are of prime importance in (1) controlling and thus conducting the polymerization process; (2) the fiber forming process, because of the strong effects on the rheological properties of the melt of polyamides; and (3) the final product characteristics, particularly in regard to the tensile properties. Therefore, more than the determination of one molecular weight is necessary for adequate polymer characterization and evaluation.

The literature includes a quite detailed discussion of molecular weight determination, polydispersity, conformational rigidity, and branching [16d]. Subjects associated with end group analysis, membrane osmometry, light scattering, viscometry, turbidimetric titration, gel permeation chromatography, and branching are discussed. The identification of textile fibers by nondestructive interference microscopy also has been reported in a discussion of the quantitative analysis of interferograms in connection with the equirefractive immersion for the classification of textile fibers [47]. The method entails the measurement of the two refractive indices in light polarized parallel and perpendicular to the fiber axis. Computerized evaluation has been used in characterization and identification of chemical fibers by infrared spectrometric methods [48].

2.2.5 Nylon-6,6 Polyamide

Nylon-6,6 is the generic term for poly(hexamethylene adipamide). It is commercially synthesized by polycondensation from hexamethylene diamine and adipic acid according to the amidation reaction of Equation 2.1:

$$n\mathrm{H_2N}-(\mathrm{CH_2})_x-\mathrm{NH_2} + n\mathrm{HOOC}-(\mathrm{CH_2})_4-\mathrm{COOH}$$

Hexamethylene diamine Adipic acid

$$\rightleftharpoons \mathrm{H}-[-\mathrm{HN}-(\mathrm{CH_2})_6-\mathrm{NH}-\mathrm{OC}-(\mathrm{CH_2})_4-\mathrm{CO}-]_n-\mathrm{OH} + 2n\mathrm{H_2O}$$

Nylon-6,6: poly(hexamethylene adipamide)

2.2.5.1 Synthetic Procedure

Zimmerman et al. [5–7] gave a comprehensive summary of this synthesis. Hexamethylene diamine melts at 40.9°C and is normally used in the form of a concentrated aqueous solution. Adipic acid has a melt temperature of 152.1°C and is used in its pure solid form. A salt solution of about 50% concentration containing precisely stoichiometric quantities of the two intermediates is first prepared. In a typical polymerization reaction, the salt solution is heated to boiling to evaporate water, possibly at elevated pressure, until its salt content reaches $\geq$60%. The concentrated salt solution is then heated gradually in a reactor as water is evaporated, typically from 212°C to 275°C at 1.73 MPa (250 psi). The polymer molecular weight will reach about 4400 at this point. The pressure is then gradually reduced to atmospheric to allow further reaction for about an hour. The polymer molecular weight is now in the range of 15,000 to 17,000, but is not quite equilibrated. All of the liquid water in the salt solution and nearly all of the potential water of reaction in the form of amine and carboxyl end groups are removed at this point. The loss of hexamethylene diamine, which boils at 200°C, is minimal. The resulting polymer is suitable for melt spinning or chip forming.

2.2.5.2 Kinetics and Thermodynamics

The equilibrium constant K_c is defined in Equation 2.5 as a function of end group and water concentrations: $[\mathrm{NHCO}][\mathrm{H_2O}]/[\mathrm{COOH}][\mathrm{NH_2}]$. For a typical reaction of high conversion and high polymer molecular weight, the equilibrium constant at 280°C is about 300 ± 50. The amide group concentration [NHCO] at high conversions is almost constant as molecular weight varies. The water concentration in the melt at a given temperature depends only on the water vapor pressure. According to Equation 2.5, therefore, the equilibrium value of $[\mathrm{COOH}][\mathrm{NH_2}]$ is proportional to the water concentration at low steam pressures and high molecular weights. The amidation reaction at high conversions is exothermic with a heat of reaction of about 25–29 kJ $\mathrm{mol^{-1}}$ (6–7 kcal $\mathrm{mol^{-1}}$)[4]. This is in the same range as the endothermic heat of vaporization of water from nylon based on equilibrium regain data extrapolated to the reaction temperature. For this reason, the decrease in equilibrium constant K_c with increasing temperature is almost exactly offset by the reduction in water content $[\mathrm{H_2O}]$ at a given steam pressure. The equilibrium value of $[\mathrm{COOH}][\mathrm{NH_2}]$ does not change significantly for some given water vapor pressure as the temperature is varied.

This polycondensation reaction follows a second-order kinetics at conversions up to about 98. It becomes a third-order reaction at higher conversion where it is catalyzed by [COOH] end groups. In the presence of water, the overall rate of reaction is a function

of $[COOH]^2[NH_2]$ for amidation and of $[COOH][H_2O]$ for hydrolysis. For nylon-6,6, the activation energy for polyamidation has been estimated at about 88 kJ mol^{-1} (21 kcal mol^{-1}). This is significantly higher than that for diffusion, which is estimated to be 59 kJ mol^{-1} (14 kcal mol^{-1}) at temperatures well above the polymer melting point. The rate of increase is about 40% for a 10°C temperature increase in the normal range of polymerization temperatures. Thus, the reaction equilibrium as manifested in Equation 2.10 is quite favorable for nylon-6,6. Under an atmosphere of steam, the reaction rate is not affected by diffusion (stirring) and by the rate of water removal up to a polymer molecular weight of about 18,000. As with [COOH] carboxyl end groups, hypophosphite salts and phosphonic acids have also been found to exert catalytic effect to the nylon-6,6 reaction at high conversions.

The molecular weight distribution of linear nylon-6,6 follows the most probable distribution of Equation 2.22. The average number polymerization degree $\overline{P}_n = 1/(1–p)$. The number average molecular weight $\overline{M}_n$ can be obtained by multiplying the respective value of $\overline{P}_n$ by the molecular weight of repeat unit. If the end groups are not widely unbalanced, an average value of molecular weight for the two kinds of end groups, 113 g for nylon-6,6, may be used. If 99% of the original end groups react, $p = 0.99, \overline{P}_n = 100, \overline{M}_n = 11{,}300$. This appears to be the low limit for most commercial nylon-6,6 today. At higher conversion, for example, $p = 0.993$, $\overline{P}_n = 143, \overline{M}_n = 16{,}140$, and $\overline{M}_w = 32{,}170$.

For linear polyamides, the viscosity of dilute or moderately concentrated solution can be related closely to $\overline{M}_w$. Thus, the molecular weight of polymer can be evaluated from $\eta_{inh} = \ln \eta_{rel}/c$. This is usually measured at a concentration of 0.5 g of polymer in 100 ml of solvent, e.g., *m*-cresol. A typical value of η_{inh} of nylon-6,6 is one for $\overline{M}_n$ of about 15,000. Another method of characterization commonly used is to measure the relative viscosity (RV) of an 8.4% solution of polymer in 90% formic acid. Typical values of relative viscosity for nylon-6,6 are in the range of 30 to 70. An RV of 41 corresponds to $\overline{M}_n$ of about 15,000, whereas an RV of 60 corresponds to about 19,000. Polymers in the lower range are used for textile yarns, and those in the higher range for industrial yarns.

2.2.5.3 Solid-State Polymerization

According to a DuPont patent, nylon-6,6 and nylon-6 can be subjected to solid-state polycondensation at temperatures below its melting point [49,50]. As an example, a nylon-6,6 prepolymer with a molecular weight of 2500 was polymerized at 216°C for 4 hr to attain a molecular weight of 16,000. Zimmerman [6] investigated the kinetics of solid-state polymerization of nylon early in 1953 [7]. He observed that the reaction is catalyzed by [COOH] end groups and follows third-order kinetics. Unlike low molecular weight prepolymers having end groups with a high degree of ionization, the polymers for solid-state polymerization are initially at high conversions and their end groups are mostly in the nonionic form. In fact, the third-order reaction rate is not quite four times as fast as expected of the melt reaction at the same temperature. The activation energy for amidation and that for diffusion of reactive ends in solid state are similar—about 84 kJ mol^{-1} (20 kcal mol^{-1}). Thus, it was suggested that the rate of solid-state polymerization is largely diffusion-controlled.

The molecular weight distribution for solid-state polymerization is about normal, if the polymer does not exceed the entanglement point. Branching occurs in the polymer and the ratio of $\overline{M}_w/\overline{M}_n$ will increase to 3.4 beyond this point.

2.2.6 Nylon-6 Polyamide

Nylon-6 is the generic name for polycaprolactam. It is almost exclusively synthesized from ε-caprolactam by a ring-opening reaction: Equation 2.3

$$\underset{\varepsilon-\text{caprolactam}}{\overbrace{HN-(CH_2)_5-C=O}} \leftrightharpoons -[-\underset{\text{Nylon 6: polycaprolactam}}{HN-(CH_2)_5-CO-}]-$$

The reaction is essentially an addition polymerization, but can be considered to be the condensation polymerization of AB-type polyamide.

2.2.6.1 Synthetic Procedure

Caprolactam melts at about 69°C. It does not polymerize upon heating to elevated temperatures. However, shortly after Carothers developed nylon-6,6, Schlack [51] of I.G. Farben discovered that the ring-opening reaction occurs readily in the presence of amine and carboxyl groups. Thus, ε-aminocaproic acid, nylon-6,6 salt, or simply water, is employed to hydrolyze lactam to form [COOH] and [NH_2] end groups. The [COOH] group catalyzes the addition of [NH_2] to the caprolactam ring. This discovery led to the polymerization of caprolactam for nylon-6.

The polymerization of caprolactam is carried out initially in the presence of water at 265°C initially under pressure. It is generally characterized by an induction period to build up the hydrolyzed products. As the end group concentrations increase, the carboxyl-catalyzed amine addition proceeds at an increasing rate and the polymer chain grows. This reaction also produces cyclic oligomers. The [COOH] and [NH_2] end groups reach a maximum concentration with time and then decreases as the monomer content depletes to equilibrium. The equilibrium constants for the end groups in nylon-6 is reportedly in the range from about the same as nylon-6,6 to somewhat above, e.g., 428 at 280°C [5–7].

2.2.6.2 Kinetics and Thermodynamics

The heat of amidation is about the same as nylon-6,6. The activation energy for polymerization is about 78 kJ mol^{-1} (18.7 kcal mol^{-1}) for the −COOH-catalyzed reaction and 88 kJ mol^{-1} (21 kcal mol^{-1}) for the uncatalyzed reaction. The activation energy of melt viscosity is about 60 kJ mol^{-1} (14.3 kcal mol^{-1}), which is almost the same as for nylon-6,6. The values of K and a in the Mark–Houwink equation, as shown in Table 2.1, are 18.0×10^4 dl/g and 0.65 in *m*-cresol at 25°C, respectively.

The molecular weights of nylon-6 are generally in the same range as nylon-6,6. Its molecular weight distribution as prepared under the above conditions is also the same as linear nylon-6,6 and other linear condensation polymers with $\overline{M}_w/\overline{M}_n = 1 + p$, or about two. However, nylon-6 and AB polyamides are unique in that a narrower molecular weight distribution can be attained by adding a bifunctional stabilizer such as the Bb-type dicarboxylic acid [37]. An AB polymer chain can only pick up one BB unit and becomes terminated with B end groups at both ends. For example, if 40 equiv. 10^{-6} g. of BB units are added and the concentration of A ends [NH_2] is reduced to 10 equiv. 10^{-6} g, $\overline{M}_w/\overline{M}_n = 1.6$. It would be possible to increase $\overline{M}_n$ by 25% in that case.

Reimschuessel reviewed the water-initiated, ring-opening polymerization of caprolactam in detail [27]. In an attempt to analyze the process from its kinetic and mechanistic aspects, the equilibrium reactions 2.11, 2.12, and 2.13 are conventionally presented as follows:

1. Ring opening

$$\underset{x}{CL} + \underset{w}{H_2O} \underset{k_1'}{\overset{k_1}{\rightarrow}} \underset{s_1}{ACA} \quad (K_1)$$

where C denotes the carboxyl group, L the lactam segment, and A the amine group.

2. Polycondensation

$$s_n + s_m \underset{k_2'}{\overset{k_2}{\rightleftharpoons}} s_{n+m} + w$$

$$\underset{a}{-\mathrm{NH_2}} + \underset{c}{-\mathrm{COOH}} \longrightarrow \underset{z}{-\mathrm{NHCO}-} + \underset{w}{\mathrm{H_2O}} \quad (K_2)$$

3. Polyaddition

$$\underset{x}{\mathrm{CL}} + \underset{s}{s_n} \underset{k_3'}{\overset{k_3}{\rightleftharpoons}} \underset{s-s_1}{s_{n+1}} \quad (K_3)$$

where x is the concentration of caprolactam, w the concentration of water, s the concentration of polymer molecules, the subscripts n and m indicate a degree of polymerization of n or m, S_1 the concentration of ε-aminocaproic acid, c the concentration of carboxyl groups, a the concentration of amine groups, and z the concentration of amide linkages. With $w = w_o - s$, $z = x_o - x - s$, and $s_2 = s$, where w_o is the initial water concentration, s_2 the linear dimer, the following rate equation may be written [9,27]:

$$\mathrm{d}x/\mathrm{d}t = -k_1[x(w_o - s) - s_1/K_1] - k_3[xs - (s - s_1)/K_3] \tag{2.32}$$

$$\mathrm{d}s/\mathrm{d}t = -k_1[x(w_o - s) - s_1/K_1] - k_2[s^2 - (x_o - x - s)(w_o - s)/K_2] \tag{2.33}$$

$$\mathrm{d}s_1/\mathrm{d}t = -k_1[x(w_o - s) - s_1/K_1] - 2k_2[ss_1 - (w_o - s)(s - s_1)/K_2] - k_3(xs_1 - s_1/K_3) \tag{2.34}$$

The kinetic and thermodynamic constants are defined as follows:

$$K_i = k_i/k_i' = \exp[(\Delta S_i - \Delta H_i/T)/R] \qquad (i = 1, 2, 3) \tag{2.35}$$

$$k_i = k_i^{\circ} + k_i^{\mathrm{c}} c \tag{2.36}$$

$$k_i^j = A_i^j \exp(-E_i^j/RT) \quad (j = \mathrm{o}, \mathrm{c}) \tag{2.37}$$

where k_i^{o} is the rate constant for the uncatalyzed reaction and k_i^{c} is the rate constant for the reaction catalyzed by carboxyl end groups.

Values for all of the kinetic and thermodynamic parameters have been reported in the literature. They were usually obtained from experiments in which caprolactam and definite amounts of water were heated in closed systems for various periods of time. From the mechanism and the corresponding rate equation, it is readily seen that for a given temperature the concentration of water is the principal process parameter. It affects both the rate and the attainable degree of polymerization. If in the kinetic experiment, therefore, any free reactor volume (vapor space) is not essentially eliminated (which may pose some experimental problems), then the effective initial water concentration is lower and consequently a lower rate of polymerization will result. This may be one reason for certain differences in values reported by different investigators. Another reason may entail different analytical approaches. Table 2.2 and Table 2.3 show the kinetic and thermodynamic parameters as reported by two different groups [52,53] for the three principal equilibrium reactions.

Both sets of parameters have been used for simulations of the hydrolytic polymerization process [52,54–56] and both appear suitable to predict general responses in different reactor systems as functions of initial composition and process parameters. Comparisons of observed

TABLE 2.2
Kinetic Parameters

	$k_i^j = A_i^j \exp.(-E_i^{0\prime}/RT)$ (i+1,2,3;j = O,C)a							
	A_i^0 (kg/mol-h)		E_i^0 (cal/mol)		A_i^c (kg^2/mol^2-h)		E_i^c (cal/mol)	
i	I	II	I	II	I	II	I	II
1	1,6940x10^6	5,987x10^5	2,1040x10^4	1,9880x10^4	4,1060x10^7	4,3075x10^7	1,873x10^4	1,8806x10^4
2	8,6870x10^9	1,8942x10^{10}	2,2550x10^4	2,3271x10^4	2,3370x10^{10}	1,2114x10^{10}	2,0674x10^4	2,0670x10^4
3	2,6200x10^9	2,8558x10^9	2,1269x10^4	2,2845x10^4	2,3720x10^{10}	1,677x10^{10}	2,0400x10^4	2,0107x10^4

Note: [a]i = 1, ring opening; i = 2, polycondensation; i = 3, polyaddition.
Source: Reimschuessel, H.K.; Nagasubramanian, K., *Chem. Eng. Sci.*, 1972, 27, 1119; Tai, K.; Teranishi, H.; Arai, Y.; Tagawa T., *J. Appl. Polym. Sci.,* 1980, 25, 77. With permission.

TABLE 2.3
Thermodynamic Parameters

	$K_i = \exp.[(\Delta S_i - \Delta H_i/T)/R](i = 1,2,3)^a$			
	ΔS_i (e.u.)		ΔH_i (cal/mol)	
	I	II	I	II
1	−7,8700	−7,8846	$2{,}1142 \times 10^3$	$1{,}9180 \times 10^3$
2	$9{,}3000 \times 10^{-1}$	$9{,}4374 \times 10^{-1}$	$-6{,}1404 \times 10^3$	$-5{,}9458 \times 10^3$
3	−6,9500	−6,9457	$-4{,}0283 \times 10^3$	$-4{,}0438 \times 10^3$

Source: From Tai, K.; Teranishi, H.; Arai, Y.; Tagawa T., *J. Appl. Polym. Sci.,* 1980, 25, 77. With permission.

and calculated data are presented in Figure 2.3 and Figure 2.4. Although the calculated data are in general consistent with the observed ones, certain discrepancies are evident. This is true even for the curves represented by the broken lines, which were calculated using the very same parameters that had been obtained by curve fitting of the experimental data represented by the solid lines [53]. These differences may be a consequence of the definition of the equilibrium constants K_i. Rather than defined by activities, these constants are defined by equilibrium concentrations. Thus they are dependent not only on the temperature but also on the initial composition (that is, the initial water concentration). Consequently, according to Equation 2.35 and Equation 2.37, all of the kinetic and thermodynamic parameters depend on the initial composition. Nevertheless, the kinetic system, as represented by Equation 2.32 through Equation 2.37, has been very useful for predicting responses to changes in process parameters and has been used as a basis for modeling and optimization of the polymerization process [52,54–58].

Both the water concentration and temperature have been identified as the principal process parameters. Their effect on the rate and extent of monomer conversion and on the rate and degree of polymerization is shown in Figure 2.5 through Figure 2.8. The effect of temperature on both reaction rate and equilibrium has been well recognized. As a consequence of the exothermic nature of the addition and condensation reactions, lower temperature is favorable for obtaining higher equilibrium values for both monomer conversion and degree of polymerization.

2.2.6.2.1 Cyclic Oligomers

The formation of low-molecular-weight cyclic polymers during the polymerization of caprolactam is of concern in regard to conversion and polymer molecular weight. These oligomers are soluble in water and in the lower alcohols. Individual members ranging from the cyclic dimer to the cyclic monomer have been identified in polymer extracts. The formation of these ring structures may be explained by intra- or intermolecular transacylation and transamidation, and direct cyclization of the corresponding linear oligomers. The concentration of the cyclic dimer amounts to about 50 mol % of the total concentration of the soluble cyclic oligomers [27]. The formation of these cyclic dimers is represented by reactions in (2.74). A kinetic model postulates that these reactions are governed by the equilibrium reactions (2.32) and (2.33).

$$\overbrace{\mathrm{NH(CH_2)_5CONH(CH_2)_5CO}} + \mathrm{H_2O} \rightleftharpoons \mathrm{H[NH(CH_2)_5CO]_2OH}$$

$$\overbrace{\mathrm{NH(CH_2)_5CONH(CH_2)_5CO}} + \mathrm{H[NH(CH_2)_5CO]_nOH} \rightleftharpoons \mathrm{H[NH(CH_2)_5CO]_{n+2}OH} \quad (2.74)$$

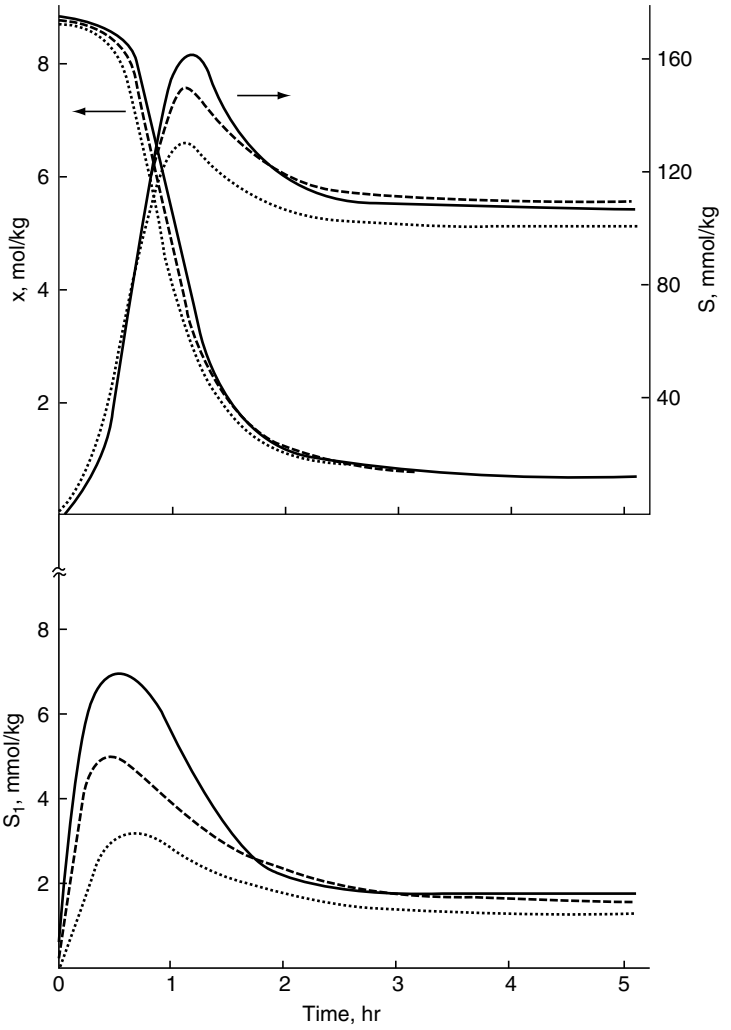

FIGURE 2.3 Comparison of observed and calculated concentration–time relationships for caprolactam (x), polymer chains (s), and amino caproic acid (S_1); $W_o = 0.82$ mol/kg, $T = 259°C$. Solid lines represent experimental data; broken lines calculated using set-II parameters; dotted lines calculated using set I parameters. (From Reirnschuesse1, H.K. and Nagasubramanian, K., *Chem. Eng. Sci.*, 1972, 27, 1119. With permission.)

The kinetic and thermodynamic parameters for these equations have already been reported in polymerization kinetics and simulation studies [59–66]. The rate constants have also been obtained by Reimschuessel [52], without considering cyclization, and by Tai et al. [53], with consideration of cyclic dimer formation. Gupta et al. [56] employed these published data in a numerical analysis of rate equations for the above equilibrium reactions to demonstrate the effects of incorporating the formation of cyclic oligomers into the kinetic scheme. There were no discernible differences for the two sets of rate constants for conversion. However, the final degree of polymerization is slightly lower, and the ratio P_w/P_n approaches a value somewhat higher with calculations based upon Arai et al. [66] than the corresponding values based upon Reimschuessel [52].

In a similar effort, Mallon and Ray [67] refined the kinetic model to include the effect of water on nylon-6 equilibria. Variations in equilibrium were attributed to microscopic states

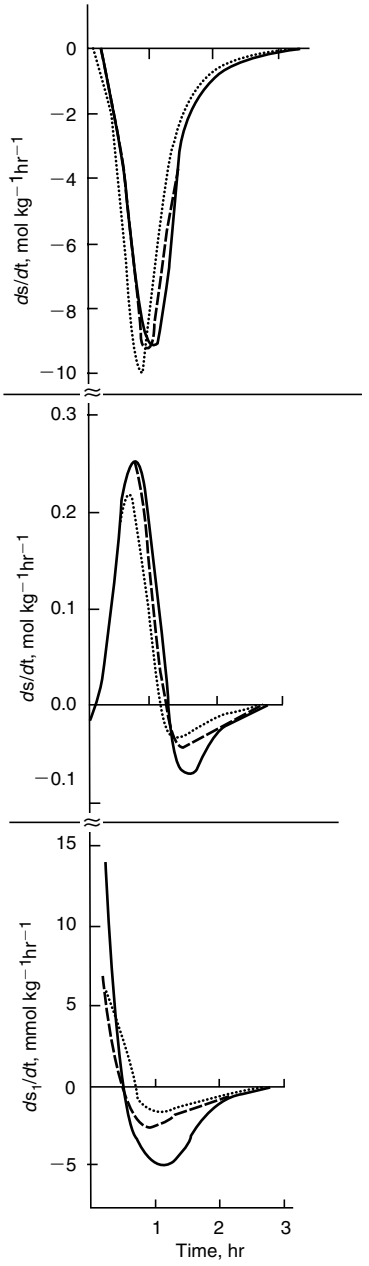

FIGURE 2.4 Comparison of observed and calculated reaction rates dx/dt; ds/dt. $W_o = 0.82$ mol/kg; $T = 259°C$. Solid lines; experimental data; broken lines calculated using set-II parameters; dotted lines calculated using set-I parameters. (From Reimschuessel, H.K. and Nagasubramanian, K., *Chem. Eng. Sci.*, 1972, 27, 1119. With permission.)

of water in nylon melt and were modeled as due to a changing dielectric constant. All reactions were assumed to be acid catalyzed. Results were good for water to polymer ratio ranging from 0.01 to 0.30 and for temperatures from 200 to 280°C. The model framework allowed the calculation of interchange rates and cyclic oligomer concentrations. Figure 2.9 and Figure 2.10 illustrate the results of the proposed model with the model of Tai et al. [68], and Wiloth's

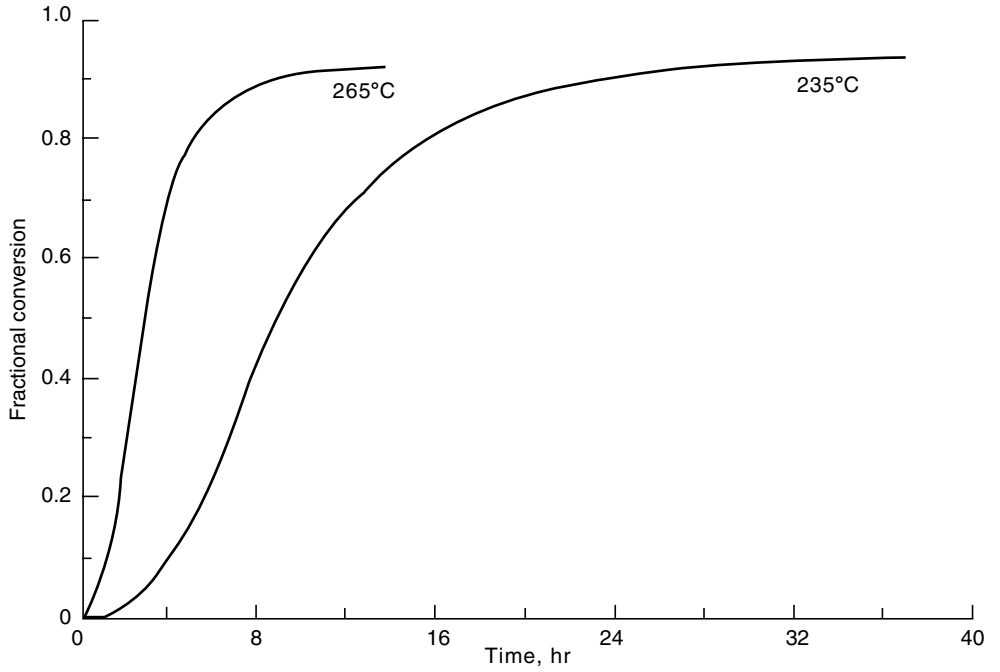

FIGURE 2.5 Effect of temperature on extent of conversion; $[W_o] = 0.02$.

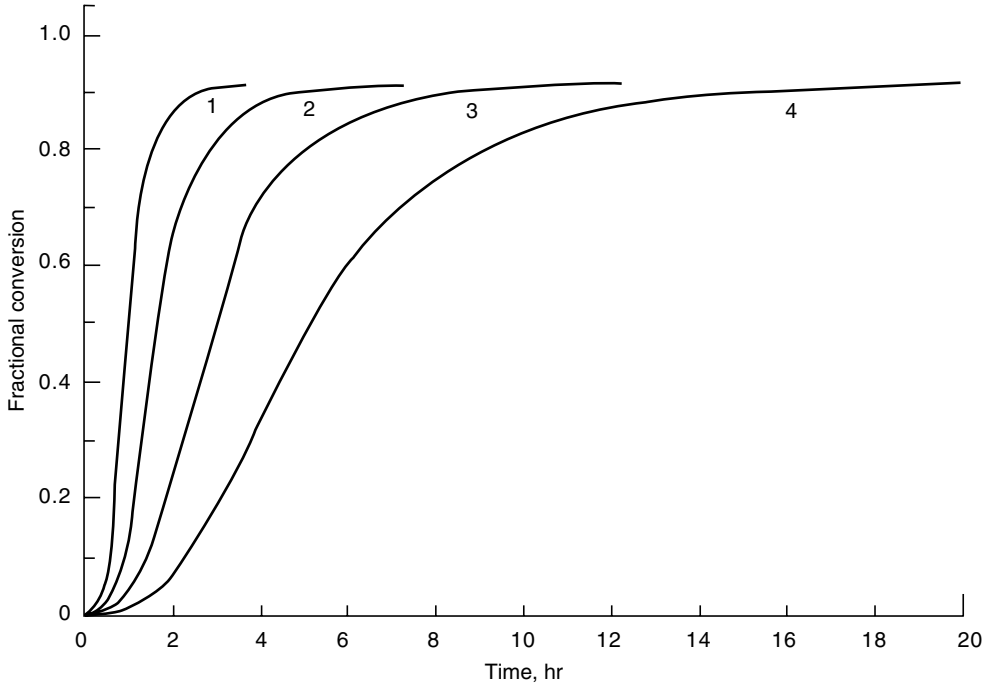

FIGURE 2.6 Effect of initial water concentration $[W_o]$ on extent of conversion; $T = 265^\circ C$; $[W_o]_1 = 0.08$; $[W_o]_2 = 0.04$; $[W_o]_3 = 0.02$; $[W_o]_4 = 0.01$.

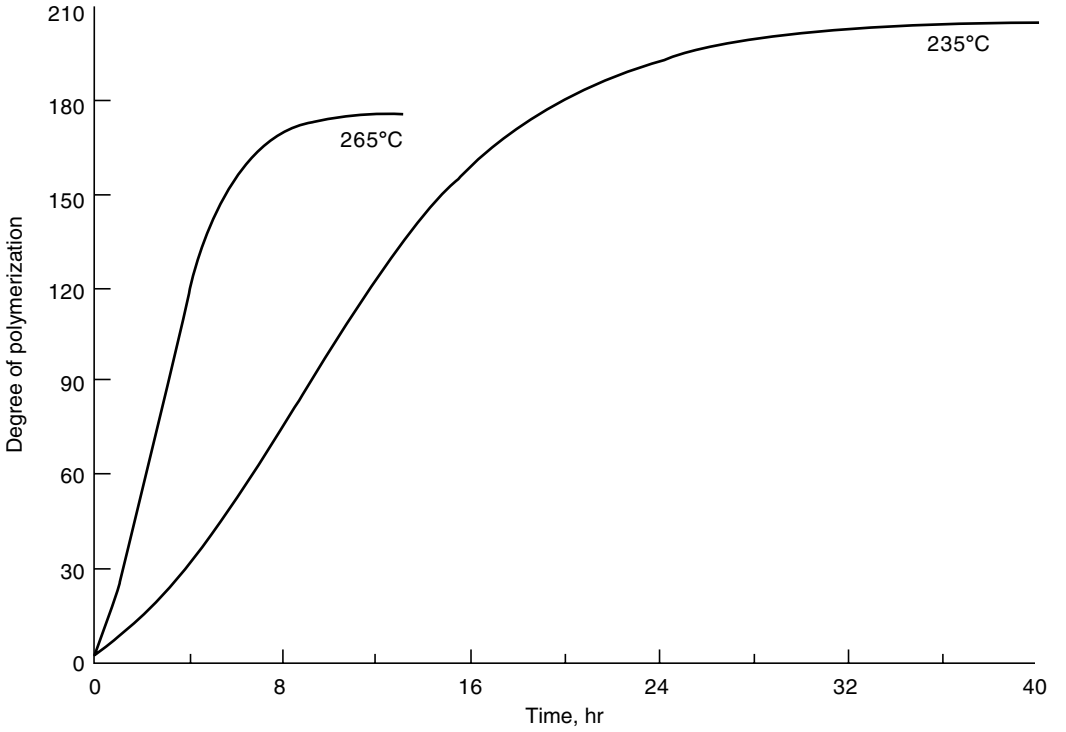

FIGURE 2.7 Effect of temperature on rate and degree of polymerization; $[W_o] = 0.02$.

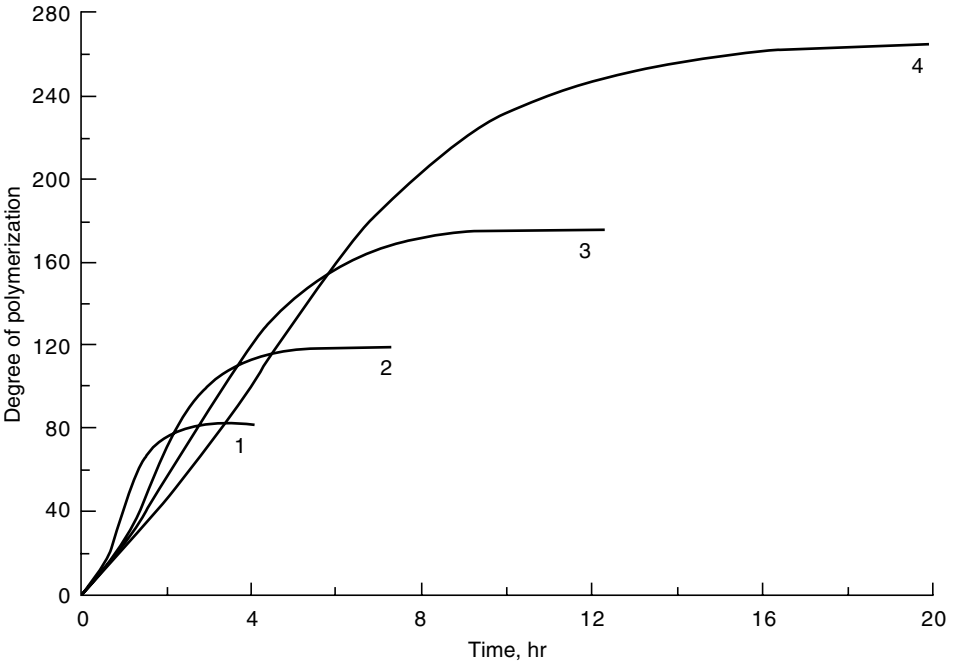

FIGURE 2.8 Effect of initial water concentration $[W_o]$ on rate and degree of polymerization; $[W_o]_1 = 0.08$; $[W_o]_2 = 0.04$; $[W_o]_3 = 0.02$; $[W_o]_4 = 0.01$.

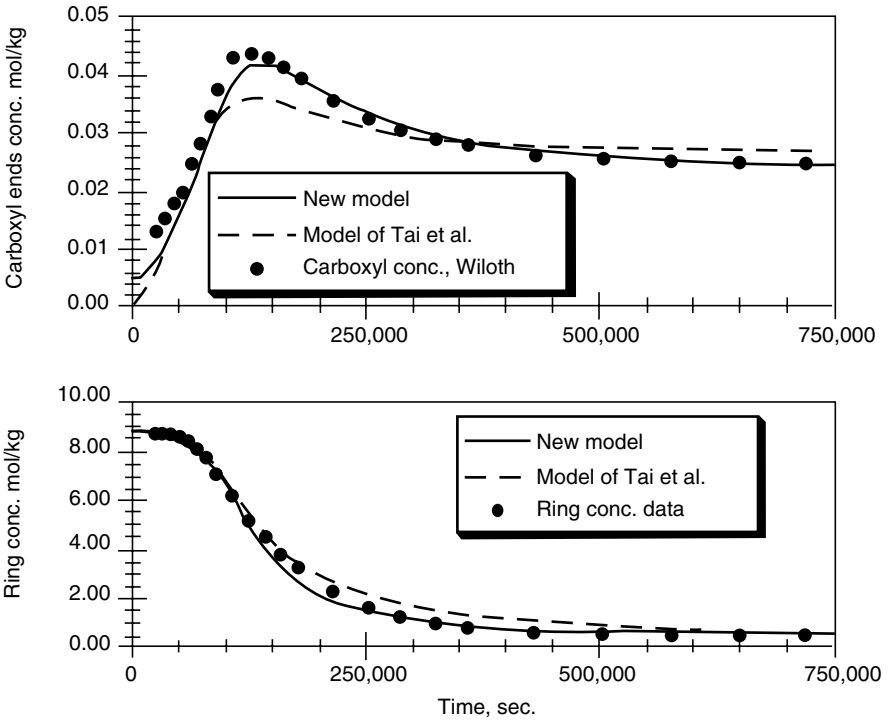

FIGURE 2.9 Polymerization at 220°C, $[W_o] = 1$ mol %. (From Mallon, F.K. and Ray, W.H., *J. Appl. Polym. Sci.*, 1998, 69, 1213–1221. With permission.)

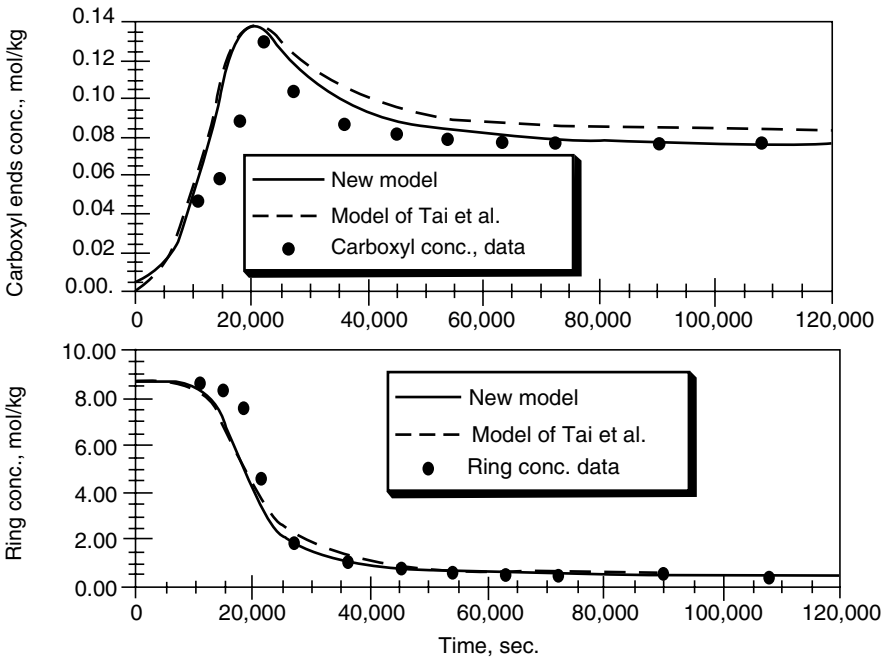

FIGURE 2.10 Polymerization at 220°C,. $[W_o] = 8$ mol %. (From Tai, K.; Tagawa, T.; *Ind. Eng. Chem. Prod. Res. Dev.*, 22, 192, 1983.)

data at 220°C for two different water concentrations: 1 and 8 mol% [69]. Wiloth carried out nylon-6 reactions with low water contents, leading to molecular weights as high as 35,000. Such molecular weights are industrially germane and are of interest to kinetic modeling. The model of Tai et al. is the standard model that assumes constant equilibrium and a mixture of second- and third-order reaction for all the reactions. At very low water content, both models follow the Wiloth data reasonably well, with the Mallon and Ray model performing somewhat better in both cases.

2.2.7 Other Polyamides

Many aliphatic polyamide compositions have been attempted in search of improved polymer end-use properties and cost advantages. Table 2.4 summarizes some of the polyamides from recent literature [5,6]. Among them, nylon-4, nylon-11, nylon-12, and nylon-4,6 are notable for industrial interests.

2.2.7.1 Nylon-3

β-Propiolactam, 3,3- and 4,4-disubstituted propiolactams can be polymerized to form unsubstituted and substituted nylon-3. Anionic polymerization was initiated by nylon-6,6 and carried out at 200–250°C. Polymers of high molecular weights were obtained from 3,3-disubstituted lactams. However, solution polymerization at 0–20°C with 25% monomer concentration in a solvent such as dimethyl sulfoxide with strongly basic activators such as potassium pyrrolidinonate also gave high molecular weights. Poly(4,4-dimethylpropiolactam) with η_{inh} of 4.5 dl/g and $\overline{M}_w$ of 50,000 was reported [70].

2.2.7.2 Nylon-4

2-Pyrrolidinone is polymerized by anionic polymerization to form polypyrrolidinone or nylon-4 [71]. The polymerization process gives a polymer of high molecular weight in 80–85% yields at temperatures below 60°C. The polymer forms a fine dispersion in hydrocarbon. It can be extracted by water to remove unreacted monomer and residual catalyst. The dispersion is suitable for dry spinning since the polymer can be readily dissolved at elevated temperatures.

2.2.7.3 Nylon-7

Polyenantholactam or nylon-7 was known as Enant in USSR. It can be synthesized from the melt polymerization of 7-aminoheptanoic acid at 260°C [72]. A polymer of η_{sp} of about 1.2 was obtained in 5 h of polymerization at 280°C in the presence of 4% water initially [73]. Its melt temperature was 230–235°C vs. 223°C for nylon-6.

2.2.7.4 Nylon-8

Capryllactam can be readily polymerized in the melt at 240°C for 24 hr with a small amount of amino acid to form polycapryllactam or nylon-8 [74,75]. It can also be polymerized rapidly with anionic initiators [76]. The polymer exhibits good thermal stability and a relatively low melt temperature of 200°C. The low melt temperature and the high cost of an intermediate have limited the usefulness of this polymer.

TABLE 2.4
Synthesis of Aliphatic Polyamides

Polymer type	Polymer intermediates	Synthetic route	M_w, M_n η_{inh}	Melt. temp. (°C)	Major uses	Ref.
AB polyamides						
Nylon-3	β-Propiolactam	Melt or solution polymerization	η_{inh} 4.5	>320	Fibers	59
3,3-dimethyl 3	3,3-Dimethyl propiolactam,			250		
4,4-dimethyl 3	4,4-Dimethyl propiolactam			296		
Nylon-4	2-Pyrrolidinone	Anionic polymerization	η_{inh} 35	260	Fibers	60
Nylon-6	Caprolactam	Ring-opening polymerization	M_n 20,000	232	Fibers, resins	
Nylon-7	ω-Enantholactam, or 7-aminoheptanoic acid	Melt amidation 200°C	η_{sp} 1.2–1.3	233	Fibers	61, 62
Nylon-8	Capryllactam	Ring opening		200		63–65
Nylon-9	ω-Aminopelargonic acid	Amidation		209		6
Nylon-10	Azacycloundecan-2-one	Ring opening		188		6
Nylon-11	ω-Aminoundecanoic acid	Melt amidation 215°C		190	Film	8
Nylon-12	Azacyclotridecan-2-one	Ring opening 300°C		170	Fibers	8, 66
AABB polyamides						
Nylon-4,2	Tetramethylene diamine Diethyl oxalate	Amidation	η_{inh} 2.7	380		67
Nylon-4,6	Tetramethylene diamine Adipic acid	Amidation 140°C Solid-phase polym	M_n 32,900	295	Fibers, resins	68, 69
Nylon-6,6	Hexamethylene diamine Adipic acid	Amidation	M_n 20,000	265	Fibers, resins	6
Nylon-6,12	Hexamethylene diamine Dodecanedioic acid	Amidation			Resins	6, 70
Aliphatic–aromatic polymers						
Nylon-4,I	Tetramethylene diamine Isophthalic acid	Amidation				71
Nylon-6,I	Hexamethylene diamine Isophthalic acid	Amidation	M_n 13,000	180–210	Resins	72–74
Nylon-6,T	Hexamethylene diamine Terephthalic acid	Interfacial amidation		370	Fibers	75
PACM,12	Bis(4-aminophenyl)methane Dodecanedioic acid	Amidation		290	Fibers	76–78

2.2.7.5 Nylon-11

Poly(aminoundecanoic acid) or nylon-11 was first synthesized by Carothers in 1935 and commercialized in France in 1955 [8]. The polymer is prepared from ω-aminoundecanoic acid by melt polymerization at 215°C under nitrogen for 3 h. This polymer is hydrophobic and has excellent electrical properties.

2.2.7.6 Nylon-12

ω-Dodecanolactam is polymerized in the melt at temperatures above 300°C with an acid catalyst [8,77]. The polymer has typically low extractable content and low melt temperature of 179°C.

2.2.7.7 Nylon-4,2

Tetramethylene diamine and diethyl oxalate were prepolymerized in a 50/50 phenol/trichlorobenzene mixture at 140°C. The prepolymer, after purification, was subjected to solid-phase polymerization under nitrogen at 250–300°C to form poly(tetramethylene oxalamide) or nylon-4,2 [78]. The polymer exhibited η_{inh} as high as 2.7 dl/g as measured from a 0.5% solution of polymer in 96% sulfuric acid. Interestingly, the polymer was soluble in trifluoroacetic acid, dichloroacetic acid, and 96% sulfuric acid, but not in 90% formic acid. It had a melt temperature of 388–392°C and heat of fusion of 148–154 J/g (35–37 cal/g).

2.2.7.8 Nylon-4,6

Poly(tetramethylene adipamide) or nylon-4,6 is prepared from tetramethylene diamine and adipic acid by polymerization in an organic solvent or by melt polymerization followed by solid-state polymerization [79,80]. The polymer melts at 295°C, about 30°C above nylon-6,6. It is more sensitive to degradation and branching. The volatility of tetramethylene diamine also makes it difficult to control the balance of end groups during polymerization. Excess diamine is added to compensate the losses. Values of $\overline{M}_n$ as high as 32,900 have been reported.

2.2.7.9 Nylon-6,12

Poly(1,6-hexamethylene dodecaneamide) or nylon-6,12 is synthesized from the polycondensation of hexamethylene diamine and dodecanedioic acid. It has been commercially produced by DuPont as a resin, Zytel* 158L [81].

2.2.7.10 Nylon-4,1

The inclusion of a ring unit in an AABB polyamide generally brings about significant changes in polymer chain structures and thermal properties. Thus, poly(tetramethylene isophthalamide) or nylon-4,I and poly(hexamethylene isophthalamide) or nylon-6,I both tend to be amorphous. They can be crystallized with great difficulties in boiling water or swelling agents [82].

2.2.7.11 Nylon-6,1

Poly(hexamethylene isophthalamide) of high molecular weights with $\overline{M}_n = 13{,}000$ for $\eta_{inh} = 0.74$ dl/g in formic acid was reported. The polymer exhibited melt temperature of 180–210°C and low crystallinity [83–85]. It is used as an engineering resin with good, high transparency and adhesive properties.

---

*Zytel—a registered trademark of E.I. du Pont de Nemours & Co., Inc., Wilmington, Delaware, USA.

2.2.7.12 Nylon-6,T

Poly(hexamethylene terephthalamide) or nylon-6,T has been investigated extensively [86]. The inclusion of a *para*-oriented phenylene ring provides a polymer of higher crystallinity, and higher melt and glass transition temperatures than that of a *meta*-oriented phenylene ring. Because of its high melt temperature of 370°C, it must be polymerized by alternative methods such as interfacial polymerization to avoid polymer degradation. This polyamide is interesting because its intermediates are inexpensive and it offers good product properties.

2.2.7.13 PACM,12

In the 1970s, DuPont commercialized a silk-like Qiana* fiber based on poly(bis[4-aminocyclohexyl]methane dodecaneamide) or PACM,12 [87]. The base polymer is synthesized from bis(4-aminocyclohexyl)methane and dodecanedioic acid. The diamine exists in three isomeric forms: *trans–trans*, *cis–trans*, and *cis–cis*. Its content of *trans–trans* isomer can be controlled by specific catalysts during its preparation. A normal diamine intermediate contained 51% *trans–trans*, 40% *cis–trans*, and 9% *cis–cis* isomers [88,89]. For Qiana fiber, the trans-trans content was about 70%. The polymer had a melt temperature of 290°C.

2.3 POLYMERIZATION PROCESSES

2.3.1 Monomer Syntheses

Nylon-6 and nylon-6,6 are the principal polyamides for commercial production of fibers and resins. The corresponding monomeric intermediates are caprolactam and the salt of hexamethylene diamine and adipic acid (HA-salt). The commercial importance of these two polyamides has stimulated considerable development and optimization of commercial processes for their monomers. In this section, both commercial processes and some of the significant experimental developments will be discussed.

2.3.1.1 Caprolactam

2.3.1.1.1 Overview

Figure 2.11 shows schematically the individual processes for the synthesis of caprolactam. The solid lines indicate processes that have been practiced commercially. As can be seen, all processes start from materials that belong to the group consisting of phenol, benzene, toluene, and cyclohexane. The chemistry of different processes has been reviewed [27,90,91]. Commercially, processes 1, 2, and 3 as shown in Figure 2.11 are important. The principal intermediates are cyclohexanone and cyclohexanone oxime for process 1, cyclohexanone oxime for process 2 [92–95], and cyclohexane carboxylic acid for process 3.

In recent years, BASF disclosed a number of processes for preparing caprolactam by the catalytic reaction of 6-aminocapronitrile (ACN) and water [96–103]. Two of these processes were reported to yield caprolactam and hexamethylene diamine simultaneously. The polymer intermediate ACN is derived from cleaving oligomers and polymers of caprolactam in the presence of a catalyst at high temperatures. Thus, it is possible to use wastes from the polymerization of caprolactam or from fiber spinning as the starting material. AlliedSignal Inc. (now Honeywell International) also reported process technology for depolarizing nylon-containing wastes to form caprolactam [104–107].

Additional synthesis routes include the catalytic aminomethylation of pentenoic acid derivatives to prepare caprolactam [108] and the catalytic conversion of a cyanopentenic

*Qiana—a registered trademark of E.I. du Pont de Nemours & Co., Inc., Wilmington, Delaware, USA.

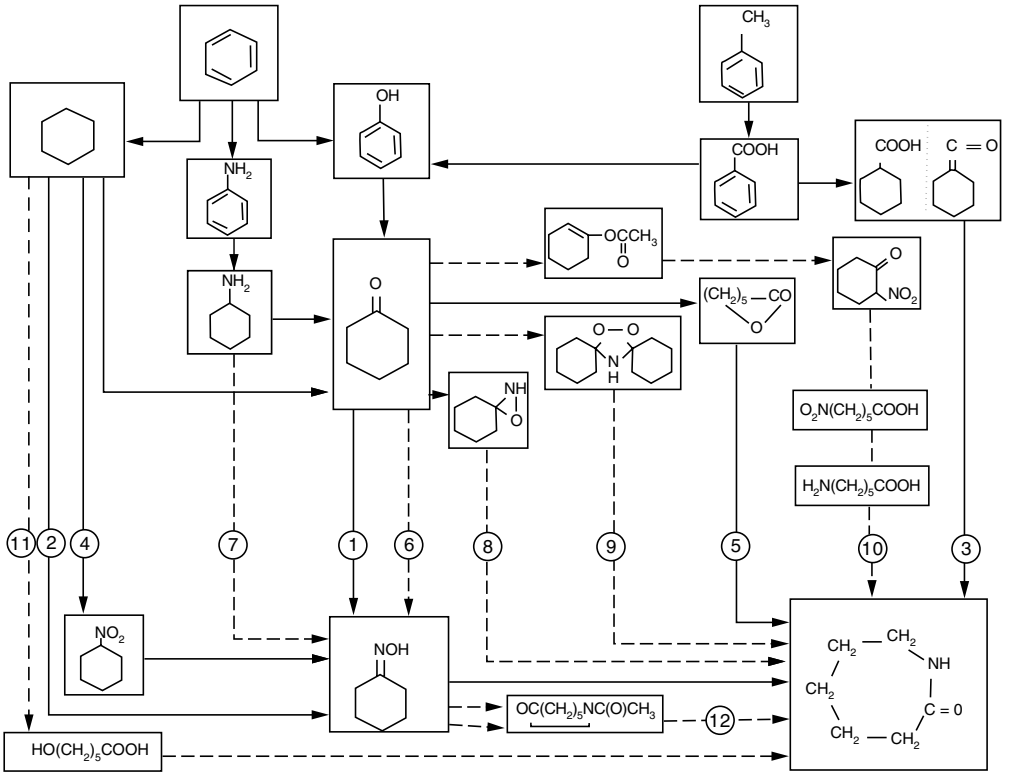

FIGURE 2.11 Block diagram of caprolactam processes.

carboxylic acid or its ester in ammonia [109]. Possible intermediates for the synthesis of caprolactam-entailing products derived from the dimerization of acrylonitril have been reported [110,111].

Procedures for the synthesis of polymer intermediate cyclohexanone:

1. Catalytic hydrogenation of phenol and subsequent dehydrogenation of the resulting cyclohexanol
2. One-step catalytic hydrogenation of phenol using palladium on carbon catalyst
3. Catalytic oxidation of cyclohexane to a cyclohexanol–cyclohexanone mixture
4. Reductive catalytic hydrolysis of cyclohexylamine in a one-stage operation

Though process 1 is still practiced, 2 and 3 are the most significant commercial processes.

Cyclohexanone oxime may be produced by:

1. Reaction of cyclohexanone with hydroxylamine (process 1, Figure 2.11)
2. Photonitrosation of cyclohexane with nitrosyl chloride (PNC process) [112,113] (process 2, Figure 2.11)
3. Hydrogenation of nitrocyclohexane [112,114] (process 4, Figure 2.11)
4. Reaction of cyclohexylamine with H_2O_2 [112,115] (process 7, Figure 2.11)
5. Ammoxydation of cyclohexanone with NH_3 and H_2O_2 [116] (process 6, Figure 2.11)

The hydroxylamine used for the reaction with cyclohexanone is obtained by the Raschig process or by catalytic hydrogenation of either nitric oxide or nitric acid. In the Raschig process, the hydroxylamine is obtained in the form of its sulfate. The raw materials for this process are sulfur dioxide, ammonia, carbon dioxide, and water. A mixture of NO and NO_2, as obtained from the catalytic oxidation of ammonia, is absorbed in an aqueous ammonium carbonate solution to yield ammonium nitrite, which is then reacted with SO_2 in the presence of ammonium hydroxide. The product of this reaction is hydroxylamine disulfonate, which converts upon hydrolysis via the monosulfonic acid hydroxylamine into hydroxylamine sulfate:

$$\begin{aligned} &NH_4NO_2 + NH_4OH + 2SO_2 \xrightarrow{5^\circ C} HON(SO_3NH_4)_2 \\ &\xrightarrow{+2H_2O,\ 100^\circ C} (NH_3OH)HSO_4 + (NH_4)_2SO_4 \end{aligned} \tag{2.38}$$

In 1967, both BASF [117] and Inventa introduced a commercial process for the catalytic hydrogenation of nitric oxide [113]. The reaction is carried out in the presence of sulfuric acid and yields hydroxylamine sulfate according to:

$$NO + 1.5H_2 + H_2SO_4 \rightarrow H(NH_3OH)HSO_4 \tag{2.39}$$

Therefore, only 0.5 mol of ammonium sulfate per mol of hydroxylamine is then produced in the subsequent neutralization with ammonia. This is half as much as in the Raschig process. Complete elimination of ammonium sulfate formation characterizes a process introduced in 1970 by Stamicarbon [118,119]. This process involves catalytic hydrogenation of nitrate ions on Pd–C in a phosphoric acid ammonium hydrogen phosphate buffering system:

$$HNO_3 + 3H_2 + H_3PO_4 + NH_4H_2PO_4 \rightarrow (NH_3OH)H_2PO_4 + NH_4H_2PO_4 + 2H_2O \tag{2.40}$$

It is carried out in a gas–liquid contactor in which hydrogen is contacted with a circulating stream containing the nitrate ions, the buffering acid, and the noble metal catalyst. Since the hydroxylammonium ion is unstable, the reaction product is directly contacted with cyclohexanone in a toluene solution to effect the formation of cyclohexanone oxime:

$$C_6H_{10}O + (NH_3OH)H_2PO_4 \rightarrow C_6H_{10} = NOH + H_3PO_4 + H_2O \tag{2.41}$$

The aqueous $H_3PO{-}NH_4H_2PO_4$ solution is reacted with a mixture of NO and NO_2, which results in the conversion of any ammonium ions to nitrogen.

$$2NH_4^+ + NO + NO_2 \rightarrow 2N_2 + 2H^+ + 3H_2O \tag{2.42}$$

Simultaneous introduction of air results in the formation of nitric acid,

$$2NO + 1.5O_2 + H_2O \rightarrow 2HNO_3 \tag{2.43}$$

which is then recycled into the process.

An interesting process developed and operated since 1962 by Toray for manufacturing cyclohexanone oxime is the photo-nitrosyl chlorination (PNC) process. It is a one-stage process in which cyclohexane is converted to the oxime hydrochloride, and may be explained by the following mechanism [120]:

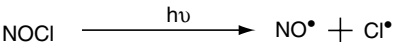

(2.44)

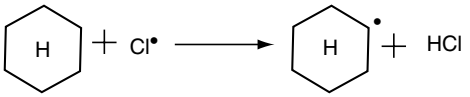

(2.45)

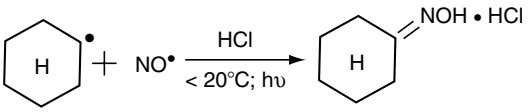

(2.46)

The nitrosyl chloride for this synthesis is obtained by a sequence of reactions that includes:

1. Oxidation of ammonia

$$2NH_3 + 3O_2 \rightarrow NO{\cdot}NO_2 + 3H_2O \tag{2.47}$$

2. Formation of nitrosyl sulfuric acid

$$2H_2SO_4 + NO{\cdot}NO_2 \rightarrow 2NOHSO_4 + H_2O \tag{2.48}$$

3. Sulfuric acid regeneration

$$NOHSO_4 + HCl \rightarrow NOCI + H_2SO_4 \tag{2.49}$$

In a process developed to commercial maturity by DuPont , and industrially practiced by this company from about 1963 to 1967 [121], cyclohexanone oxime is obtained by a route that encompasses the nitration of cyclohexane to nitrocyclohexane and the reduction of the latter to the oxime, which is converted to caprolactam by the Beckmann rearrangement. According to U.S. Patent 2,634,269, nitrocyclohexane can be converted directly to caprolactam in the gas phase at 250–450°C using a polyborophosphate catalyst.

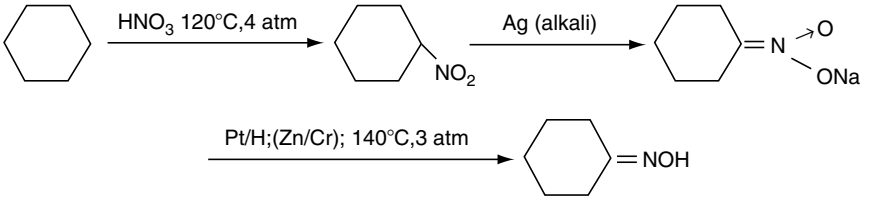

(2.50)

Cyclohexanone oxime processes that have not been commercially practiced include:

1. The Kahr process [115], in which cyclohexylamine is catalytically oxidized with hydrogen peroxide
2. The ammoxidation process developed by Tao Gosei Chern. Ind. Co. [116], entailing the direct reaction of cyclohexanone, ammonia, and hydrogen peroxide in a liquid phase in the presence of a tungstic acid catalyst:

$$C_6H_{10}O + NiI_3 + H_2O_2 \xrightarrow{(H_3PW_{12}O_4).8H_2O} C_6H_{10}NOH + 2H_2O \tag{2.51}$$

The cyclohexanone oxime obtained by any of these processes (1, 2, 4, 6, and 7, in Figure 2.11) is converted to caprolactam by the Beckmann rearrangement in oleum. The resulting caprolactam sulfate is neutralized with ammonia and purified. The neutralization process yields about 2 ± 0.2 kg of ammonium sulfate/kg of caprolactam. The lactam purification may entail extraction with organic solvents (toluene, benzene, chlorinated aliphatic hydrocarbons) followed by extraction of the organic solution with water and subsequent isolation of the lactam by either crystallization or distillation. Newer developments are concerned with the gas-phase catalytic rearrangement of cyclohexanone oxime using a boric acid on carbon catalyst in a fluidized-bed operation [122].

Union Carbide Corp. developed a process using cyclohexanone as a principal intermediate and used this process commercially in 1966. According to the following reaction scheme, cyclohexanone is oxidized to caprolactone with peracetic acid, which is obtained by the reaction of acetaldehyde and hydrogen peroxide. The caprolactone is then converted to caprolactam by reaction with ammonia at high temperature and high pressure (process 5, Figure 2.11). The only by-product is acetic acid; the amount of acetic acid obtained is about 1 kg/kg of product [123].

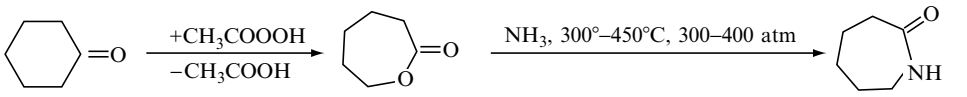

(2.52)

Cyclohexanone is also the starting material for process 8 (Figure 2.11). This process does not appear to be commercially practiced. It is characterized by the formation of cyclohexanonisoxim (3,3′-pentamethylene oxaziridine) upon treatment of cyclohexanone in a toluene solution with ammonia and sodium hypochloride [124]:

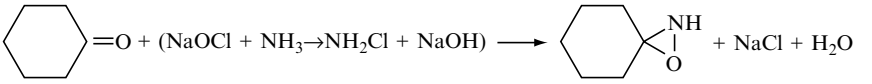

(2.53)

Process 9 (Figure 2.11) refers to the reaction of cyclohexanone with hydrogen peroxide and ammonia resulting in 1,1′-peroxy dicyclohexylamine via either of the following two routes:

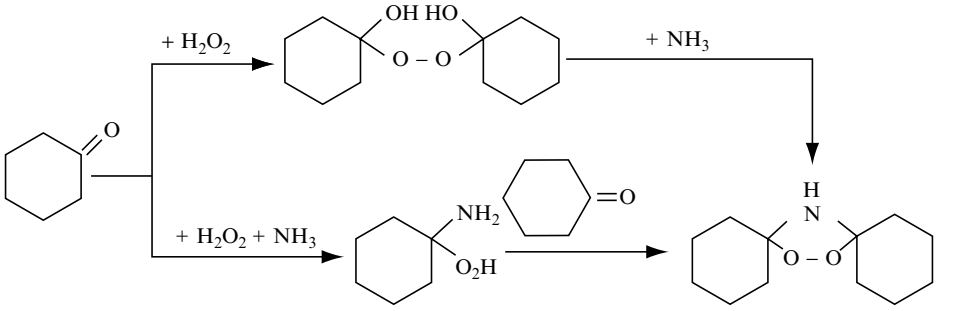

(2.54)

Cleavage of 1,1′-peroxy dicyclohexyl amine then yields caprolactam with regeneration of one equivalent of cyclohexanone according to the reaction [125,126]:

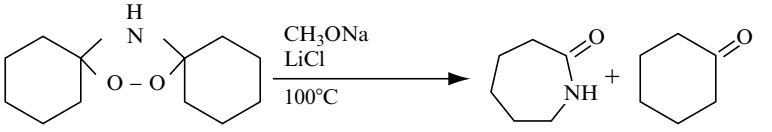

(2.55)

The Techni-Chem. process (process 10, Figure 2.11) that started from cyclohexanone also did not develop beyond pilot plant operations [127]. It is characterized by the following reaction scheme entailing (1) acylation of cyc1ohexanone with ketene, (2) nitration of the resulting cyclohexenyl acetate with concurrent deacetylation to 2-nitrocyc1ohexanone, (3) hydrolytic cleavage to ε-nitrocaproic acid, (4) hydrogenation to ε-aminocaproic acid, and (5) cyclization to caprolactam:

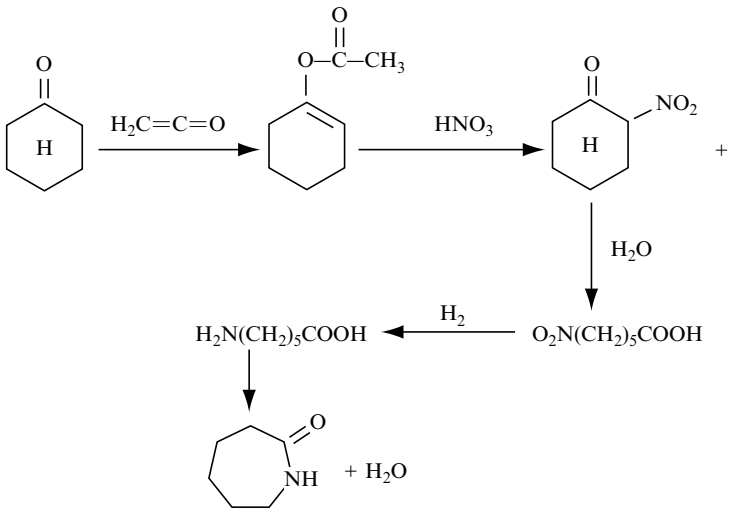

(2.56)

(2.57)

The acetic acid obtained in the nitration step is recycled to the ketene generator.

Toluene is the starting material of a commercial process developed by SNIA Viscosa [128] (process 3, Figure 2.11). It involves the reactions shown in the following scheme:

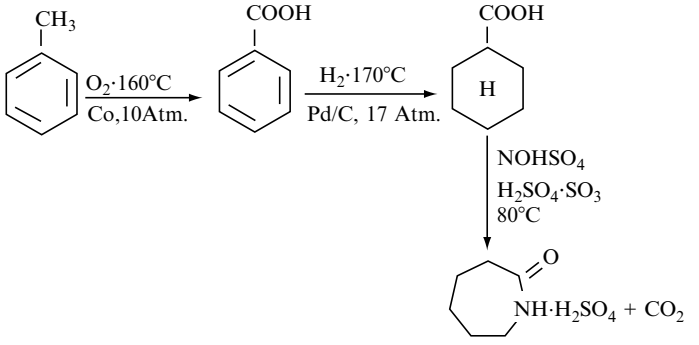

(2.58)

Toluene is oxidized in liquid phase to benzoic acid, which is subsequently hydrogenated to cyclohexane carboxylic acid. Reaction of this acid with nitrosylsulfuric acid in oleum then results directly in the formation of caprolactam sulfate by a mechanism that entails simultaneous nitrosation, decarboxylation, and rearrangement of the formed oxime.

Several modifications improved this process. One such process consisted in converting the cyclohexane carboxylic acid either with oleum or by thermal dehydration at 600°C into pentamethylene ketene, which then converted readily into caprolactam under mild conditions on treatment with nitrosylsulfuric acid.

$$C_6H_{11}COOH \xrightarrow[-H_2O]{H_2SO_4\cdot SO_3} C_6H_{10}C{=}O \xrightarrow[-CO_2]{NOHSO_4} \text{caprolactam} \tag{2.59}$$

In 1974, SNIA revealed a further modification of this process that resulted in eliminating ammonium sulfate formation [129]. In this modified process, the product of the reaction between cyclohexane carboxylic acid and nitrosyl sulfuric acid is slightly diluted with water and treated with an alkylphenol to extract the caprolactam, which is then purified by distillation. The sulfuric acid is mixed with a fuel and thermally cracked to sulfur dioxide, which is recycled into the process.

Processes 11 and 12 (Figure 2.11) also demonstrate approaches for the manufacture of caprolactam without producing ammonium sulfate. Developed by Kanegafuchi [130], process 11 involves oxidation of cyclohexane and reaction of the oxidation products with ammonia and hydrogen in the presence of a copper chromite catalyst. The reaction is conducted at 200–300°C and at pressures up to 3 atm. Process 12 (Figure 2.11) was developed by Kanebo [131]. It entails acetylation of cyclohexanone oxime with either ketene or acetic anhydride, vapor-phase rearrangement over a SiO_2–$A1_2O_3$ fixed-bed catalyst at 150°C to *N*-acetyl caprolactam,

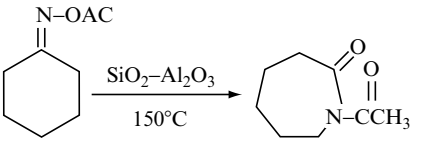

(2.60)

and transacetylation according to

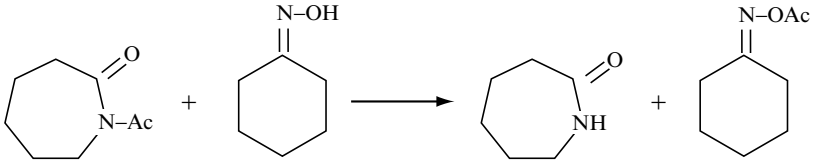

(2.61)

employing temperatures up to 100°C. The mechanism of the rearrangement may entail coordination of the acetyl carbonyl with the acidic silica–alumina catalyst and thus may be similar to the one that governs the boric oxide catalyzed vapor-phase rearrangement as reported by BASF [132].

2.3.1.2 Adipic Acid

Approaches for the synthesis of adipic acid are shown in Figure 2.12. The basic raw materials are benzene, cyclohexane, phenol, acrylates, and butadiene. The principal commercial processes are based on the oxidation of cyclohexane, which usually proceeds in two stages. The first step entails oxidation with air, yielding either a mixture of cyclohexanone and cyclohexanol (process 1, Figure 2.12) or predominantly cyclohexanol (process 2, Figure 2.12). These reaction products are oxidized in the second stage with nitric acid to adipic acid. Process 1 employs a soluble cobalt oxidation catalyst [133], reaction temperatures in the range of 150–160°C, pressures between 800 and 1000 kPa, and catalyst concentrations of 0.3–3 ppm. At conversions of 5–10%, the selectivity with respect to the cyclohexanone–cyclohexanol mixture is about 70–80 mol %, with an alcohol/ketone ratio of about 2:1. In process 2 the oxidation is carried out in the presence of boric acid or its anhydride. This results in mixtures particularly

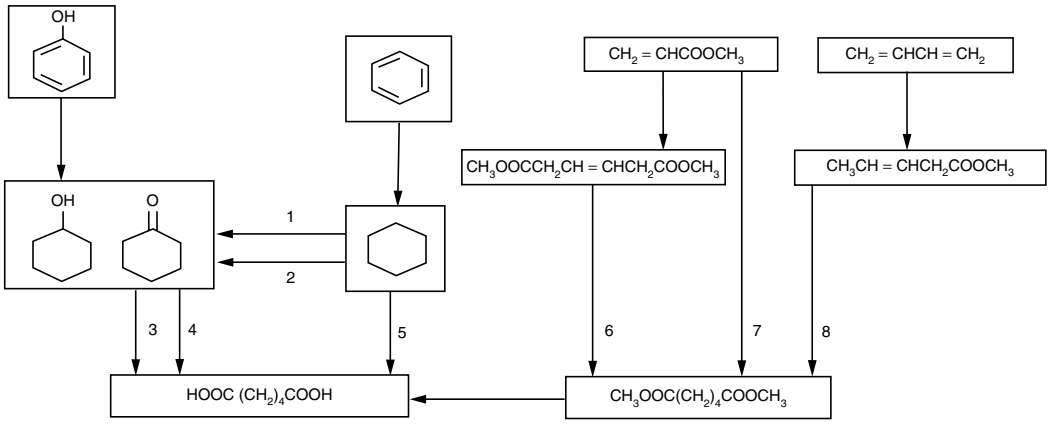

FIGURE 2.12 Block diagram of adipic acid processes.

rich in cyclohexanol. In this process the reaction temperatures are in the range of 170–180°C. At a conversion of about 15%, the selectivity is about 85% for a mixture characterized by an alcohol/ketone ratio of more than 10:1 [134]. The oxidation processes have been largely improved through changes in oxidizing agents and catalyst compositions [135–138].

Hydrogenation of phenol may yield, depending on the type of catalyst and operating conditions, predominantly either cyclohexano1 or cyclohexanone. Although ketone is preferred for the production of caprolactam, alcohol is the more desirable product for the manufacture of adipic acid. The hydrogenation is usually carried out in the liquid phase using nickel on silica catalyst, with temperatures at about 140°C, and hydrogen pressures between 0.2 and 1.8 MPa [139]. At 99% conversion, selectivity is higher than 97%.

Although air oxidation of the cyclohexanone–cyclohexano1 mixtures on a Cu–Mn catalyst in acetic acid [140] is possible, the principal commercial operations entail oxidation with nitric acid. The reaction is usually carried out at 60–80°C and pressures of 0.1 to 0.4 MPa, employing 50–60% nitric acid and a copper–vanadium catalyst containing between 0.1 and 0.5% Cu and 0.1 and 0.2% V [141]. The yields of adipic acid are in the range of 90–96%. The main by-products are succinic acid and glutaric acid. Their concentration generally increases as the purity of the feed mixture decreases. The adipic acid is isolated by crystallization and purified by recrystallization from water.

Single-step oxidation of cyclohexane to adipic acid (process 5, Figure 2.12) has been demonstrated [142]. This process involves a liquid-phase air oxidation using acetic acid as a reaction medium and cobalt acetate as an oxidation catalyst. The reaction temperatures are in the range of 70–90°C. At residence times of 6–10 h, conversions to about 80% were obtained with selectivities to adipic acid of 70–75%. Several alternate processes have been described for the oxidation of cyclohexane to form adipic acid [143–148].

Routes 6 and 7 in Figure 2.12 are based on methylacrylate, which may be converted to the adipic acid ester by electrolytic coupling. The corresponding technology has been reviewed quite extensively [149–151]. More recent developments have been concerned with catalytic coupling processes [152,153] using catalysts such as $PdC1_2$, $Pd(PPh_3)_2Cl_2$, $RuCl_3$, Ru(acac), $Fe(CO)_5$, and $Ca(acac)/AlR_3$. Reaction conditions are reflected in the following typical experiment: when a mixture of 100 m1 of methy1acrylate, 0.2 g of $PdCI_2$, and 0.3 g of benzonitrile under nitrogen was heated at 80°C for 35 min, 45% of methyl acrylate was converted. The reaction product contained 92% dimethyl hexenoate (linear dimer), 3% dimethylmethyl pentenoate (branched dimer), 3% oligomers, and 2% methyl propionate. Hydrogenation of the linear dimer and subsequent hydrolysis of the resulting dimer

readily yield adipic acid. An alternate method [154] to process 6 involves the hydrolysis of dimethyl adipate in a 30-tray column at 95–105°C and atmospheric pressure yielded a bottom effluent of 31% adipic acid. This process constitutes a simple continuous reaction operation.

Process 8 in Figure 2.12 indicates an interesting approach. This process involves a two-step carbonylation of butadiene [155]. In the first step butadiene is reacted with carbon monoxide and methanol in the presence of dicobaltoctacarbonyl and a heterocyclic structure containing a tertiary nitrogen moiety (pyridines, pico1ines, quinoline, isoquinoline):

$$CH_2 = CHCH = CH_2 + CO + CH_3OH \rightarrow CH_3CH = CHCH_2COOCH_3 \qquad (2.62)$$

The reaction is carried out at 120°C and at pressures of 60 MPa. The selectivity with respect to the methyl 3-pentenoate is 98%. About 1% each of the branched isomer and the saturated ester is formed. After removal of unreacted butadiene, the second-step carbonylation is carried out at about 185°C and 3 MPa:

$$CH_3CH = CHCH_2COOCH_3 + CO + CH_3OH \rightarrow CH_3OOC(CH_2)_4COOCH_3 \qquad (2.63)$$

This second step yields about 85% of the dimethyl adipate. The main by-products are about 10% dimethyl methyl glutarate, 3% dimethyl ethyl succinate, 1% dimethyl diethyl succinate, and 1% methyl pentanoates. The dimethyl adipate is isolated by distillation and converted to adipic acid by hydrolysis.

Burke discloses a two-step process for the conversion of butadiene to adipic acid at high yields [156]. The first step is the hydrocarboxylation of butadiene to form 3-pentenoic acid. The second step is the hydrocarboxylation of 3-pentenoic acid with carbon monoxide and water in the presence of a rhodium-containing catalyst, an iodide promoter, and certain inert solvents such as methylene chloride. The first reaction step gives also a significant by-product of γ-valerolactone and a minor by-product of α-methyl-γ-butyrolactone. These lactones can be converted to adipic acid by modified catalyst compositions [157–159]. In a related work, pentenic acids or esters are used as the starting intermediates for conversion to adipic acid [160–166].

2.3.1.3 Hexamethylene Diamine

The block diagram in Figure 2.13 shows the process reactions for syntheses of hexamethylene diamine. This diagram includes processes (8–10) that had been developed to some degree of commercial maturity but do not appear to be practiced commercially. Process 8 is included because it starts from furfural, a material independent of hydrocarbon feedstocks. Process 9, developed by Toray [167], involves first the catalytic gas-phase reaction of caprolactam with ammonia at 300°C to amino capronitrile as the principal product at conversions of up to 75%. The subsequent step is the hydrogenation of the nitrile group. In process 10, developed by Celanese [168], caprolactone is first hydrogenated at 250°C and pressures of 25–30 MPa to hexanediol-1,6 in very good yields using Raney-cobalt or a copper–chromite catalyst. Subsequent catalytic conversion of the hydroxyl groups to amino groups using Raney-nickel proceeds at higher temperatures and pressures [169], to a yield of about 90% with the production of many by-products that complicate further purification.

The commercial processes for the manufacture of hexamethylene diamine entail hydrogenation of adiponitrile. It is a continuous liquid-phase process [170] that is usually conducted at 75°C and 3 MPa pressure in the presence of a chromium-containing Raney-nickel catalyst and aqueous sodium hydroxide:

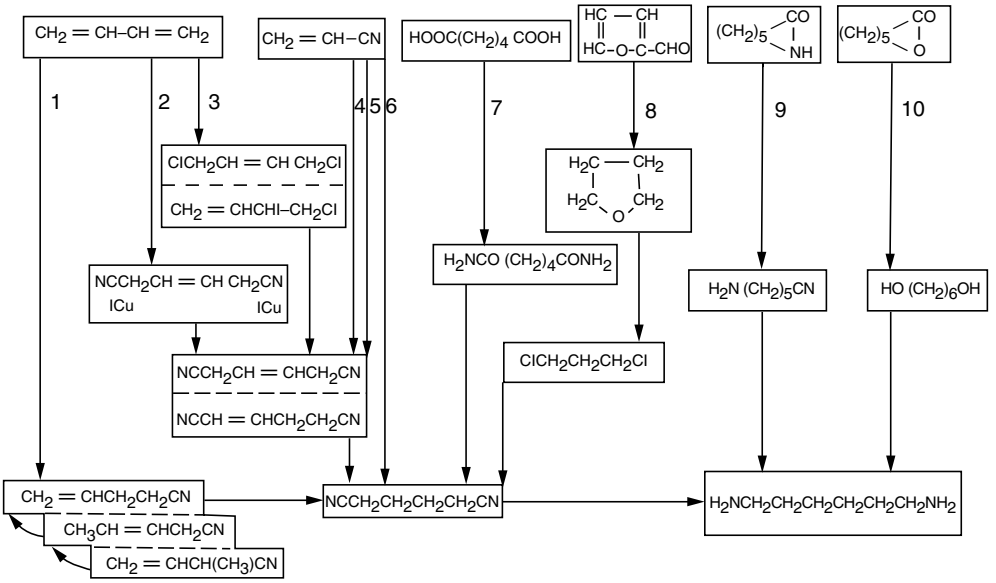

FIGURE 2.13 Block diagram of hexamethylene diamine processes.

$$NC(CH_2)_4CN \xrightarrow{H_2(2MPa),\ 75^\circ C,\ Cr/Ni,(NaOH,\ H_2O)} H_2N(CH_2)_6NH_2 \qquad (2.64)$$

Yields are in the range of 99%.

Adiponitrile in turn is obtained from processes starting from (a) adipic acid, (b) butadiene, and (c) acrylonitrile. The process starting from adipic acid (process 7 in Figure 2.13) is rather well developed and used by most of the major raw material suppliers. It consists of a gas-phase reaction between adipic acid and ammonia at about 270°C at atmospheric pressure. In the presence of dehydration catalysts, such as phosphonic acid or a mixture of phosphoric and boric acids, the reaction proceeds via the formation of adipic acid amide to adiponitrile with about 90% yield.

In the first butadiene process (process 3 in Figure 2.13) developed by DuPont [171], chlorine is reacted with butadiene at about 200°C in a mole ratio of 4:1. At a 95% yield this reaction results in the formation of both 1,4-dichlorobutene and 1,2-dichlorobutene. Treating this mixture with HCN at 130–150°C in the presence of HCl acceptors such as $CaCO_3$ yields 1,4-dicyanobutene-2, which upon treatment with a basic catalyst, isomerizes to 1,4-dicyanobutene-1. Hydrogenation at 250°C and at atmospheric pressure in the gas phase using a palladium catalyst yields hexamethylene diamine directly.

A newer DuPont process [172] is characterized by the direct addition of HCN to butadiene (process 1 in Figure 2.13). It is essentially a two-stage process. The first step is a vapor-phase operation. A gaseous mixture of butadiene, hydrogen cyanide, nitrogen, and hydrogen chloride in a ratio of 1:1:1:0.1 is contacted at about 215°C and at atmospheric pressure with a copper magnesium chromite fixed-bed catalyst for about 50 min. In an essentially quantitative conversion, the reaction product consists of 88% of a mixture of linear pentenenitrile isomers and 12% of branched 2-methylbutenenitriles:

$$CH_2{=}CHCH{=}CH_2 \xrightarrow{+HCN} \begin{cases} \rightarrow CH_2{=}CH{-}CH_2CH_2CN + \text{isomers} \\ \rightarrow CH_3CH(CN)CH{=}CH_2 + \text{isomers} \end{cases} \qquad (2.65)$$

The second step entails catalytic isomerization of the 2- and 3-pentenenitriles to 4-pentenenitrile and the addition of a second mole of HCN:

$$CH_3CH = CHCH_2CN \rightarrow CH_2 = CHCH_2CH_2CN \xrightarrow{HCN} NC(CH_2)_4CN \tag{2.66}$$

At about 98% conversion, hexamethylene diamine is obtained in 90% yield. The process is a liquid-phase operation, carried out at 120°C. The catalyst is a triphenyl phosphite–Ni(O) complex. It appears that the addition of a promoter such as zinc chloride to the nickel ligand results in a composition that catalyzes the conversion of 2-methylbutenenitrile (the undesired branched isomer) into the linear 3-pentenenitrile [173], which may be recycled into the second process step for isomerization to 4-pentenenitrile.

The approach for process 2 in Figure 2.13 has been developed by Exxon [174]. In this process, butadiene reacts with cuprous cyanide in the presence of iodine, yielding a cuprous iodide complex of 1,4-dicyanobutene-2. This is decomposed with aqueous hydrogen cyanide resulting in the liberation of the dicyanobutene, regeneration of cuprous cyanide, and formation of hydrogen iodide, which on oxidation to iodine can be, together with cuprous cyanide, recycled to the first process stage:

$$\begin{aligned} &CH_2 = CHCH = CH_2 \xrightarrow{CuCN/I_2} [ICuNCCH_2CH = CHCH_2CNCuI] \\ &\xrightarrow{(HCN)} NCCH_2CH = CHCH_2CN + CuCN + HI \end{aligned} \tag{2.67}$$

$$2\,HI \xrightarrow{1/2\,O_2} I_2 + H_2O \tag{2.68}$$

The isolated 1,4-dicyanobutene-2 is hydrogenated successively to adiponitrile and hexamethylene diamine.

Processes 4, 5, and 6 in Figure 2.13 are based on acrylonitrile. Among them, process 6 is the oldest. Introduced in 1965 as a technical process by Monsanto [175], it involves the electrolytic dimerization of acrylonitrile to adiponitrile. The process is carried out in a system of electrolytic cells containing sulfonated polystyrene membranes. An aqueous solution of tetraethylammonium-*p*-toluyl sulfonate is used as the catholyte and aqueous sulfuric acid as the anolyte. Using a 40% aqueous solution of acrylonitrile at temperatures of 25–35°C, the following reaction sequences occur:

$$\text{Anode: } H_2O \rightarrow 2H^+ + 1/_2O_2 + 2e \tag{2.69}$$

$$\text{Cathode: } 2CH_2 = CHCN + 2H_2O + 2e \rightarrow NC(CH_2)_4CN + 2OH^- \tag{2.70}$$

The reductive dimerization thus proceeds at the cathode, occurs at a pH of 7–9, and yields more than 90% adiponitrile at a conversion of acrylonitrile of about 50%. By-products are 2% *bis*(cyanoethyl) ether, 0.5% hydroxy propionitrile, 2.5% propionitrile, and about 4% high boilers. The adiponitrile is purified by liquid–liquid extraction and distillation.

Processes 4 and 5 in Figure 2.13 are more recent developments entailing dimerization of acrylonitrile. Although formally analogous to the Monsanto process they are quite different because they proceed via catalysis rather than electrolysis. One of these processes developed by Halcon [176] involves liquid-phase reaction of acrylonitrile at 30°C under a nitrogen pressure of 0.7 MPa in the presence of a two-component catalyst system.

The catalyst system consists of a combination of a tertiary amine, either acyclic or heterocyclic, with a Lewis acid. The reaction yields 2-methylene glutaronitrile:

$$2CH_2{=}CHCN \xrightarrow{\text{Zn-tosylate/N(Et)}_3} \begin{matrix} CH_2 \\ \| \\ NCCCH_2CH_2CN \end{matrix} \tag{2.71}$$

In a second step, the glutaronitrile is isomerized to the desired linear 1,4-dicyanobutene. This reaction is carried out at 255°C in the presence of catalytic amounts of lithium cyanide and appears to proceed via the formation of 1,2,4-tricyanobutane:

$$\begin{matrix} CH_2 \\ \| \\ NCCCH_2CN \end{matrix} \xrightarrow{+HCN} \begin{matrix} CH_2CN \\ | \\ NCCHCH_2CH_2CN \end{matrix} \xrightarrow{-HCN} \begin{cases} NCCH{=}CHCH_2CH_2CN \\ NCCH_2CH{=}CHCH_2CN \end{cases} \tag{2.72}$$

The same 1,4-dicyanobutenes can be obtained directly by a process disclosed by ICI [177]. According to this process, acrylonitrile is dimerized in an anhydrous proton donor solvent in the presence of a phosphinite, phosphonite, or phosphite catalyst at temperatures of about 60–80°C in an inert atmosphere:

$$2CH_2{=}CHCN \xrightarrow[\text{t-butyl alcohol}]{CH_3C_6H_4P(OCH_3)_2 \text{ at } 60^\circ C} \rightarrow \begin{cases} NCCH{=}CHCH_2CH_2CN \\ NCCH_2CH{=}CHCH_2CN \end{cases} \tag{2.73}$$

At 25% conversion after a reaction time of 1.5 h, yields in excess of 90% have been reported. Conventional processes may readily hydrogenate the linear dicyanobutenes.

2.3.2 Industrial Processes

Although industrial polymerization processes are generally treated as proprietary information, general description of polymerization technology, including flow sheets and schematic diagrams of polymerization processes and reactors, can be found in the literature [27,178–182]. The following sections discuss some general aspects of industrial polymerization processes.

2.3.2.1 General Operations

2.3.2.1.1 Monomer Preparation

The monomer feed preparation section is designed for obtaining carefully controlled monomer composition. This is particularly critical in case of the nylon-6,6 manufacture, where proper stoichiometry must be assured for the preparation of the HA-salt. Nonequivalence of the two monomers may, according to Equation 2.6, significantly affect the attainable molecular weight. The salt may be prepared either by reacting an aqueous dispersion of the diacid with an aqueous solution of the diamine or by mixing alcoholic solutions of the two components. In the latter case, a rather pure salt precipitates that may be used directly for making an aqueous feed solution of about 50% salt concentration. The monomer feed preparation in the nylon-6 process is concerned mainly with producing compositions of molten caprolactam with proper amounts of water and additives such as acids, or bases,

pigments, delustrants, antistatic agents, and materials imparting stability against light and heat. Additives of this type, of course, are also used in the nylon-6,6 process.

The monomer compositions are then fed into the polymerization reactor system where the conversion of monomer to polyamide takes place. The polymerization of the HA-salt is either preceded or, in the initial stages, accompanied by evaporation of the water used to dissolve the salt. This evaporation process requires proper temperature and pressure control to prevent solidification of any prepolymer formation and to eliminate or at least minimize any loss of diamine. Since only catalytic amounts of water are used in the caprolactam polymerization process and only a single monomer is present, there is no need for an analogous step for this process. The polymerization of either monomer system is then conducted either in a batch or in a continuous operation using equipment ranging from simple autoclave reactors to multistage flow reactor systems. The process is carried out at temperatures in the range of 250–280°C for periods of about 12 h to more than 24 h. It results in a polymer melt that is either transferred directly to spinning units for filament formation or extruded in the form of ribbons that are subsequently cut into chips. For nylon-6,6, except for drying of the chips, neither the polymer melt nor the chips need further treatment prior to the melt-spinning operation. This is not true for nylon-6 because the polymerization does not result in complete conversion of the caprolactam but in equilibrium.

2.3.2.1.2 Polymer Purification

The quantity of the residual monomer depends on the reaction temperature. At the temperatures used in industrial operations, it amounts to about 8–9%. In addition, there are about 3% oligomers of low molecular weight that are mostly cyclic. Since subsequent processing as well as performance characteristics in many applications is adversely affected by both the residual monomers and the oligomers, it is necessary to remove them from the polymer. This can be accomplished either by hot-water extraction or by vacuum evaporation. The latter is usually part of an integrated continuous operation. In this case, the molten equilibrium polymer is fed into a suitable apparatus, such as a thin-film evaporator, in which most of the monomer and part of the cyclic oligomers are distilled from the melt under vacuum. The efficiency of this operation depends upon the vacuum applied, the residence time, and the design of both the equipment and process, especially of the part that is concerned with condensation and transfer of the cyclic oligomers. Concomitant with the vacuum distillation of the monomer and oligomers is usually an increase of the polymer molecular weight as a result of intercatenary condensation. The polymer melt emerging from the vacuum stage can then be converted directly to filaments or to polymer chips. The chips are usually cylindrically shaped, about 3×3 mm.

If the process does not include a vacuum stage for the removal of residual monomer and oligomers, then hot-water extraction is required. In this case, the molten polymer is extruded in the form of rods of about 3 mm in diameter, which are quenched in water and cut into chips of about 3 mm in length. These chips are then extracted with water at temperatures slightly below the boiling point. The extraction process can be carried out batchwise or continuously in countercurrent operation. The residence time for this diffusion-controlled process is about 8–12 h. The extracted chips must then be dried. This process again can be done batchwise or continuously. The use of vacuum tumble dryers at temperatures of 100–120°C and final pressures of 0.1 torr is most common for batch operation. Rotary dryers or towers are used in continuous processes in which the chips are dried countercurrently with circulating nitrogen. Depending on the particular process and constitutional factors such as molecular weight and type of end groups, residence times in the range of 20–50 h may be required to reduce the water content of the chips to a level suitable for various subsequent melt-processing operations. The residual water content of the chips used in most commercial processes ranges from 0.02 to 0.1%.

Since both extraction and drying steps require long residence times because of the diffusional resistance of the solid nylon, vacuum evaporation appears to be a more attractive mode of operation. However, it is less effective in removing the water-soluble constituents of the equilibrium polymer. The corresponding polyamide usually contains a higher concentration of oligomers when compared with a water-extracted one. Although the total amount of residual water-soluble compounds in extracted commercial nylon-6 is generally below 1%, concentrations of 2.8–3.8% are characteristic of products from which monomer and oligomers are removed by vacuum evaporation. This may be too high for some uses and product requirements. Even if the performance of vacuum evaporation can be improved to meet quality requirements, the route via chip extraction will continue to be practiced, especially in cases where flexibility with respect to subsequent processing steps and product characteristics is of primary concern.

2.3.2.1.3 Monomer Recovery

Although the monomer recovered from the nylon-6 melt by vacuum distillation may be directly recycled into the monomer feed section, the monomer recovered by extraction of the solid chips is usually purified by liquid–liquid extraction and distillation. In case of nylon-6, the corresponding aqueous solutions are generally combined with those leaving the polymer waste recovery section in which the polyamide waste, generated in the various process stages (Figure 2.26), is hydrolyzed to the corresponding monomers with superheated steam.

2.3.2.2 Nylon-6 Polyamide

Although the syntheses of aliphatic polyamides are well established, process modifications are continually developed either to produce specific products or to produce polyamides more economically. According to BASF in Ger. Offen. DE 3,134,716/17 (1983), caprolactam is polymerized in a perpendicular tubular reactor consisting of discrete zones. The resulting polyamide is claimed to be more easily dyed. In a later BASF disclosure [183], a moist inert gas is employed to remove unreacted monomer and oligomers from the unextracted polymer to obtain polycaprolactam of high molecular weight. The preparation of high-molecular-weight polycaprolactam by the removal of water from the melt by nitrogen in the polycondensation stage at normal pressure has also been reported [184]. A similar process also has been described, which entails the removal of water from a flowing film by nitrogen where the flow rate of the nitrogen controls the relative viscosity of polyamide [185]. DuPont disclosed a continuous process that employs a multistage reactive distillation column to produce nylon-6 [186,187]. A feed stream containing a major portion of caprolactam and prepolymer and a minor portion of aminocapronitrile is fed to the column in which the feed stream flows countercurrent to a steam stream. In an another disclosure [188], 6-aminocapronitrile is polymerized to form a prepolymer in a tubular reactor. The liquid prepolymer passes through a flasher at atmospheric pressure to evaporate excess water and volatile products, and is crystallized at 140–160°C.

Unitika patent JP 60,248,730 deals with a process to produce high-molecular-weight polyamides in which molten linear polyamides are treated with adducts of bisoxazolines and dicarboxylic acids. Continuous polymerization resulting in high-molecular-weight nylon-6 entailing the degassing of a thin film is described in the East Ger. DD 234,430 patent. The solid-phase polymerization of polycaprolactam has been reported to increase the polymer molecular weight [189,190]. Barnes and Gottund. [191] discuss the use of certain quaternary ammonium compounds such as methyl tributyl ammonium chloride as accelerator for the polymerization of caprolactam. Such a modification enhances the rate and yield of polymerization significantly at temperatures below 115°C.

2.3.2.3 Nylon-6,6 Polyamide

In the preparation of nylon-6,6 salt, DuPont discloses a process for making highly concentrated solutions of nylon salt at maximum solubility [192]. In the first step of this process, a concentrated salt solution for nylon-6,6 is made with 73.5–77.5 wt% of adipic acid and 22.5–26.5 wt% of hexamethylene diamine at 55–60°C. The solution contains 60–69.5 wt% solute as compared to an ordinarily stoichiometric solution containing 56% diacid and 44% diamine with a maximum solute concentration of about 59 wt%. The second step is to remove water from the solution by evaporation to a solution concentration of 93–96 wt%. When the concentrated solution is ready to be polymerized, addition hexamethylene diamine is added to complete the reaction. A process with similar reaction modifications is developed to prepare an essentially anhydrous mixture of adipic acid and hexamethylene diamine [193]. The reaction mixture is heated to 120–135°C to allow evaporation of water while reacting. The resulting product has a ratio of adipic acid to hexamethylene diamine of 81:19. The molten acid-rich mixture is withdrawn in a continuous process.

As an alternate intermediate, adiponitrile is employed to react with hexamethylene diamine and steam in a multistage distillation column to prepare nylon-6,6 [194]. The process is carried out in the presence of an oxygen-containing phosphorous catalyst at an elevated temperature and pressure. Nylon-6,6 of high molecular weight can be produced by the postpolymerization of lower molecular weight polymer in the molten state in the presence of a phosphonic acid catalyst [195] or in the solid state [196]. In a different approach, a prepolymer is formed in a reactor system.

2.3.2.4 Other Polyamides

The synthesis of a number of polyamides other than nylon-6 and nylon-6,6 has already been discussed in Section 2.2.7. In recent investigations, nylon-12,14 with a long alkane segment was investigated for its crystallization behavior [197]. Copolymers of butylene terephthalate and 1,4-diaminobutylene terephthalate (PB/4-T) were synthesized from the diamides of diaminobutane and dimethyl terephthalate (DMT) with butane diol and more DMT in a concentration range of up to 50% nylon-4,T [198]. The polymerization conditions were similar to those for poly(butylene terephthalate), i.e., melt polymerization followed by solid-state postcondensation. At increasing nylon-4,T content in the copolymers, the melting temperatures increased strongly, heats of fusion decreased slightly, and glass transition temperatures increased linearly. The torsional moduli above the glass transition temperature also increased. Gonsalves and Chen reported the synthesis of copolymers of nylon-2,6,6 and nylon-6,6 by interfacial polymerization of *N*-glycyl hexane diamine and hexane diamine with adipoyl chloride [199]. The molecular weights of these copolymers were relatively high according to intrinsic viscosity measurements and GPC analysis. The copolymers had similar solubility features as nylon-6,6. The copolymers were semicrystalline. Both melting and glass transition temperatures showed a minimum at around 20–30% nylon-6,6 content. The copolymers with relatively low melting temperatures could conceivably be melt-spun into fibers without appreciable thermal degradation.

New block copolymers of nylon-6-*b*-polyimide-*b*-nylon-6 were prepared by first synthesizing a series of imide oligomers end-capped with phenyl 4-aminobenzoate [200]. The oligomers were then used to activate the anionic polymerization of molten caprolactam. In the block copolymer syntheses, the phenyl ester groups reacted quickly with caprolactam anions at 120°C to generate *N*-acyllactam moieties, which activated the anionic polymerization. In essence, nylon-6 chains grew from the oligomer chain ends. All of the block copolymers gave higher moduli and tensile strengths than those of nylon-6. However, their

elongations at break were much lower. The thermal stability, chemical resistance, moisture resistance, and impact strength were dramatically increased by the incorporation of only 5 wt% polyimide in the block copolymers.

2.3.2.5 Nanocomposites

A new composite material was introduced in 1987 with the discovery of a nylon-6/clay hybrid (NCH) [201]. The hybrid was prepared by the *in situ* thermal polymerization of ε-caprolactam with 8% or less montmorillonite, the clay material containing 1-nm thick exfoliated aluminosilicate layers. It exhibited a truly nanometer-sized composite of nylon-6 and layered aluminosilicate. Figure 2.14 depicts conceptually the NCH synthesis and its fine structure. The NCH exhibited high modulus, high strength, and good gas-barrier properties. The unique and superior properties led to the commercialization of NCH. It has also created a new class of nanocomposites and worldwide interest.

Variations in the preparation of nanocomposites have now been investigated extensively. Liu et al. [202] proposed the preparation of nylon-6/clay nanocomposites by a melt-intercalation process. They reported that the crystal structure and crystallization behaviors of the nanocomposites were different from those of nylon-6. The properties of the nanocomposites were superior to nylon-6 in terms of the heat-distortion temperature, strength, and modulus without sacrificing their impact strength. This is attributed to the nanoscale effects and the strong interaction between the nylon-6 matrix and the clay interface. More recently, nanocomposites of nylon-10,10 and clay were prepared by melt intercalation using a twin-screw extruder [203]. The mechanical properties of the nanocomposites were better than those of the pure nylon-10,10.

García et al. [204] prepared composites of nylon-6 polymer with nanometer-sized silica (SiO_2) filler by compression molding. The addition of 2 wt% SiO_2 resulted in a friction reduction from 0.5 to 0.18 when compared with neat nylon-6. This low silica loading led to a reduction in wear rate by a factor of 140, whereas the influence of higher silica loadings was less pronounced.

2.3.2.6 Process Simulation

Advances in the areas of instrumental analysis and numerical computations have made possible meaningful improvement of the polymerization processes.

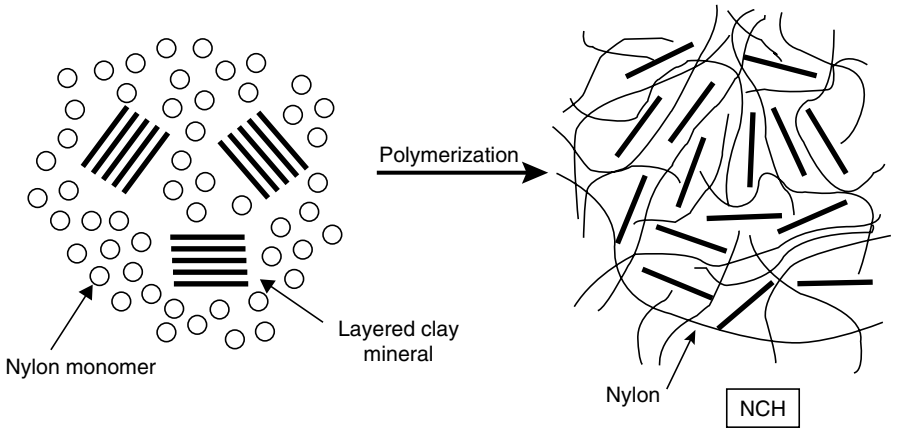

FIGURE 2.14 Conceptual depiction of NCH synthesis and fine structure. (From Kawasumi, M., *J. Polym. Sci. A: Polym. Chem.*, 2004, 42, 4, 819–824. With permission.)

2.3.2.6.1 Staged Polymerization

The optimal process is distinguished by two principal stages. The first entails operations at high water concentrations and high temperatures, resulting in high rates of monomer conversion. In the second stage, low water concentrations and low temperatures characterize the approach to high degrees of polymerization and conversion. The transfer of the reacting mass from the first to the second stage therefore entails the removal of any free water. The additional reactor element to accomplish this may be either a separate unit or a part of the reactor systems in either of the two stages. To realize the effects of a low temperature on conversion and polycondensation equilibrium would necessitate cooling of the polymer mass when conversion equilibrium is approached. Since a highly viscous material is involved, such an additional process step requires a more complex reactor system. Further complications may also result from the concomitant increase of the melt viscosity. Most industrial processes, therefore, operate the essential polymerization stage as much as possible under isothermal conditions employing the highest permissible reaction temperature. The latter is determined by the boiling point of the caprolactam and the extent of undesirable side reactions. In such a case, the optimizing functions depend only on the water concentration; the optimizing criterion being the minimum time required to obtain the desired degrees of polymerization and conversion. The optimum water concentration is either the upper or lower limiting value: the upper with respect to the rate of conversion, the lower with respect to the condensation equilibrium.

A simulation for such a two-stage process is shown in Figure 2.15 in comparison with the course of polymerization for the one-stage process at 265°C. On the basis of the assumption that there are no operational limitations for realizing ideal piston flow and instantaneous removal of water, Figure 2.15 shows that in the two-stage process the desired degree of polymerization is obtained in less than half the time required for the one-stage process.

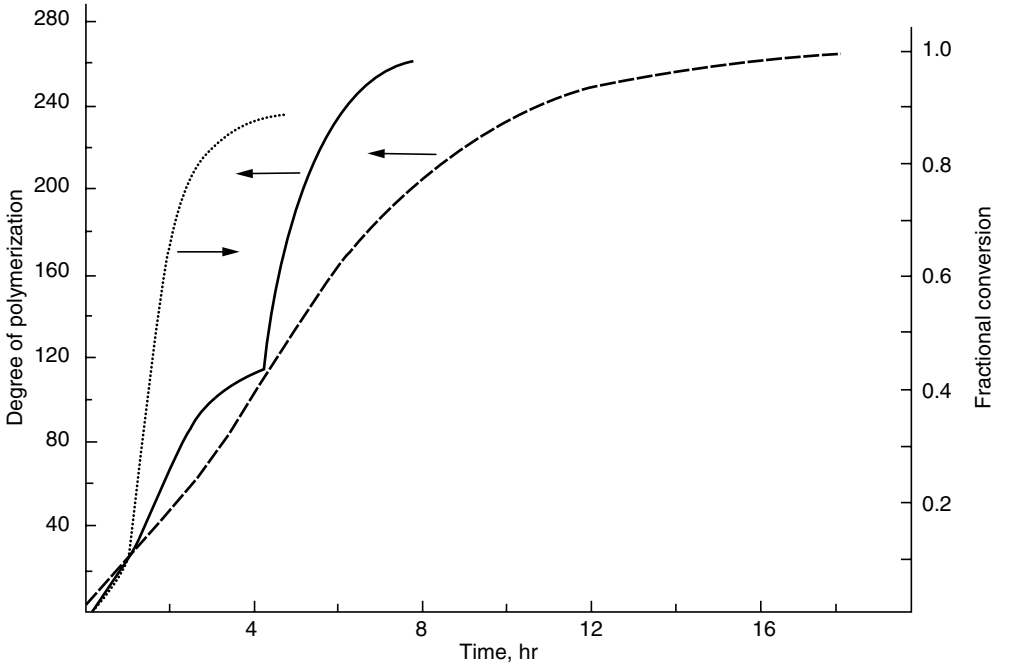

FIGURE 2.15 Course of polymerization for two-stage process. Solid line: two-stage process, initial water concentration; $[W_o]_{init} = 0.04$ mol/mol CL; free water removed at conversion equilibrium; dotted line: conversion at $[W_o]_{init} = 0.04$; broken line: one-stage process, $[W_o] = 0.1$.

Commercial process designs reflect the awareness of the advantage of operating the polymerization process in two distinct stages that are characterized by water content that approaches the upper working limit in the first stage and the lower one in the second stage. The most favorable mode of operation, however, depends on many factors, such as specific product requirements, the availability of reactors that provide the desired performance with regard to heat and mass transfer, and flow patterns.

2.3.2.6.2 Reactor Designs

Industrial processes entailing both batchwise and continuous operations use reactor systems that include autoclaves, with and without internal heat exchangers and stirrers, simple tube reactors, cascades of stirred tank reactors, and combination reactors containing both tubular and back-mix units. Relatively simple reactor systems that meet the considered requirements to some degree have been employed in industrial operations. Most of them are tubular flow reactors that in ideal operations are characterized by true plug flow, which is a condition that cannot readily be realized. Consequently, and also for the achievement of good heat transfer, processes have been proposed and practiced that utilize a cascade of stirred-tank reactors or a combination of such a cascade and tubular plug flow reactor. In this combination, the cascade constitutes the first stage and the tubular reactor the second one.

Principally, this process of polymerization consists of N stirred reactors followed by a tubular reactor as shown schematically in Figure 2.16. To obtain the highest possible rates of conversion, the reactor segment consisting of the stirred tanks 1 to $N+1$ is essentially a closed system and, as such, the first process stage. Removal of the free water is carried out in the Nth tank, from which the polymer melt is fed into the tubular reactor where the final degree of polymerization is obtained. Processes of this type have been quantitatively treated [54,55]. The overall rate of reaction of this multistage process depends, of course, considerably upon the removal of water from the polymer melt after the first process stage. With both diffusion and reaction, this process is obviously governed by mass transfer rates. The diffusion of both caprolactam and water in nylon-6 melts has been studied by Nagasubramanian and Reimschuessel. [205], and the diffusion coefficients of both caprolactam and water were estimated for nylon-6 equilibrium polymers at 265°C to be $D_m = 8 \times 10^{-8}$ cm^2/s and $D_w = 2.5 \times 10^{-4}$ cm^2/s, respectively. It was found that the diffusion of water out of the melt is very rapid and appears to be governed primarily by the boundary conditions for the melt surface rather than by the extent and rate of surface generation. These boundary conditions themselves are controlled by the respective modes of operation, which may be characterized by the use of steam pressure, inert gas flow, or vacuum. With respect to the caprolactam in the equilibrium polymer, a rather different situation prevails. Due to the low value of D_m, the rate at which caprolactam evaporates from the polymer melt depends mainly upon the surface area and thus on the rate of surface regeneration. Processes characterized by the direct vaporization of caprolactam from the polymer melt, therefore,

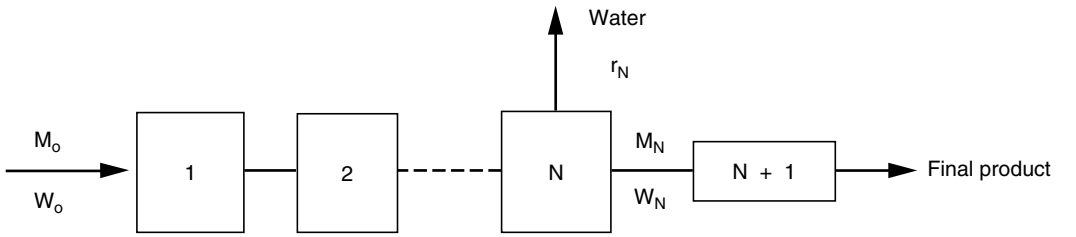

FIGURE 2.16 Combination reactor system.

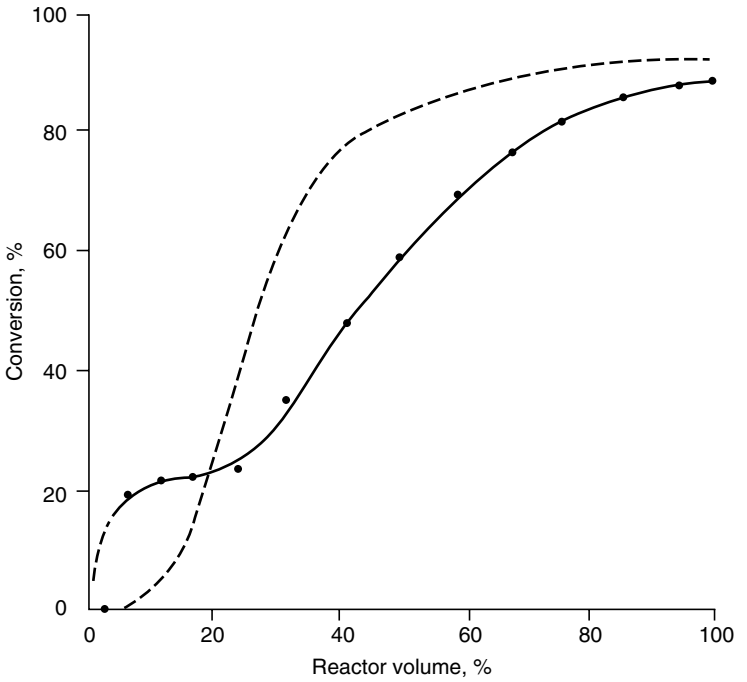

FIGURE 2.17 Conversion as a function of reactor volume for a reactor with back-mix flow in the first stage. (From Bayer, Ger. Patent 2,848,951.)

require more sophisticated operations and equipment than the more conventional ones in which the unreacted monomer is removed from the quenched polymer by hot-water extraction.

The concept of combining back-mix units with tubular plug flow reactors characterizes particularly large capacity reactor systems [181,182]. Compared with ideal plug flow reactors, higher initial conversion rates have even been claimed for a commercial reactor containing a type of back-mix section as the first stage [181]. Figure 2.17 shows the lactam conversion as a function of the reactor volume. The solid curve represents the observed course of conversion, and the broken line the one calculate for plug flow according to data of Reimschuessel and Nagasubramanian [52].

In recent years, twin-screw extruders are increasingly employed as commercial reactors for the polymerization of nylons. Such a reactor system offers the advantages of controlled plug flow, good mixing and heat transfer, and control of reaction time. Nascimento et al. investigated the finishing stage of nylon-6,6 polycondensation in a twin-screw extruder reactor [206,207]. Experimental results from industrial and pilot plants were employed to build various process models. They reported reasonable agreement between their models and industrial data and were able to achieve an increase in industrial production of about 20%.

2.3.2.6.3 Solid-State Polymerization

As discussed earlier, solid-state polymerization reactions are used to increase the degree of polymerization in the production of nylon-6 and nylon-6,6. The solid-state polymerization process has been studied by process simulation. Mallon and Ray [208] developed a comprehensive model to handle the reactions in polymers undergoing polycondensation reactions in the solid state. The polymer crystalline fraction is modeled as containing only repeat units,

thus concentrating end-groups and condensate in the amorphous fraction. In addition, many effects such as variable crystallinity and gas-phase mass transfer are included in a general framework. This model is compared to poly(ethylene terephthalate) and nylon reaction data with good results. In a separate study, Yao et al. [209] employed a complex model to describe dynamic changes in polymer property profiles of degree of polymerization, temperature, and moisture content over the height of the reactor and within the polymer particles. The model was further simplified by deriving appropriate expressions for heat- and mass-transfer coefficients and performing a lumped heat- and mass-transfer analysis. Good agreement between simplified and complex models is obtained, indicating that the simplified model can be used in place of the complex model if the polymer properties' profiles within individual particles are not of particular concern to the model user.

2.4 PREPARATION OF POLYAMIDE FIBERS

2.4.1 Melt Spinning

Polyamide fibers are basically converted from polyamide polymers by melt spinning. As shown schematically in Figure 2.18 [210], the classic melt spinning process usually encompasses several process steps: polymer melting, transporting, spinning through a spinneret to form multiple filaments, quenching, finish application, and take-up. This is followed by fiber drawing, comingling (interlacing), and package formation. In many cases, the drawing

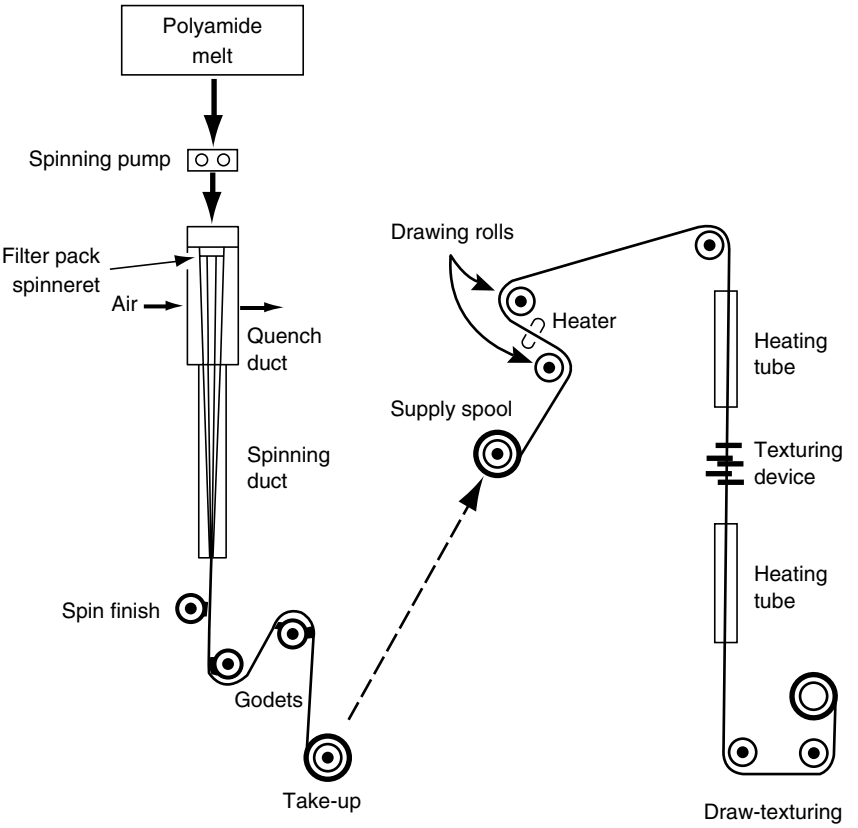

FIGURE 2.18 Traditional two-step melt spinning from chip.

process is integrated with spinning to form a one-step process. By changing the operating conditions of various process steps in a manufacturing process, different fiber structures and properties can be obtained for different applications.

The molten polyamide obtained either directly from the polymerization vessel or by melting the polymer chips via an extruder or a melt tank is delivered to an accurate metering device called a spin pump. The spinning temperature is usually 30°C higher than the polymer melting point. For nylon-6 with a melting point of 220°C, the spinning temperature is generally targeted at 260–270°C, and around 290°C for nylon-6, with a melting point of 260°C. It is very important to dry the polyamide chip to a consistent moisture level (about 0.12%) for successful spinning. Otherwise, poor spinning yield and poor fiber quality may result from polyamide degradation.

The spin pump (metering pump) delivers the molten polymer to a spin pack, which consists of a top cap and a breaker plate to distribute polymer evenly, then into a filtration media and out of the spinneret. The filtration media contains either different layers of special sand, layers of different size of stainless steel screens, or sintered metals. In addition to removing the foreign particles, gel particles and undesirable conglomerate additives, filtration may also improve the polymer melt homogeneity due to its torturous path and high shear of the filtration media.

The spinneret is similar to a showerhead, which converts the polymer melt into filaments. The orifices of the spinneret are normally round, thus producing filaments with a round cross section. In general, most nylon fiber products requiring high strength in tire cord, rope and cordage, and sling airbag, have round cross sections. However, for textile and carpet applications, fibers with modified cross sections have been developed to achieve different aesthetics such as luster, opacity, and insulation, walk resistance, etc. A fiber with a complex cross section can be used as a filtration medium for air or liquid. Figure 2.19 illustrates examples of nonround filament cross sections, including that of a $T_m = \Delta H_m/\Delta S_m$ TRIAD* fiber [211].

Spinneret orifice length/diameter ratio (L/D) and the orifice layout in the spinneret strongly influence filament uniformity and production yield. In general, an L/D ratio of 3 eliminates the entrance effect of the polymer flow through the orifice, a minimum upstream pressure of >600 psi for uniform distribution of polymer flow across the spinneret, and a shear rate at wall below 5000/s to avoid melt fracture are considered as a ''rule of thumb'' in spinneret design. Therefore, different polymer types (viscosity), molecular weight, and throughput rate may require different spinneret orifice dimensions for high yield and uniform fibers.

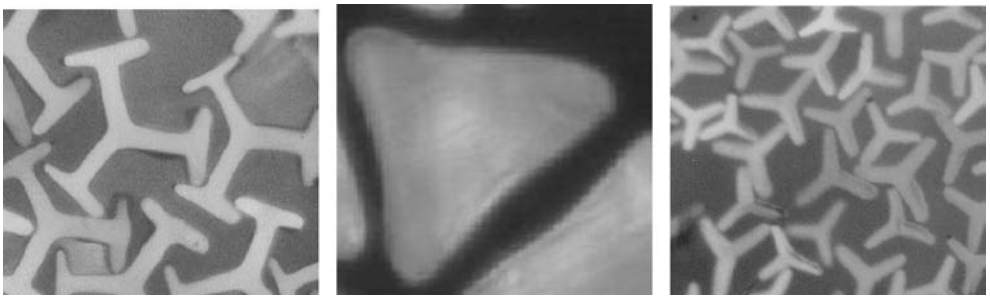

FIGURE 2.19 Examples of nonround fibers. (From http://FRAM.com/Honeywell International, FRAM Consumer Products Group, products (accessed September 2004). With permission.)

*TRIAD—a registered trademark of FRAM, Honeywell International, Consumer Products Group, Danbury, Connecticut, U.S.A

2.4.2 Dynamics of Melt Spinning

The melt spinning speed refers to how fast the yarn is taken up on the first godet roll (take-up roll). This is the most important area in fiber spinning and the dynamics is very complicated. Key process parameters such as the throughput rate (jet velocity) through the spinneret, the quenching rate (the rate of cooling to solidify the fiber), the take-up velocity (stretching rate dv/dl), and the dynamic viscosity of the polymer as a function of temperature, are mainly responsible for the physical properties of the resulting fiber. Theoretical studies by computer modeling to relate fiber properties to spinning conditions, heat transfer, polymer rheology, kinetics of crystallization, and molecular orientation have been formulated and resolved in the last 30 years. These results provide a guideline to study the process–structure–properties relationship. However, experimental studies and actual measurements are still the most reliable method to obtain an insight of the fiber properties.

A principle factor for correlating fiber properties to spinning conditions is the velocity gradient (q). It is related to the jet velocity (v_j), the take-up velocity (v_t) and the distance from the spinneret (l) at which the filament cross section becomes constant.

$$q = (v_t - v_j)/l \tag{2.74}$$

For a given Δv (dv/dl), the distance l is a function of the melt viscosity, which depends on the quenching temperature and its gradient. The elongational flow in melt spinning affects the molecular orientation, the extent of which results from the competition between the velocity field and thermal motion, the latter being controlled by temperature and viscosity [212]. Therefore, the temperature profile of the filament bundle in the quenching zone is of great importance, especially for those with a large number of filaments in the bundle. Significant differences in birefringence, diameter, tenacity, and elongation have been reported from the windward and leeward segments of the filament bundle. Filaments from the windward (cooler) part were characterized by larger diameters, lower birefringence, lower tenacity, and higher elongation after draw than the filaments from the leeward (warmer) part of the bundle.

2.4.3 Quenching

As the molten filaments emerge from the spinneret, they are cooled by air and sometimes by water. Most melt-spinning operations use air as the cooling medium. The quench air temperature is in the range of 18–20°C and relative humidity in the range of 55–65%. Both temperature and humidity of the air used for quenching must also be controlled because of their effects on orientation and eventual crystallization.

There are at least three major quenching approach systems: cross flow, radial inflow, and radial outflow as illustrated in Figure 2.20 [213]. The key objective is to provide uniform cooling to each individual filament so that all the filaments will have the same morphology and properties within the yarn bundle. If not done correctly, the end-product will be nonuniform, which may result in streaky carpet or streaky fabric because the dye uptake rate is affected by fiber morphology. Therefore, the spinneret layout, the velocity and the flow pattern of the quench air in turbulent or laminar flow, and the take-up speed of the fiber are very important to fiber uniformity. Considerable effort has therefore been directed toward the development of quench stacks designed to achieve uniform air velocities across the filament bundle and to eliminate any turbulence. Additional approaches to reduce filament nonuniformity involved specially designed spinnerets [214]. With the advent of the high-speed computer, flow modeling via computation of flow dynamics by finite element analysis (CFD)

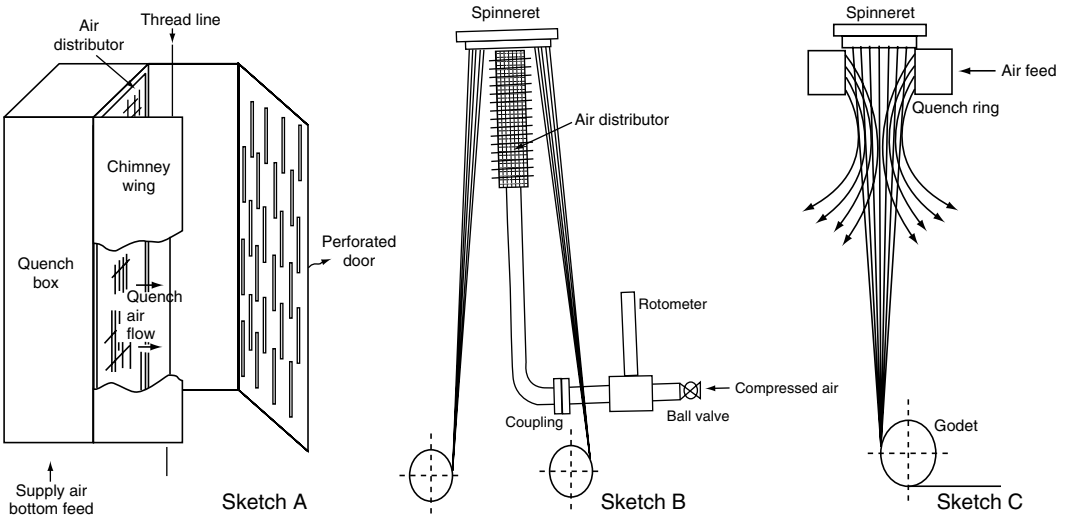

FIGURE 2.20 Quench air systems: A. cross flow; B. inflow; C. outflow. (From James, A., *Intl. Fiber J.*, 1999, 101–103. With permission.)

is currently used to design the quenching hardware by visualizing the interaction between the quench air flow and the filaments to maximize the yarn uniformity.

2.4.4 Spin Finish

As the filaments solidify and travel downstream at high speed, the surface friction through air generates static electricity, which makes the filament bundle less cohesive. To facilitate drawing and downstream processes, a finish emulsion with an antistatic agent, lubricating oils, bactericides, an antisoil agent, etc., are used to "wet" the fiber bundle by a kiss roll or meter finish device. Most of nylon-6 and nylon-6,6 spin finishes are water-based. The amount of finish (water) applied on the yarn may act as a plasticizer to lower the glass transition temperature and change the rate of crystallization once the yarn is wound up on the package. In general, the "wet pick-up" of the finish is about 10% by weight of the fiber to achieve the equilibrium moisture level for the downstream process, and the finish on yarn (FOY) is in the range of 0.2–1% of the fiber weight. Although the effect of the spin finish is an important aspect in fiber production, rather little has been reported in corresponding investigations [215,216].

2.4.5 Drawing

To develop the fiber strength, polymer molecules in both the crystalline and the noncrystalline regions are further oriented by elongating the fiber between two rolls at different speeds. The ratio of the two rolls is called the draw ratio. Higher draw ratio generally leads to higher molecular orientation and thus higher fiber strength. Drawing devices such as heated rolls with different surface roughness, draw pin, or draw point localizer, etc. are used to control the drawing profile. Mostly, increasing the drawing speed (higher elongation rate), drawing at a temperature lower than appropriate, or increasing the orientation of the feeder yarn from the spinning process decreases the fiber uniformity and quality. Therefore, spinning and drawing are best operated as an integral process to control the fiber morphology, physical properties, and end-uses.

2.4.6 Process Integration

To increase process efficiency and reduce production costs, an industrial effort has succeeded in integrating the spinning and drawing processes. Therefore, there are now three different types of spinning process arrangements. Each of these processes gives a different set of yarn properties and morphology.

1. Separate spinning and drawing: a two-step process
2. Stack-draw process: a one-step process
3. Spin-draw process: a one-step process

Figure 2.21 illustrates the two-step spinning and drawing process. The take-up speed is generally around 1000 m/min to make "undrawn" yarn of low orientation. The undrawn yarn is "lagged" in storage for 4–12 h and then drawn at about 3:1 draw ratio to develop the

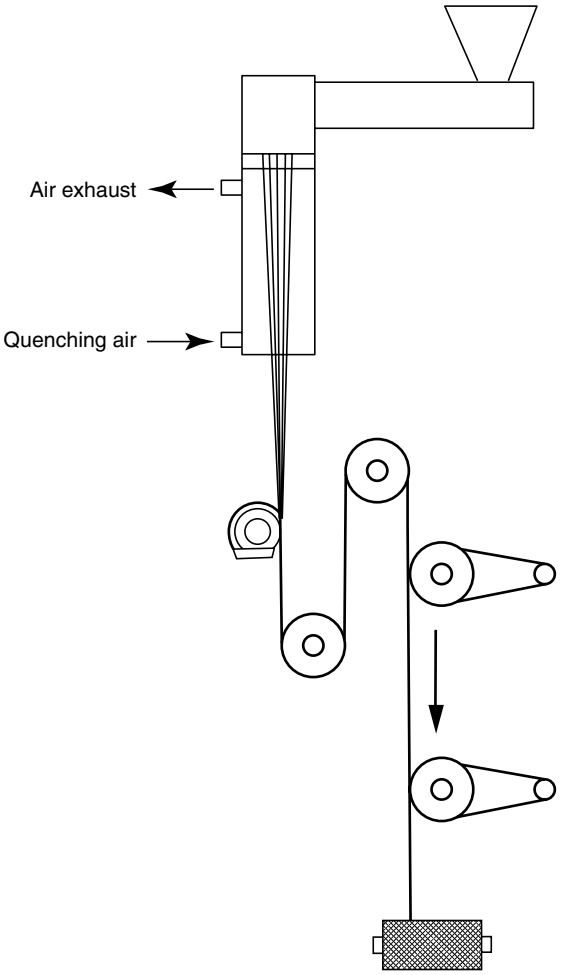

FIGURE 2.21 One-step stack draw process. (From Tam, T.Y. and Lin, C.Y., A unique one-step process of achieving fully oriented yarn properties with <1500 m/mintake-up speed, Fiber Society Spring Conference, Princeton, New Jersey, June 1996. With permission.)

fiber strength. The process of this type, as shown in Figure 2.18, yields a fully drawn yarn (FDY). Additional twisting step to provide the filament bundle cohesiveness is generally followed in the same process. Thus, the process is also called a draw-twist process.

Figure 2.21 illustrates the one-step stack-draw process. The take-up speed of this one-step process is greater than 3000 m/min. The product is known as the partially oriented yarn (POY). The combination of drawing and textile finishing seems suited particularly for the production of POY at high spinning speeds.

Figure 2.22 illustrates the one-step spinning followed immediately by drawing and lagging. The take-up speed of this process ranges from 600 to 3000 m/min, coupled with immediate drawing on the panel. The resulting product is a fully drawn yarn.

2.4.6.1 Draw-Twisting

Polyamide filaments produced in high-speed operations that do not combine spinning and drawing processes must be subjected to a subsequent draw-twisting process to develop more useful properties. Since this process is performed in the solid state, the resulting orientation is

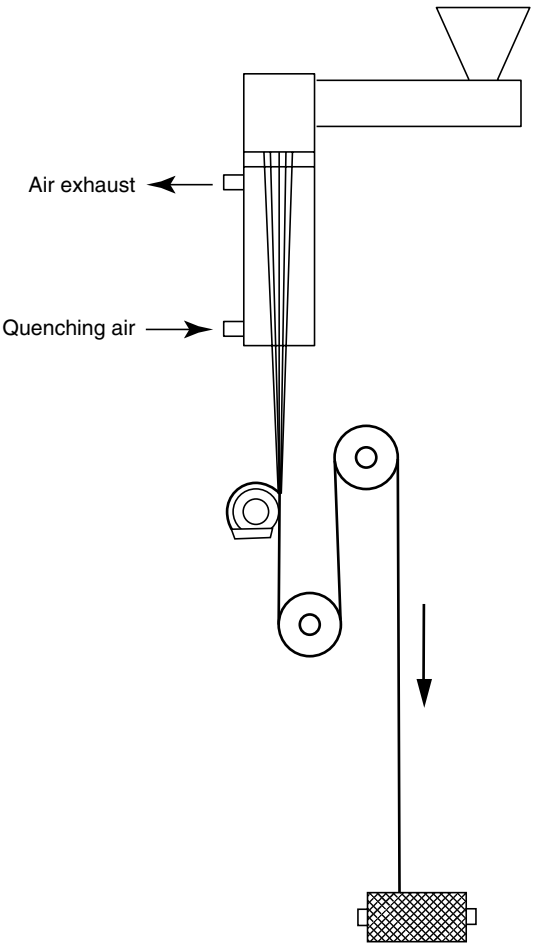

FIGURE 2.22 One-step spin-draw process. (From Tam, T.Y. and Lin, C.Y., Fiber Society Spring Conference, Princeton, New Jersey, June 1996. With permission.)

mainly controlled by the draw (deformation) ratio and is less affected by relaxation factors (molecular motions). Thus the drawing rate and temperature in the draw-twisting process are of less importance than they are in the spin-draw process.

2.4.6.2 Spinning–Drawing–Texturing

BCF production can be converted into a one-step spinning–drawing–texturing process for carpet and other applications. In this process, the yarn is generally spun at a take-up speed of about 2000 m/min, immediately drawn on panel at a draw ratio from 1.1 to 2.5, and passed through a texturing device to develop a crimped fiber. The crimped fiber will continue onto a perforated drum to be cooled before it is wound up on a package. Alternatively, an undrawn yarn spun earlier can be used as a feeder yarn to be drawn and textured as above.

2.4.7 High-Speed Spinning

For polyamide fibers, increasing the spinning speed increases productivity as well as the preliminary orientation of polymer molecules with respect to the fiber axis. This leads to a reduction of the extensibility of the spun filaments and the extent to which they can be drawn. It can result in acceptable product variation at certain speed limits, or reduce the fiber tenacity attainable in a high-tenacity fiber process. It can also reduce the draw ratio in the stack-draw process. These difficulties have been mitigated by reducing the filament quenching in spinning to reduce the preliminary molecular orientation. This can be achieved by the use of hot tubes below the spinneret, or the use of high-velocity air to enhance the filament stretching at a high temperature closer to the spinneret. The spinning parameters that affect the molecular orientation also affect crystallization during the spinning process, but in the opposite direction. Thus crystallinity increases with delayed cooling and filament thickness and decreases with increasing take-up velocities [217]. These effects, particularly in nylon-6,6, may be somewhat effaced due to orientation-induced crystallization during the melt-spinning process.

The categorizing of orientation obtained by this spinning process is classified as low-oriented yarn (LOY, produced at rates up to 1800 m/min), medium-oriented yarn (MOY, produced at rates in the range of 2000–3000 m/min), partially oriented yarn (POY, produced at rates 3000–4000 m/min), and highly oriented yarn (HOY, produced at rates higher than 4000 m/min). High-speed spinning at take-up speed in the range of 6000 m/min yields fiber properties that appear adequate for apparel applications. Partially oriented polyamide filaments obtained at take-up speeds of 2500–4500 m/min are characterized by elongations of about 40–100% and are suitable for draw-texturing operations at drawing velocities between 700 and 800 m/min [207,218].

The effect of molecular weight on high-speed melt spinning of nylon-6 has been studied [219]. In as-spun filaments, higher molecular weights led to high modulus and tenacity and lower elongation to break.

There have been many attempts to change the melt flow properties of a polymer by incorporating a small amount of an anisotropic or an immiscible polymer. For example, Brody [220,221] demonstrated a windup speed up to 5000 m/min by adding a small amount of copoly(chloro-1,4-phenylene ethylene dioxy-4,4′-dibenzoate/terephthalate) (CLOTH) or copoly(4-hydroxybenzoic/6-hydroxy-2-naphthoic acid) into nylon-6,6. More recently, Vassilatos [222] disclosed the melt spinning of nylon-6,6 at speeds up to 6000 m/min with the addition of a minor amount of liquid crystalline polymers such as CLOTH. This technique clearly offsets some of the cost advantages of high-speed spinning.

The development of high-speed winding equipment has made the application of the high spinning speeds feasible. Equipment has been developed that realized spinning speed up to

6000 m/min. Modern operations utilize microprocessors to control the winding of the filament on cylindrical bobbins to obtain a "ribbon-free random wind" (RFRW).

2.4.8 Textile Finishing Operations

Textile finishing generally comprises operations such as rewinding, warping, twisting, and texturing. In the warping procedure, an extensive number of filaments are wound concurrently on a warp beam at a rate of 700–1000 m/min. In subsequent steps, the bobbins produced in this way are placed directly on a weaving machine. More recent developments are concerned with combining this process step with a drawing operation. Twisting and texturing, as discussed earlier, are parts of the integrated draw-twisting and spinning–drawing–texturing processes.

2.4.8.1 Texturing

Texturing procedures comprise mechanical distortions of the filaments to improve fiber characteristics such as the apparent volume (bulk), stretching properties (elasticity), shape (appearance), and the perceived feel (touch, handle) of the fiber material. The textured yarns are either fine tex* (1.7–2.2 tex) or heavy tex (110–400 tex) materials. The former are used in apparel applications, mainly for woven and knitted stretch fabrics; the latter are used primarily for carpets. A considerable number of processes and techniques have been developed for the production of textured filaments. A compilation of relevant processes has been presented by Wagner [223].

There are two types of texturing operations: crimping and jet texturing. The classic crimp texturing technology is used in the two-step spinning and drawing process for staple fibers. In this two-step operation, the fiber is first spun into a large container. About 20 to 30 of these tow containers are combined together to make a 30,000-denier tow. This big tow is drawn normally at a 3:1 draw ratio to develop its strength. The drawn tow of about 10,000-denier is continually forced into a stuffer box to be "crimped." The crimp is two-dimensional and the normal intensity is from 9 to 12 CPI (crimp per inch). The "crimped" tow is immediately heat-set and is cut to different lengths of about 7–7.6 cm (2.75–3 in.) or to customer specifications. The typical denier range is from 10 to 15 dpf (denier per filament) for carpet fiber.

Another texturing technology used in conjunction with process (1) is the Sintex texturing technology for three-dimensional texturing. An undrawn yarn is first spun. The undrawn package is then drawn at about 3:1 draw ratio and immediately fed into a texturing jet and wound upon a package. The product is about 1200 denier and typically contains 70 filaments.

Jet texturing is the new technology employed in the one-step spinning–drawing–texturing process (3). In this process, the yarn is spun, immediately drawn on panel without packaging and immediately textured on panel with a texturing jet, cooling drum, and finally wound up on a package.

2.4.8.2 False-Twist Texturing

The most important recent development, applied for the manufacture of about 90% of textured filaments, utilizes a process based on torsion mechanical–thermal procedures. The operation consists of three basic steps: high-twist twisting, fixation of the twist, and detwisting of the twist. In the process known as false-twist texturing, these three procedures are carried out in one process step. Rather detailed descriptions of this procedure are given

*1 tex = 0.11 denier = $1 \times 10-4$ kg/m; tex = weight in grams of 1000 meter filament; dtex (decitex) = weight in grams of 10000 meter filament.

in the literature [224,225]. The efficacy of this texturing process has been greatly improved by resolving problems concerning a bearing-free support of the spindle in the texturing aggregate. Adjusting the ratio of the driving wheel diameter to the spindle to about 20:1, revolutions of 106/min and rates to 200–300/min were possible. Twist is defined as the ratio of the spindle revolutions to the delivery rate of the filaments. If the twist of the filament amounts to or exceeds 150 twists/m, the material must be exposed to temperatures ranging from 60 to 80°C to stabilize the induced twist.

Considerable improvement in the production rates resulted from the introduction of frictional texturing [226]. This process uses friction wheels. Essentially, one wheel revolution produces a fiber characterized by a twist number that parallels the ratio of the friction wheel diameter to the fiber diameter. Industrially practiced frictional texturing processes use a variety of wheels and are characterized by a delivery rate that approaches values in the range of 1000 m/min^{-1}. Gall presents a detailed account of this process [224].

Kuznetsov and Usenko have presented some aspects related to the texturizing technology, employing false-twisting operations and discussed ultrahigh frequency heating for thermal fixation of textured fibers [227]. The manufacture of textured yarns of polyamide conjugate fibers (mixtures of nylon-6,6 and nylon-6) is described in a Toray Industries patent [228], which refers to a process operating at 15°C and 3000 turns/m. Conjugate yarns that yield crimpable polyamides are described in a number of patents: a Toyobo patent [229] relates to yarn compositions constituted mainly of nylon-4,6 and nylon-6,6, in which the two polymers were spun into side-by-side conjugate yarns. Toray patents [230] pertain to diverse polyamide compositions yielding self-crimpable composite fibers.

False-twisting is most widely used for texturing fine tex yarns. In the first step, they are heated to about 220°C and 185°C in the cases of nylon-6,6 and nylon-6, respectively. This is followed by twisting to introduce 30–40 turns/cm using spindle or friction devices. The yarn is then cooled and untwisted. The resulting product is characterized by good elasticity. If bulk is required, the yarn is either subjected to a second heat–twist–untwist step or treated with steam or hot water in an autoclave.

2.4.8.3 Crimp Texturing

The edge-crimping process results a textured yarn by passing the filaments over a heated roll and then drawing them across a blunt knife edge at an acute angle. This results in compressed and stretched filament segments, causing the development of a textured structure upon relaxation. The texturing efficacy does not equate the results attained with the false-twisting process.

Used mainly for heavy tex yarns, gear crimping produces a textured material when drawn filaments are passed through sets of meshing gear teeth. The process may or may not involve external heating of the filaments, but heat-setting is necessary for adequate crimp permanence.

In stuffer box crimping (and in the related Spunise process), yarn is heated and forced into a stuffer box (a heated chamber) where it bends, folds, and forms random crimp that is heat-set. In the mechanical process, the yarn is forced into the box through pairs of feeder rolls, whereas in the aerodynamic process, the yarn is transported into the crimping chamber via a jet by a gaseous medium, usually superheated steam [231]. In both cases, the crimped yarn is pulled from the stuffer box after a controlled residence time and at a constant rate. The principal application of this process is the texturing of fibers having titers* in the range of 600 to 4000 dtex. This class includes carpet fibers for which this process is primarily applied.

---

*The titer is the weight of 1000 meter filament and is defined by the relation Titer = M*1000/(Shy*Nd), where M = amount of polymer fed to the spinneret in g/min, Shy = take-up velocity in m/min, and Nd = number of filaments pro spinneret.

2.4.8.4 Commingling, Interlacing, and Air-Jet Texturing

Since a yarn bundle consists of multiple filaments, it is difficult, if not impossible, to further process the yarn into a final product such as carpet or fabric via weaving or tufting processes. The methods to provide filament cohesiveness include twisting in the draw–twist process as mentioned above, commingling, or interlacing. The commingling process is conducted by passing the yarn bundle in and out of a commingling jet where a high pressure, turbulent air inside the jet chamber entangles the filaments together into nodes with uniform spacing. These nodes transform loose filaments into a continuous yarn bundle suitable for weaving, tufting, knitting, and the like.

The design of a commingling jet affects the appearance of an entangled yarn. Some commingling jets produce the node and antinode feature, while some produce a continuous interlaced cohesive yarn bundle without the distinct nodes. In addition, by controlling the feed speed and take-up speed (called overfeed) with a specially designed jet, one can obtain a bulky, air-textured yarn for end uses like luggage fabric, backpack, etc.

2.4.9 Winding and Yarn Package

After the commingling or twisting step, the yarn is finally ready to be wound up on a bobbin. To produce a stable package, winder settings like the wind ratio, helix angle, winder tension, finish or moisture content of the fiber, and the fiber properties must be optimal. As mentioned earlier, in the high-speed spinning of nylon-6, the fiber is not stable at the take-up speed of 1200–3000 m/min for a polymer of 55 FAV (formic acid viscosity). The fiber will grow or elongate as it is being wound up on the package. Good package formation cannot be provided under this circumstance.

2.5 STRUCTURES AND PROPERTIES OF POLYAMIDE FIBERS

2.5.1 Polymer Chain Structure

The structure of polyamide fibers is defined by both chemical and physical parameters. The chemical parameters are related mainly to the constitution of the polyamide molecule and are concerned primarily with its monomeric units, end-groups, and molecular weight. The physical parameters are related essentially to chain conformation, orientation of both polymer molecule segments and aggregates, and to crystallinity.

This characteristic for single-chain aliphatic polyamides is determined by the structure of the monomeric units and the nature of end groups of the polymer molecules. Thus, in accordance with Equation 2.1 through Equation 2.3, these polyamides are represented by either of the two general structures:

1. X,Y polyamides

$$R' - [\,[-HN-(CH_2)_X-NH-CO-(CH_2)_{Y-2}-CO-]]_n-R$$

2. Z polyamides

$$R' - [-HN-(CH_2)_{z-1}-CO-] - R''$$

where $R' = H$, C(O)R; $R'' = OH$, NHR; $n >> 1$; and R = aliphatic or aromatic residue.

For the Z-type polylactams, recent literature has reviewed the molecular and electronic structures of lactams in considerable detail [16a]. Rudolf Puffr's review is concerned with the electronic structure of the amide group and the corresponding responses of molecular parameters. He refers to sp^2-hybridization of the nitrogen and carbonyl carbon atoms, the essential coplanarity of the atoms forming the amine group, the torsion angle about the amide bond, and the spatial electron distribution of the amide group. Conformational characteristics depend on the ring size of the particular lactam and encompass planar structures to puckered rings. In addition to some physical properties, he also addresses acid–base features comprising the acidity of both the NH and CH_2 moieties, characteristics of lactam salts, amide electrophilicity, hydrogen bonding, self-association, amine–water interaction, hydrogen donor complexes, protonation, and inorganic electron acceptor complexes entailing molecular acceptors and metal cation acceptors.

2.5.2 Characteristics of Crystalline and Amorphous Structures

Linear aliphatic homopolyamides are partially crystalline materials. Therefore they are characterized by both an unordered amorphous state and an ordered crystalline state. The latter may exhibit polymorphism. The extent to which each state or specific modification is represented depends, for a given chemical structure, considerably on processing conditions and treatment operations. It affects the properties of the shaped polyamide product. Thus the corresponding structure parameters are of importance for optimizing fiber processes as well as for assessing the performance of fiber products in particular applications.

2.5.2.1 Crystalline Forms

The crystal structure of polyamides results from the conformation of the macromolecules and their lateral packing. Generally, the packing of polymer chains will be such that the occupied volume is at a minimum, thereby minimizing the potential energy of the structure, but maintaining appropriate distances for intermolecular forces between adjacent chain segments. In polyamides, these intermolecular forces are both van der Waal's bonds and hydrogen bonds. The latter, involving the NH and CO moieties, cause the formation of sheet-like arrangements between adjacent chains. The stacking of these hydrogen-bonded sheets controls the size and shape of the unit cell. Since the nature of the bonds in the chain direction is different from that of the lateral bonds, the unit cells of polyamides are generally characterized by monoclinic, triclinic, and rhombic lattices. Hexagonal lattices indicate usually metastable mesomorphic modifications. The general conformation of the chain segments in the unit cell and their mode of packing are the basis for classification with regard to the crystalline forms of various polyamides. One is characterized by fully extended chain segments and is referred to as the α-structure; the other γ-structure consists also of extended segments, which however are twisted or contain some kink, resulting usually from rotation about the $–CH_2NHCO–$ unit [232]. Polyamides of the nylon X,Y-type with even–even carbon atom numbers crystallize mainly in the α-form, whereas those with odd–odd, even–odd, and odd–even numbers crystallize usually in the γ-form. Polyamides of the nylon Z type with even numbers crystallize generally in the γ-form for $Z > 8$. Nylon-4 and nylon-6 can crystallize in either the α- or the γ-form. However, the predominant structure of these two polyamides is the α-form. The two structures are interconvertible. The γ-form can be converted to the α-form by either treatment with aqueous phenol or the application of stress at high temperatures, whereas the α-form can be converted to the γ-form by treatment with aqueous iodine–alkali iodide solutions [233–238].

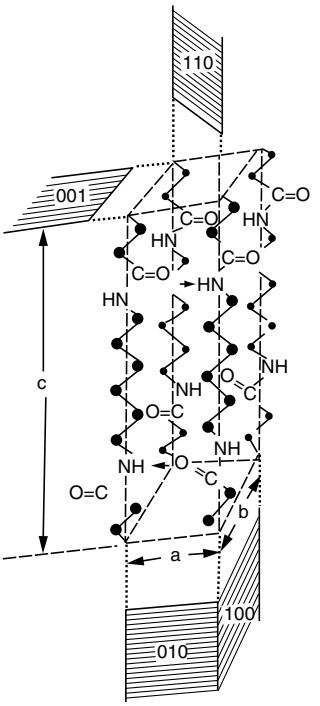

FIGURE 2.23 Unit cell of nylon-6,6.

Nylon-6,6 and nylon-6 are the two polyamides that are of most importance for commercial fiber production. The stable structure of both is the α-form and as such is comprised of stacks of sheets of planar hydrogen-bonded extended-chain segments [238,240]. These sheets are characterized in nylon-6,6 by a parallel alignment of the adjacent extended molecules, which are spaced with a perpendicular chain-to-chain distance of 0.42 nm and which are successively displaced in chain direction by a distance corresponding to one chain atom. The stacking of the hydrogen-bonded sheets entails a perpendicular sheet-to-sheet distance of 0.36 nm and a displacement of each successive sheet of about 0.5 nm in the chain direction. This arrangement results in a triclinic structure. The corresponding unit cell is characterized by identity of the crystallographic period and the chemical repeat unit. There is one extended chemical repeat unit per unit cell [239]. Figure 2.23 shows a schematic drawing of the unit cell and the principal crystallographic planes.

In nylon-6, the hydrogen-bonded sheets of the α-form are characterized by an antiparallel alignment of the extended chain segments. This opposite directionality of the CONH segments makes possible complete formation of unstrained hydrogen bonds. The stacking of the resulting planar sheets is marked by an alternating up-and-down displacement of about 0.37 nm parallel to the chain direction. The resulting structure is monoclinic. The crystallographic repeat unit of the unit cell corresponds to two extended monomer units, and the unit cell consists of four extended-chain segments; it contains, therefore, eight monomer units [240]. Figure 2.24 shows a schematic presentation of the unit cell and the principal crystallographic planes.

The distances between both the hydrogen-bonded chain segments and the sheets linked by van der Waal's forces are about the same as those found for nylon-6,6, namely 0.44 and 0.37 nm, respectively [240]. Although in these structures, due to the relatively strong hydrogen bonds, the chain-to-chain distances do not easily change, sheet-to-sheet distances are more

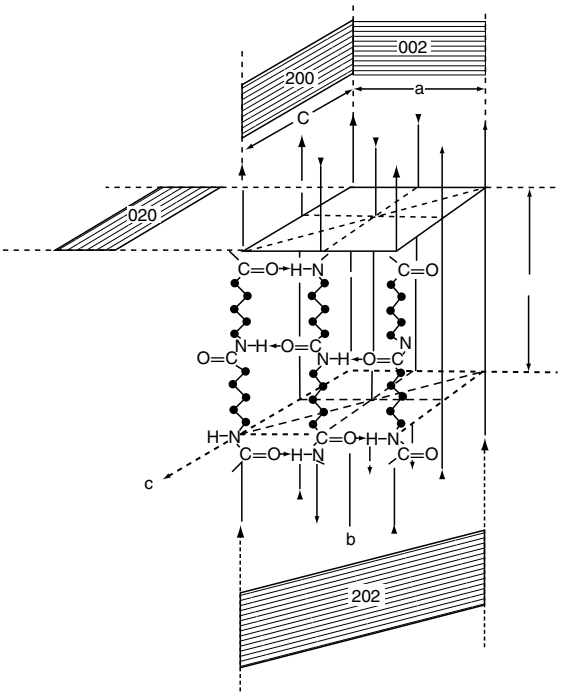

FIGURE 2.24 Unit cell of the monoclinic α-form of nylon-6.

readily affected and susceptible to changes in response to conditions of crystallization and applied external forces. This anisotropy of the intermolecular forces is responsible for the polymorphism that characterizes most aliphatic polyamides.

Stable polymorphic modifications are possible usually in systems distinguished by directionality, which in polyamides is caused by steric polarity resulting from the invariable sequence of the CONH groups. As is shown schematically in Figure 2.25, steric polarity is absent in polyamides of the X,Y-type but is a distinct characteristic of the Z-type polyamides.

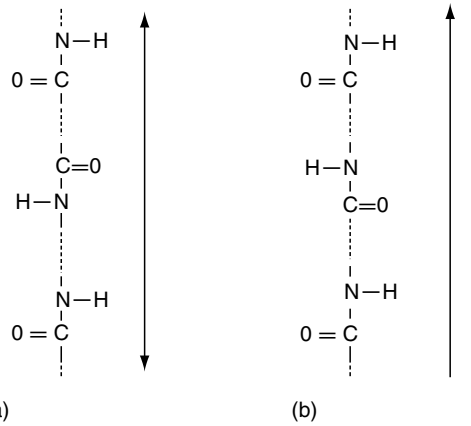

FIGURE 2.25 Steric polarity in polyamides: (a) nylon X,Y; (b) nylon Z.

Any lattice disorder may correct itself readily due to the lack of directionality of the X,Y-type nylon chain molecules. The x-ray diagram of nylon-6,6 filaments of high axial orientation, for instance, shows a medicinal reflection and layer-line streaks. This was initially explained as a result of an alternating up-and-down displacement of the hydrogen-bonded lattice planes similar to the stacking arrangements, characterizing the α-form of nylon-6 [239]. It was therefore considered a definite polymorph referred to as β-form. Another explanation, however, involves the postulation of rudimentary and intermediate stages in a continuous process of the formation of an ordered α-structure [241,242]. Indeed, upon annealing, this β-form converts readily into the α-form.

Rudimentary organization of chain segments may also be the cause for the formation of a similar metastable mesomorphic modification of nylon-6 upon rapid quenching of the molten polyamide [243]. The resulting structure is pseudo-hexagonal, since the corresponding x-ray diagram shows only a single reflection, but it is in general less well understood. It may be considered a bundle-like arrangement that consists of chain segments of both parallel and antiparallel directionalities with statistically changing equidistant bonding along two crystallographic axes [244,245]. This pseudo-hexagonal structure has been referred to as a γ-form [232,234,246–250], a β-form [251], and a pleated α-form [252]. This structure is formed and is stable within the temperature range of 100–150°C. Upon annealing or any proceeding process of crystallization, adjacent chains organize according to their directionality to form stacks of lattice planes. The resulting structure is characterized by an antiparallel arrangement of adjacent chain segments, either within the individual lattice planes or between successive planes. The antiparallel alignment of extended chain segments within the lattice planes characterizes, as discussed earlier, the α-form, whereas parallel directionality within the lattice planes is now generally referred to as the γ-form. In both forms, hydrogen bonding is complete between the amide functions of adjacent chain segments within the individual lattice planes, as shown by infrared studies [248,253]. Both crystallographic period and chain packing of the γ-form are different from those of the α-form; there is no alternating up-and-down displacement of the hydrogen-bonded sheets in the chain direction, such as the shift of (3/14)b in the α-form. Both forms have the same chain arrangement in the basal plane [236], as can be seen in Figure 2.26.

To realize complete hydrogen bonding between parallel chain segments, the latter cannot be in a planar zigzag conformation, but are, as has been pointed out earlier, slightly twisted due to a rotation by about 60° about the $-CH_2NHCO$ unit. This results in a lowering of the height of the unit cell to 1.688 nm from the 1.724 nm of the α-form.

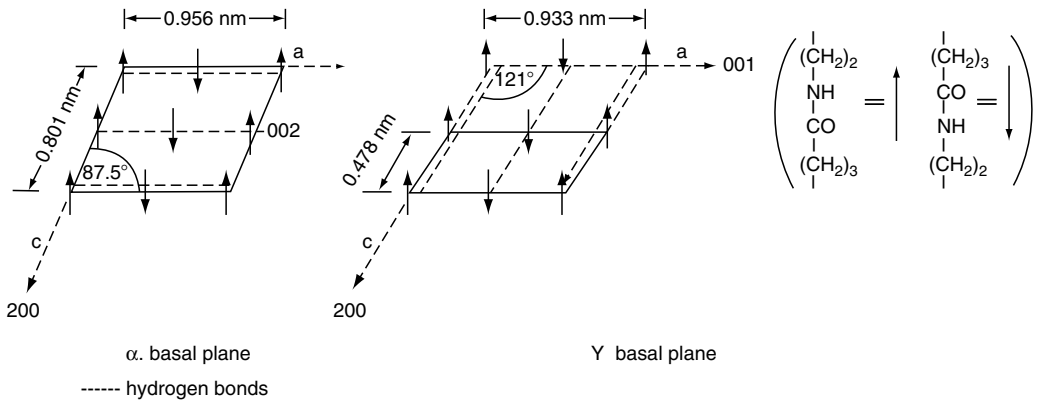

FIGURE 2.26 Schematic presentation of chain arrangement and hydrogen bonds in the basal planes.

2.5.2.2 Crystalline Structures in Fibers

Nylon-6 fibers obtained by melt spinning contain mixtures of the different crystal modifications, the concentrations of which depend upon the conditions of spinning, drawing, and annealing. Thus, fibers produced by conventional operations at moderate spinning speeds contain about equal amounts of α- and γ-forms. Annealing these fibers at temperatures up to about 100°C in the presence of moisture and up to about 150°C in dry conditions results in moderate increases of both forms, with the α-form slightly favored. At annealing temperatures higher than about 100°C, and in the presence of moisture, conversion of the γ-form to the α-form occurs. On drawing at low temperatures, the ratio of the concentrations of the two forms changes, although a mixed structure is retained. Increasing the draw temperature results in an increased conversion to the α-form; in combination with increasing draw ratios, the amount of the γ-form becomes negligible [254,255]. All this indicates that the α-form is energetically favored and is thus the more stable structure. However, fibers spun at high take-up speeds (<3000 m/min) have the γ-form as the predominant structure. Spinning at these very high winding speeds entails an orientation-induced crystallization process; obviously, the kinetics of this process favors the γ-form [254].

A pure γ-form can be obtained by an α-crystal-to-γ-crystal transition, which can be effected by treatment with a solution of iodine in aqueous potassium iodide [232,233, 236,237,248,249,256–267]. The pure γ-form resulting from this process is stable to the extent that it can be annealed and may retain any initial uniplanar axial orientation [236,249]. Although its structure has been considered nearly hexagonal [249,268], pseudohexagonal [237], and orthorhombic [257], it is characterized by a monoclinic geometry [236,249]. The corresponding unit cell has the following dimensions: $a = 0.933$ nm, $b = 1.688$ nm (fiber axis), $c = 0.478$ nm, $\beta = 121°$, and it contains two chain segments each consisting of two monomer chemical units. The crystal-to-crystal transition may be explained by a mechanism that entails interaction of the iodine with the amide group. This interaction results in both the breaking of the hydrogen bonds between antiparallel chain segments within the sheet-like structures and omits twisting the amide moiety out of the plane of the main chain axis by about 60°. This rotation reduces the distance between the amide groups of neighboring sheets to such an extent that after the removal of iodine, hydrogen bonds form between these amide groups. Thus, in accordance with the chain arrangement shown in Figure 2.6, a structure emerges that is composed of hydrogen-bonded sheets of parallel chain segments [249,263,264].

Consistency with x-ray diffraction data has been indicated in a study of iodine-complexed nylon-6 films using polarized resonance Raman spectroscopy [269].

Although both this γ-form and the α-form may be considered well-established structures, it has been realized that perfection of the crystal lattices and the dimension of the unit cells may be affected by processing conditions [245,247], particularly in the fiber-forming process. Thus the monoclinic α-structure as represented in Figure 2.4 may be considered a limiting form that can be observed only in certain crystalline aggregates such as well-developed spherulites. The monoclinic α-type structure observed in nylon-6 obtained by conventional molding, extrusion, and melt-spinning operations is less perfect and may be characterized by differing lattice parameters [245]; therefore, it has been called a "paracrystalline α-form" [247]. Indeed, the densities obtained upon extensive annealing of both highly oriented and nonoriented fibers were slightly above 1.17 g/cm^3 [236,270] but did not approach the value of 1.23 g/cm^3 calculated for the ideal monoclinic α-form [240]. From the relation between the heat of fusion and the specific volume [250], as well as from x-ray data [257], a density of 1.19 g/cm^3 was determined for the perfect monoclinic γ-form as obtained by the iodine treatment; the corresponding experimentally obtainable values were in the range of

1.14–1.15 [271]. The structure of iodide ions in iodinated nylon-6 and the outgrowth of hydrogen bonds between parallel chains have been discussed [272].

The limiting value for the density of the pseudohexagonal structure was found to be 1.13 g/cm^3, whereas a value of 1.084 g/cm^3 has been reported for the amorphous phase [236]. For nylon-6,6, values of 1.233 and 1.12 g/cm^3 for the triclinic crystal [273] and the amorphous phase [274], respectively, were found.

2.5.2.3 Structural Models

The crystalline and noncrystalline phases in polyamide fibers do not appear to be governed by what may be defined as thermodynamic equilibria, nor is there evidence for definite boundaries between a ''phase,'' characterized by a simple or complex state of order and an essentially amorphous ''phase.'' It is therefore quite obvious that the morphological structure of nylons cannot be described adequately in terms of a simple two-phase model according to which ideally ordered crystallites exist together with completely amorphous domains. This model constitutes merely one of the two limiting cases; the other is that of a paracrystal according to which all deviations from the ideal crystal are ascribed to defects and distortions of the crystal lattice [275–277].

The paracrystal model is rather convenient for explaining some observations, such as the broadening of the x-ray diffraction pattern and the essentially linear relationship between the melting temperature and the specific volume of nylon samples that are characterized by rather different thermal and processing histories [278]. On the other hand, , for example, both the existence of a glass transition, which is affected by plasticizing agents, and the observed relationships between density and the diffusion and absorption of water and dyes are less compatible with this model. These phenomena and processes seem to be more readily explained in terms of a two-phase model.

The fact that certain structure-related phenomena tend to support one model, whereas others can be explained adequately only in terms of the other, underlines the limiting nature of either of the two concepts. The actual morphological structure of nylon is more complex and may involve paracrystals of any of the possible polymorphic forms, mesomorphic regions, and essentially amorphous domains. This is also indicated by a multiple melting phenomenon [279] that was investigated by high-temperature x-ray techniques and differential scanning calorimetry, and has been explained based on three phases — crystalline, intermediate, and liquid amorphous [280].

The micromorphology of the ordered phases depends upon the conditions of crystallization and may be characteristic of that of flat dendrite crystals, lamellae, fibrillar and globular aggregates, and rhombohedric single crystals. The thickening of these crystals may be the result of either superimposition of lamellae or spiral growth originating from screw dislocations [281].

The thickness of the lamellae depends on the crystallization temperature and is usually in the order of 6–10 nm. The macromolecules are normal to the lamellae and are folded back and forth on themselves. A single-polymer molecule may belong to more than one lamella, especially in polymers crystallized from the melt. Such interlamellar bonding increases as the molecular weight increases. Chain-folding also exists in some of the fibrous or ribbon-like structures in which nylons may crystallize. These structures are presumed to be the degenerated forms of lamellae. The structure of the observed globular particles appears to be unknown.

The ordered structures discussed thus far are sometimes incorporated into superstructures, which are mainly, but not exclusively, formed upon crystallization from the melt. These superstructures are spherical aggregates, range in sizes from submicroscopic dimensions to millimeters in diameter, and are called spherulites. They can be recognized in the polarized